NOISE SOURCES CHARACTERIZATION OF AUTOMOTIVE HVAC SYSTEMS

NOISE SOURCES CHARACTERIZATION OF AUTOMOTIVE HVAC SYSTEMS

By

VAHID MADANI

A Thesis

Submitted to the School of Graduate Studies

in Partial Fulfillment of the Requirements

for the Degree

Master of Applied Science

McMaster University

MASTER OF APPLIED SCIENCE (2002) McMaster University

(Mechanical Engineering) Hamilton, Ontario

TITLE: Noise Sources Characterization of Automotive HVAC Systems

AUTHOR: Vahid Madani, M.Sc.

SUPERVISOR: Dr. Samir Ziada, Professor
Department of Mechanical Engineering
McMaster University

NUMBER OF PAGES: xiv, 103

Abstract

The noise sources and mechanisms of the front and rear HVAC systems of an automotive are characterized experimentally. The front system has three main outlet ducts equipped with louvers and operates in two modes of bypass and recirculation. The inlet and outlet sides of the rear system are both located in the cabin; hence, it always works only on the recirculation mode. The outlet duct of the rear system is covered by a ten-hole curved plate which is found to be a strong source of noise. Both systems are tested at the highest possible flow rate, as it is the most annoying condition of noise generation. The noise coming out of each duct of the front and rear systems and their fan units are measured separately. Since the fan is an important part of the systems, it is studied at different speeds with more details. In order to compare the effect of the noise generated by the fan section with the noise produced by the complete system, the impeller is replaced with a speaker generating an overall sound level similar to the fan noise. Under this condition, the flow noise due to the evaporator core, distributive ducts and louvers are cancelled. It is concluded that at low frequencies the duct flow-noise is dominant. At high frequencies, the effects of both duct flow-noise and fan noise are

important. To find out how the combination of the outgoing sound from the vents and fans inlet affect on the driver and passengers, some measurements are carried out inside the cabin of the automobile.

Acknowledgments

I would like to express my sincerest gratitude to Dr. S. Ziada for his guidance, instruction, helpful advices, encouragement and financial support in the course of this project. His patience and understanding is greatly acknowledged.

I would also like to appreciate the Climate Control Division of Ford Oakville Assembly Plant for providing the HVAC systems, fans, related components and on-site test facilities.

To the technicians in the Department of Mechanical Engineering: Dave, Ron, Andrew and Joe, thanks for your tremendous assistance.

I would like to thank the members of the FIV research group for all those invaluable suggestions and discussions.

Lastly, but not least, I would like to thank my friends and family for their constant support and encouragement.

Contents

Nomenclature

c	speed of sound, m/s
d	duct diameter, m
f	frequency, Hz
j	$\sqrt{-1}$
n	normal unit vector
p	pressure, Pascal
St.	Strouhal number
t	time, second
T_{ij}	Lighthill's Stress Tensor
u, v	velocity components, m/s
V	impeller tip velocity, m/s
Z	number of impeller blades
ρ	air density, kg/m^3
μ	shear viscosity, kg/m.s
ω	vorticity, 1/s

List of Figures

List of Tables

Chapter 1

Introduction

The interior acoustic comfort of automobiles has considerably developed over the last two decades. Yet car manufacturers and system suppliers are looking for more control of sound emission as the demand for the higher levels of driver and passenger's satisfaction is continually growing. The interior environment of automobile is acoustically dominated by the following sources:

- External aerodynamic noise
- Road noise
- Engine noise
- Heating, ventilation, and air conditioning (HVAC) system noise
- Exhaust noise

Among the above sources, HVAC noise has been least investigated. Air temperature, humidity and air quality of the HVAC systems have been improved, but it has not been extensively studied from the air-borne noise aspect. As a matter of fact, HVAC systems

are no longer evaluated only by the airflow performance, but today sound quality is an important criterion that should be considered.

An automotive air conditioning system is typically compact. The fan or blower provides air movement and circulation. It is possible to change the flow air speed to make an appropriate heat exchange balance at heating, cooling or evaporator section to create a pleasant climate condition inside the car. The fact is the noise control and reduction of automotive air conditioning systems is a difficult research topic. The main constraint is the packaging space limitation which results in a highly complex flow field inside the system, as shown in Figure 1.1. There is not enough length for flow to develop and expand through plenums and ducts. The sudden changes in duct size and direction of the airflow generate shedding vortices, separation, turbulence and unwanted flow circulation

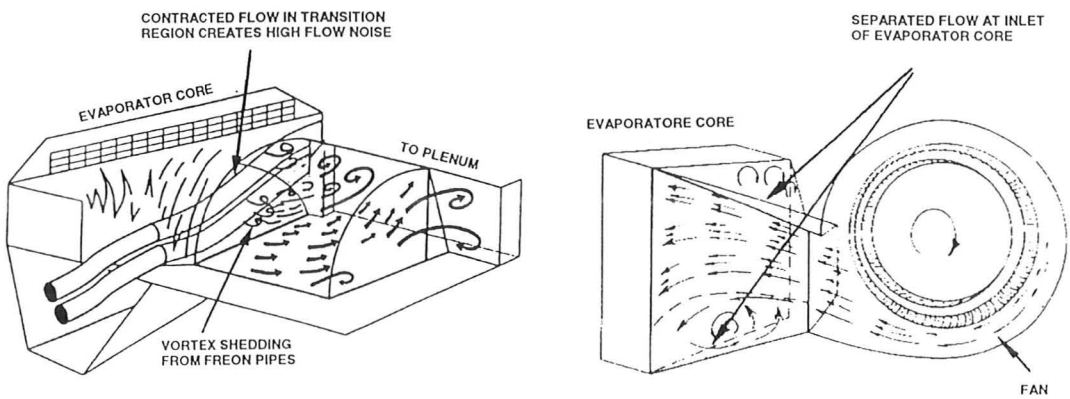

Figure 1.1: The region between evaporator core and plenum (left), area between fan and evaporator core (right), Brungart *et al.* (1992)

inside the fan and the air ducts. Therefore, this kind of flow field wastes fan power and produces high sound pressure levels. Besides, due to the packaging constraint and proximity of all the possible noise sources such as fan, evaporator core, flow ducts and louvers, identification of dominant noise sources needs a systematic detailed investigation. It will be demonstrated that noise generated by the HVAC system is broadband; however, it should be remembered that air rush noise, which produced in the range of 150-350 Hz, is very critical and greatly contributes to fatigue and excessive discomfort for the driver and passengers.

Fan or blower is normally described as a device to move the air within a fluid system. In automotive air conditioning systems, centrifugal fans push the air through the ducts and the core section. The system's resistance to flow results in an increase in pressure from inlet to discharge. Against the centrifugal pumps and compressors, centrifugal fans produce very small pressure rise; hence, the air can be considered completely incompressible. As explained before, the fan rumble noise which occurs at low frequencies is extremely bothering, as depicted in Figure 1.2. Many investigators have tried to reduce the noise levels of the fans and most of them could find very effective methods for some certain cases that will be reviewed in the next chapters.

During every design or optimization procedure for automotive HVAC system, the challenge is to reduce the noise generated by fan, evaporator core, ducts, louvers or any other part without any serious effects on the aerodynamic performance and manufacturing cost. These two limits are now added to the packaging constraint. That is

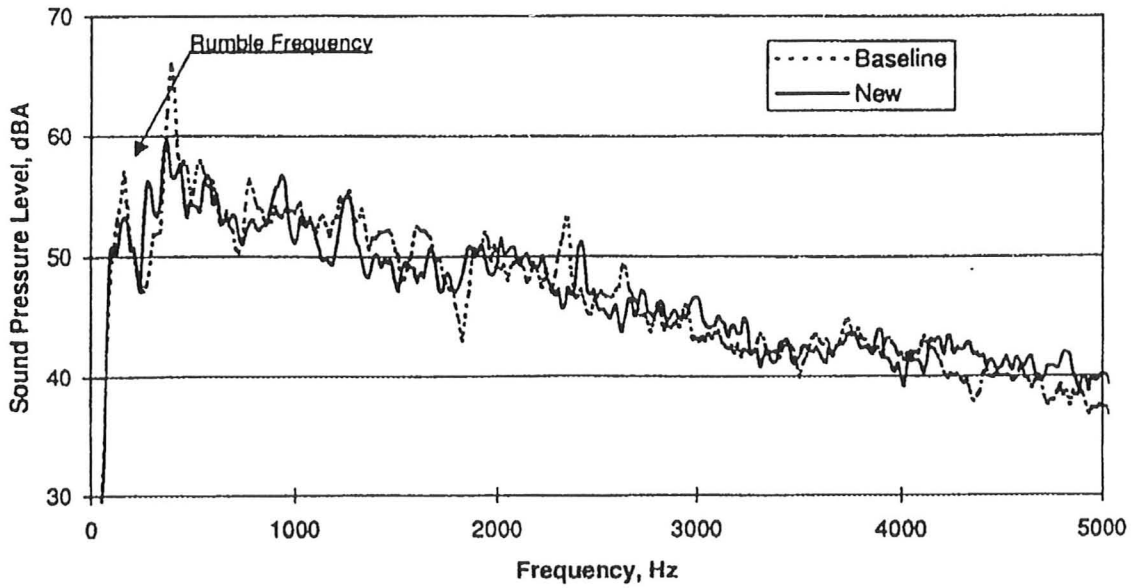

Figure 1.2: Sound pressure level spectrum for a typical fan; solid line indicate the modified fan, Humbad *et al.* (1996)

why after many years from manufacturing of new generations of automobiles, engineers still believe that design, redesign and improvement of air conditioning and ventilation systems of automobiles is a demanding task. To the author's knowledge, there is only one comprehensive investigation conducted on determination of the HVAC system noise sources, published by Brungart *et al.* (1992). This study, which was performed in an anechoic room, contains schematics of intensity vector distribution around a complete HVAC system. Flow visualization revealed the locations of highly turbulent flow which is a source of noise. Based on the measured intensity vectors, it is concluded that the fan is the dominant noise source. However, there is no information related to the spectra and the levels of the noise propagating inside the automobile from the duct outlets, and how these outgoing sound pressures could be related to the noise level of the fan. These

concerns are important because outgoing noise from the vents is the main noise that driver and passengers bear.

The motivation for this study came from a long-term research project intending to design and produce an excellent automobile in the country. Alleviation of interior air-borne noise was one of the main branches of this project.

As stated before, any attempt in order to reduce or control the noise of the air conditioning systems will not be successful unless the causes and locations of the major sources are clarified. Therefore, the present study is concentrated on the phase of noise sources characterization. Here, the total levels and spectra of the noise coming out of each vent of the HVAC systems and centrifugal fan parts will be measured and discussed.

Following this introduction, a literature review of the flow-induced noise in automotive air conditioning systems and fans is presented. Performance and aerodynamic noise aspects of forward-curved fans will be discussed. Since, most of the previous works have focused on the fan noise control; the automotive HVAC research background will not be too long. Chapter 3 contains a detailed explanation about the experimental apparatus and the method that used to measure and analyze the data. In chapter 4, results of all tests for the complete front and rear HVAC systems and their fans alone for both inlet and outlet sides will be presented and discussed. Thereafter, using the cancellation of flow-noise effects by replacement of the fan with a speaker, attention is focused on which sections are the main sources of noise. An in-car measurement was carried out to realize how the measured data are related to noise levels in the cabin of the automobile. These measurements also show the most critical locations inside the cabin. Chapter 5

includes a summary of the results of this study and some helpful recommendations for further investigations.

Chapter 2

Literature Review

2.1 Introduction

This chapter is a review of literature on flow-induced noise applied to centrifugal fans and automotive air conditioning systems. Section 2.2 discusses the fundamental theory of flow-generated noise in general. In section 2.3, performance and aerodynamic noise related to centrifugal fans are discussed. Previous investigations on automotive HVAC systems are reviewed in section 2.4. Last section deals with some interesting research works on HVAC fans using numerical methods.

2.2 Theory of Flow-Induced Sound

Historically, understanding of aeroacoustics was introduced by Lighthill (1952), Curle (1955), and Ffowcs Williams and Hawkins (1969). Most of the recent progress on blading noise has been based on their investigations. Lighthill's acoustic analogy is based on a comparison of the acoustic wave equation with the governing equation on the flow field. Goldstein (1974) presented one of the best formats of the final equation as follow:

$$\frac{\partial^2 \rho'}{\partial t^2} - c_0^2 \nabla^2 \rho' = \frac{\partial^2 T_{ij}}{\partial y_i \partial y_j} \tag{2.1}$$

where $\rho' = \rho - \rho_{steady\ state} = \rho - \rho_0$. The source term, which is called as Lighthill's turbulence stress tensor, is given by:

$$T_{ij} = \rho_0 v_i v_j + \delta_{ij}[(p - p_0) - c_0^2 \rho'] - S_{ij} \tag{2.2}$$

where S_{ij} is the shear stress tensor of shear viscosity μ, bulk viscosity σ, and fluid velocity vector v_i:

$$S_{ij} = \mu\left(\frac{\partial v_i}{\partial y_j} + \frac{\partial v_j}{\partial y_i}\right) + (\sigma - \tfrac{2}{3}\mu)\delta_{ij}\frac{\partial v_k}{\partial y_k} \tag{2.3}$$

Goldstein also showed that T_{ij} is approximately equal to $\rho v_i v_j$ inside the flow and approximately equal to zero outside this region. Therefore, the following approximation to Lighthill's stress tensor is ended up, neglecting the density fluctuations within the moving fluid:

$$T_{ij} \cong \rho_0 v_i v_j \tag{2.4}$$

However, since the radiated sound energy is only a few percentage of the fluid flow energy, Reynolds stress $\rho v_i v_j$ can be determined without any knowledge of the sound field. Hence, the right hand side of the equation 2.1 is a known sources term. One more point about equation 2.1 is that it is basically similar to the governing wave equation on a quadrupole acoustic field with a strength equal to $\partial^2 T_{ij} / \partial y_i \partial y_j$. Lighthill's equation is a consequence of the conservation of mass and momentum laws; or rearranged form of the Navier-Stokes and continuity equations. Hence, in order to determine the sound field

characteristics, the complete nonlinear equation should be solved inside the acoustic source region. This is a challenging job even for the case of a simple flow field. Today, numerical methods have an important contribution in this regard. Curle later modified Lighthill's equation to include the effects of solid bodies.

In case of existence of solid boundaries, monopole, dipole and quadrupole can be present at the same time, as well as the diffracting and reflecting sound waves. However, based on the order of magnitude analysis, dipole sources are the only dominant ones. Doak (1960) extended Curle's work and showed that for a solid body in a low speed flow, the noise sources are due to the distribution of surface stresses which consist of shear stresses and surface pressure. The former is usually much smaller and can be ignored. Ffowcs-Williams and Hawkins developed the boundary layer noise theory in the presence of arbitrary moving surfaces for subsonic and supersonic speeds.

While Lighthill's theory describes the sound intensity in terms of the statistical characteristics of the turbulent source region, it is unable to detect the vortex dynamics that is undoubtedly a major source of noise. In fact, Lighthill's theory is not able to answer which characteristics of the eddy motion are noise producing. Powell (1960 & 1964) examined the sound generation theories from this special viewpoint. His final equation contained the term $\vec{\omega}\times\vec{u}$ which incorporates the noise due to the stretching of vortex lines by an imposed velocity $\vec{u}$:

$$\frac{\partial^2 \rho}{\partial t^2} - c_o^2 \nabla^2 \rho = \nabla\left[\rho(\vec{\omega}\times\vec{u}) + \nabla(\frac{\rho u^2}{2}) - u\frac{\partial \rho}{\partial t} - \frac{u^2}{2}\nabla p + \nabla(p - \rho c_o^2)\right] \tag{2.5}$$

where $\vec{\omega}$ is the vorticity vector that is equal to the curl of the velocity. Thereafter, Howe (1975) derived a similar equation for convected sources in nonisentropic flows using the equations of continuity, momentum and the first law of thermodynamics. Mueller (1979) and Howe (1998) published two comprehensive texts on this subject. The former contains analytical methods for modeling acoustic problems including vorticity and entropy fluctuations as sources of sound.

2.3 Centrifugal Fans

A centrifugal fan or blower is the air-moving component in all automotive heating and air conditioning systems. In operation, the fan or impeller is rotated by an electric motor. The rotation of the fan's blades imparts kinetic energy to the air in the form of a velocity change, which produces airflow and pressure difference.

Figures 2.1 and 2.2 show the blower housing or scroll and impeller of an automotive HVAC system fan. Based on the shape of the blades, centrifugal fans are mainly divided into three categories, shown in Figure 2.3. The magnitude and direction of the air at the blade tips are represented. The total velocity of the air leaving a blade tip $\vec{V}_{blade,total}$ equals the air velocity relative to the blade tip $\vec{V}_{blade\,tip}$ plus the tangential velocity of the blade tip $\vec{V}_t$:

$$\vec{V}_{blade,total} = \vec{V}_{blade\,tip} + \vec{V}_t \tag{2.6}$$

where $\vec{V}_t = r\omega$, r and ω are radius of the blade tip and radial speed of the impeller, respectively. The magnitude of $\vec{V}_t$ is equal to the volume flow rate divided by the total

area of the flow paths between adjacent blades at the blade tips. In Figure 2.3, if the magnitudes of $\vec{V}_t$ were the same, the flow rate and impeller size would be identical. Three main groups of centrifugal fans are as follows:

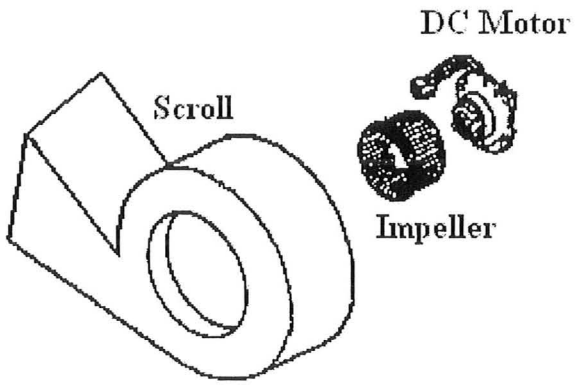

Figure 2.1: Components of a typical fan of an automotive HVAC system

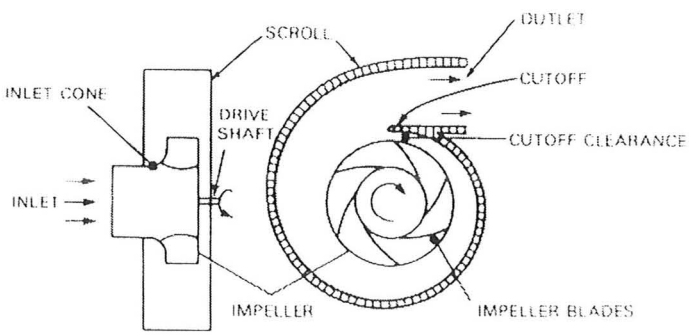

Figure 2.2: Schematic of main parts of a centrifugal fan, Blake (1986)

A. Forward-Curved: This group is extensively used in various industrial applications. The tip of the blades is curved in the direction of rotation. From figure 2.3, it is obvious that for same total velocity, air leaves the impeller at a velocity greater than the impeller tip speed; hence, forward-curved fans run at low speeds and have low efficiency. That is why they require greater input power for the same flow rate and pressure. This kind of fans is usually light and may have from 24 to 64 blades. Since, automotive blower fans are usually of the forward-curved type, it will be discussed with more details.

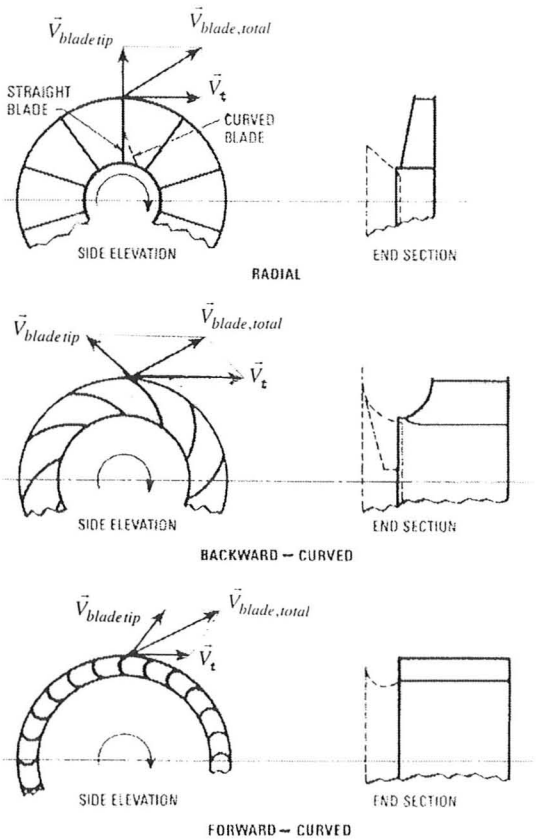

Figure 2.3: Schematic of radial, forward- and backward-curved fans, Jorgensen (1999)

B. Backward-Curved: This class of fans is more efficient than the previous group. The tip of the blade is curved away from the direction of rotation and run at higher speeds. They contain 10 to 16 blades and are used for general heating, ventilating, and air-conditioning systems, but automotive.

C. Straight Radial: This is the simplest type of centrifugal fans. They have low efficiency and about 6 to 10 blades. They are used widely for high-pressure industrial applications.

2.3.1 Forward-Curved Fans: Performance

Forward-curved blades fans are the most common blowers in automotive HVAC system industries. The impeller is located in blower scroll that guides the air streamline and flow at an increasing radius of curvature to further increase the static pressure. Typically, the total pressure rise is between 250 and 1000 Pascal, and the range of the impeller tip speed is from 2000 to 4000 RPM. The flow in fan system is totally considered incompressible as the Mach number never exceeds 0.15. Near the peak static operation, forward-curved fan efficiencies range from 0.35 to 0.45, and decrease to zero at no-pressure rise condition. The peak static point is also in the range of lowest noise level, but at higher flow rates it could increase by up to 15 dB. Figure 2.4 shows a typical performance curve for forward-curved fan.

As observed in Figure 2.2, two important parts of any centrifugal fan are impeller and scroll. The impeller increase the kinetic energy of the air and the scroll, or housing, directs the flow into, around, and out of the impeller and provide a smooth path

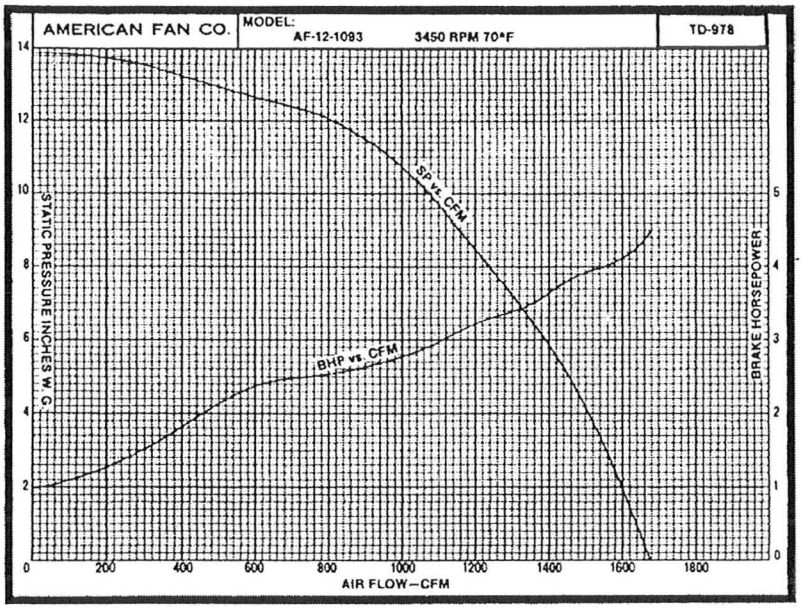

Figure 2.4: Performance curve of a forward-curved fan, American Fan Co.

to discharge of the high-energy air. The inlet flow accelerates in two steps. First, when it turns radially to enter the impeller blades, and the second time is when the moving blades impose a tangential force. Obviously, as a result of this process, there should be a reduction in static pressure, which could be determined by the Bernoulli equation. This pressure variation reaches its maximum immediately after the cutoff area and gradually reduces to a minimum on the discharge side of the cutoff. The spiral shape of the scroll provides the required area for diffusion, although in the best case, only 50 to 60 percent of the exit area is occupied. The exit flow from the blades has high-velocity jet characteristics, as it can be seen in Figure 2.5. Since, the flow along the blade span and the jet-wake region are highly separated, the potential flow solution has a drastic

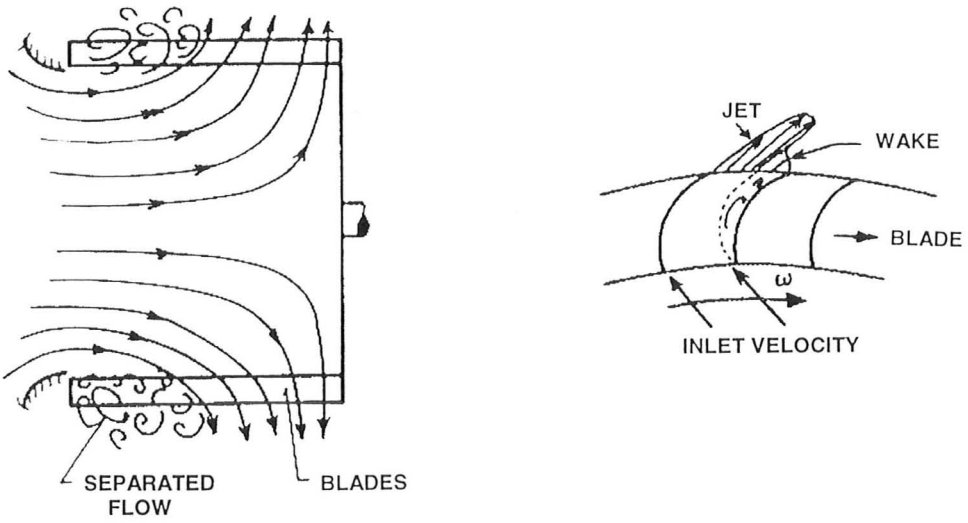

Figure 2.5: Streamlines in and around the blades, Kind and Tobin (1990)

discrepancy from the measured velocity. Therefore, any theoretical analysis of the flow field inside the forward-curved fan is difficult.

2.3.2 Forward-Curved Fans: Aerodynamic Noise

The first investigation on centrifugal fan noise is the research work of Howes and Real (1958). They used an in-duct method to measure the sound levels of a forward- and backward-curved fans. Their results were not very useful because their measurements were not in the typical rotor case, but totally in stall condition. Five years later, Huebner (1963) published a paper indicating two mechanisms for fan noise. The first is the siren tone resulting from the interaction of rotating and stationary parts of a centrifugal fan; and the second is vortex noise. According to his measurements, he concluded that small

height rotors generate sharp peaks in the spectra while larger height rotors do not show any discrete frequency peaks. Probably, the first attempt to reduce the centrifugal fan noise was made by Lyons and Platter (1962) and Embleton (1963). They found that the location of cutoff has a significant role in reduction of noise at blade pass frequency. Embleton also tried to decrease the noise level by making slots on the blades surfaces in order to delay the flow separation, but it was not very effective. Chanaud (1965) studied the fan noise using measurement of the sound level from an uncased forward-curved fan. He ended up that the broadband aerodynamic sound from an uncased centrifugal fan can be interpreted to be a result of radiation from randomly oriented dipole sources within the flow. However, all of his results were not very helpful and accurate because of the breakdown of the flow field around the impeller. Smith *et al.* (1974) studied the effect of cutoff distance on both noise and performance. They reported a rise in efficiency and a sudden reduction in pure tone noise as a result of increasing the cutoff distance. In 1975, Mugridge developed equations to predict the noise generated by centrifugal fans. This work was based on the noise generated due to inlet turbulence and separated boundary layer. Krishnapa (1979) made measurements on a wide variety of mostly heavy industrial centrifugal blowers. He found a strong dependency of noise levels on the mass-flow-pressure characteristic, especially in the frequency band containing tones. Kind and Tobin (1990) studied the performance and flow field of three squirrel-cage centrifugal fans. This work was not directly related to noise measurement, but it revealed some important characteristics of flow field which are important to characterize the noise sources. They concluded for larger ratio of rotor exit to inlet area, the separation of inlet

flow is more intensified. This phenomenon is an essential factor in producing complex flow field containing nonuniform and reverse flows over much of the operating range. Humbad *et al.* (1998) improved the sound quality of an automotive air conditioning blower by modifying the cutoff and scroll geometries which reduced the blade passage tone noise. This progress was gained without losing the airflow performance. They used an anechoic room for the measurement of the sound pressure level.

Most of the published papers in 1980's and early 1990's on blading noise have been related to axial fans because of their broad range of applications in aeronautical industries. The fact is the basic mechanisms of flow-noise generation are the same for both axial and centrifugal types. The first solution of the wave equation 2.1 was developed by Ffowcs Williams and Hawkins (1969); however, the notation that Goldstein (1974) used is easier to understand and allows studying different flow-noise sources with presence of moving surfaces:

$$\rho'(\vec{x},t) = \frac{K\partial^2}{\partial x_i \partial x_j} \int_{v_c(t_0)} \left[\frac{T_{ij}}{r|C|}\right] dv(\sigma) - \frac{K\partial}{\partial x_i} \int_{A(t_0)} \left[\frac{f_i}{r|C|}\right] dA(\sigma)$$

$$- \frac{K\partial}{\partial x_j} \int_{v_c(t_0)} \left[\frac{\rho_0 a_j}{r|C|}\right] dv(\sigma) + \frac{K\partial^2}{\partial x_i \partial x_j} \int_{v_c(t_0)} \left[\frac{\rho_0 V_i V_j}{r|C|}\right] dv(\sigma) \qquad (2.7)$$

where $K = 1/4\pi a_0^2$, $\vec{r}$ is the vector between the locations of source and observer (i.e.; $\vec{r} = \vec{x} - \vec{y}$), $C = 1 - (\vec{r}/r)(\vec{V}/c_0)$ which is the Doppler factor, and f_i represents the force exerted by the boundaries on the fluid per unit area, $f_i = n_i S_{ij} - n_j(p - p_0)$; where n_i is unit vectors normal to the surface elements. For isentropic changes in the fluid, one may assume $p' = c_0^2 \rho'$. The first term on the right hand side of equation (2.7) is similar to the

Lighthill integral for an unbounded flow that corresponds to the noise generation due to volume sources. This indicates a field of moving quadrupoles due to the applied fluctuating shear stress. Ffowcs Williams and Hawkins have shown that interaction of inlet flow with the flow around the blades of a fan could be a very good example of sound generation due to the fluctuating shearing stress. Later on, Morfey (1971) and Goldstein *et al.* (1974) showed separately that quadrupole noise is important only when the compressibility effects should be taken into account, especially when the speed of blade reaches $M = 0.8$. Hence, for small centrifugal blowers, this phenomenon is negligible. The second term of equation 2.4 contains the effects of unsteady forces applied by the solid surfaces on the flow. Since the unsteady forces can be simply assumed as a series of moving dipoles, this term represents dipole noise. The third and forth terms are related to blade thickness noise that contain the volume displacement effects on the moving surfaces, and sometimes called monopole noise. Since, the blade tip speed of small centrifugal fans is much less than the range of transonic velocities, blade thickness noise cannot be considered as a crucial noise generating factor. Therefore, from the theoretical viewpoint, monopole and quadrupole noise mechanisms are not important for small blowers. This will be examined in chapter 4.

Unsteady blade forces are commonly discussed in centrifugal fans because the flow field is spatially non-uniform due to the strong change of the flow velocity vector. The best classification of this kind of force related to the fan noise generation mechanisms has been published by Neise (1988). If the inlet flow velocity fluctuations are periodic, the spectra of the noise generated by incident turbulence are discrete; and if

random, the spectra are broadband. In the case when separated flows and turbulent boundary layers exist, the noise will be generated due to the pressure fluctuations applied to the blades. This mechanism will be intensified if it happens around the blade trailing edge. Flow instability in the laminar boundary layer on the blade suction side could produce disturbances which interact with blade trailing edge and generate sound waves. This phenomenon is sometimes called vortex shedding noise or vorticity noise.

Shepherd and Lafontaine (1992) used Particle Image Velocimetry (PIV) to map the instantaneous velocity distribution in a centrifugal fan scroll. Figure 2.6 shows the vorticity contours in different blade angles. The thick solid line demonstrates the instantaneous location of blade, near the cutoff, rotating anti-clockwise. The figure clearly represents that the most important noise source is the interaction of the shedding vortices from the blade with the cutoff. The dark areas around the blade tip are due to vorticity shed from blade shear layer.

Another source of unsteady blade forces is rotating stall. It occurs as a result of secondary flows which make the suction side of the blade relatively blocked. This phenomenon, in turn, may generate low frequency pressure pulsation, noise and vibrations.

Ishihara and George (1994) investigated the noise sources in a forward-curved centrifugal fan using several flow visualization methods. Figure 2.7 demonstrates the result of their oil flow method. Figure 2.7a shows the re-circulated flow through the cutoff clearance and back in through the rotor. This is a major source of noise. In Figure 2.7b some inward flow under the impeller is observed. The re-circulating nature is still

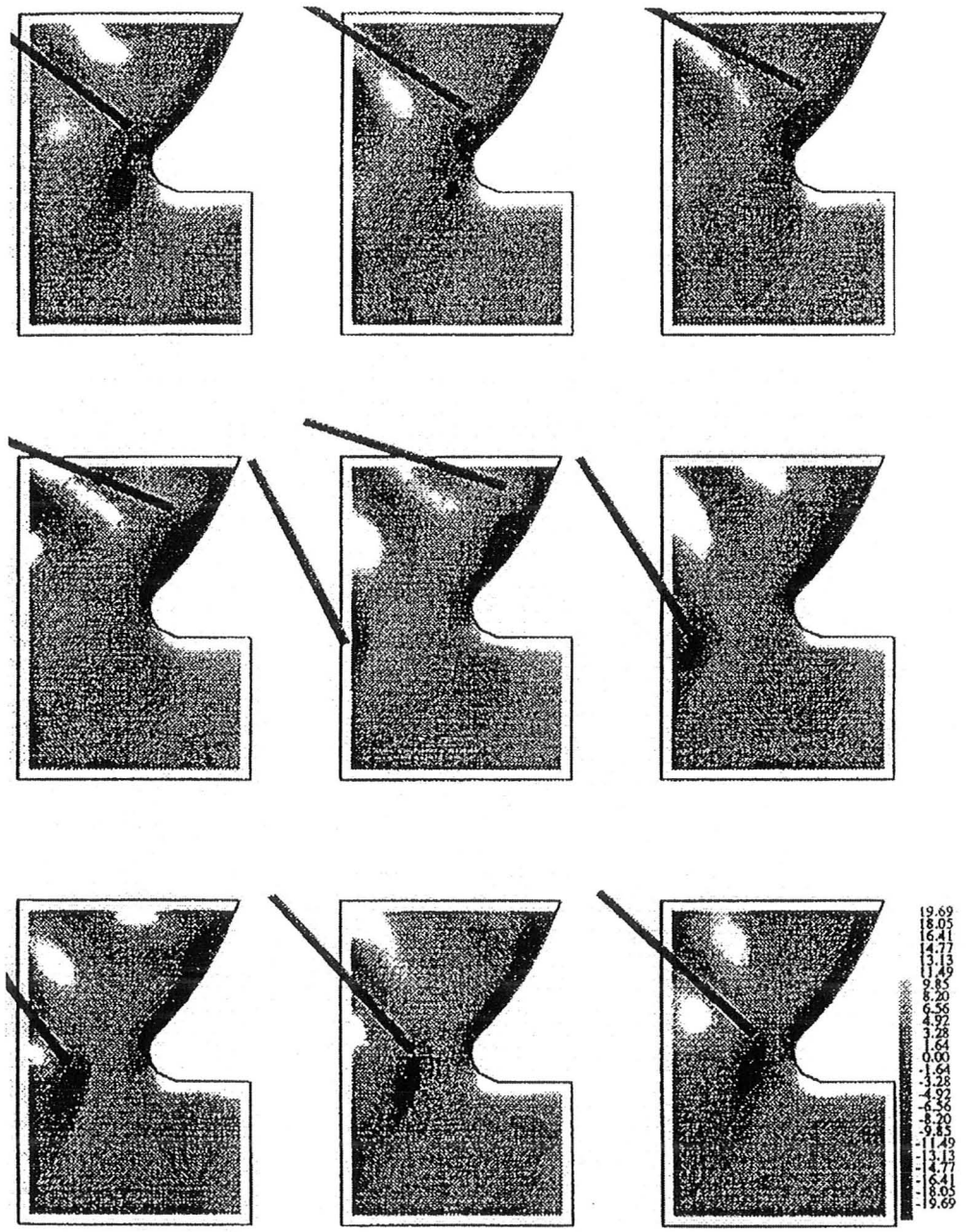

Figure 2.6: Vorticity distribution at different blade angles, Shepherd and Lafontaine (1992)

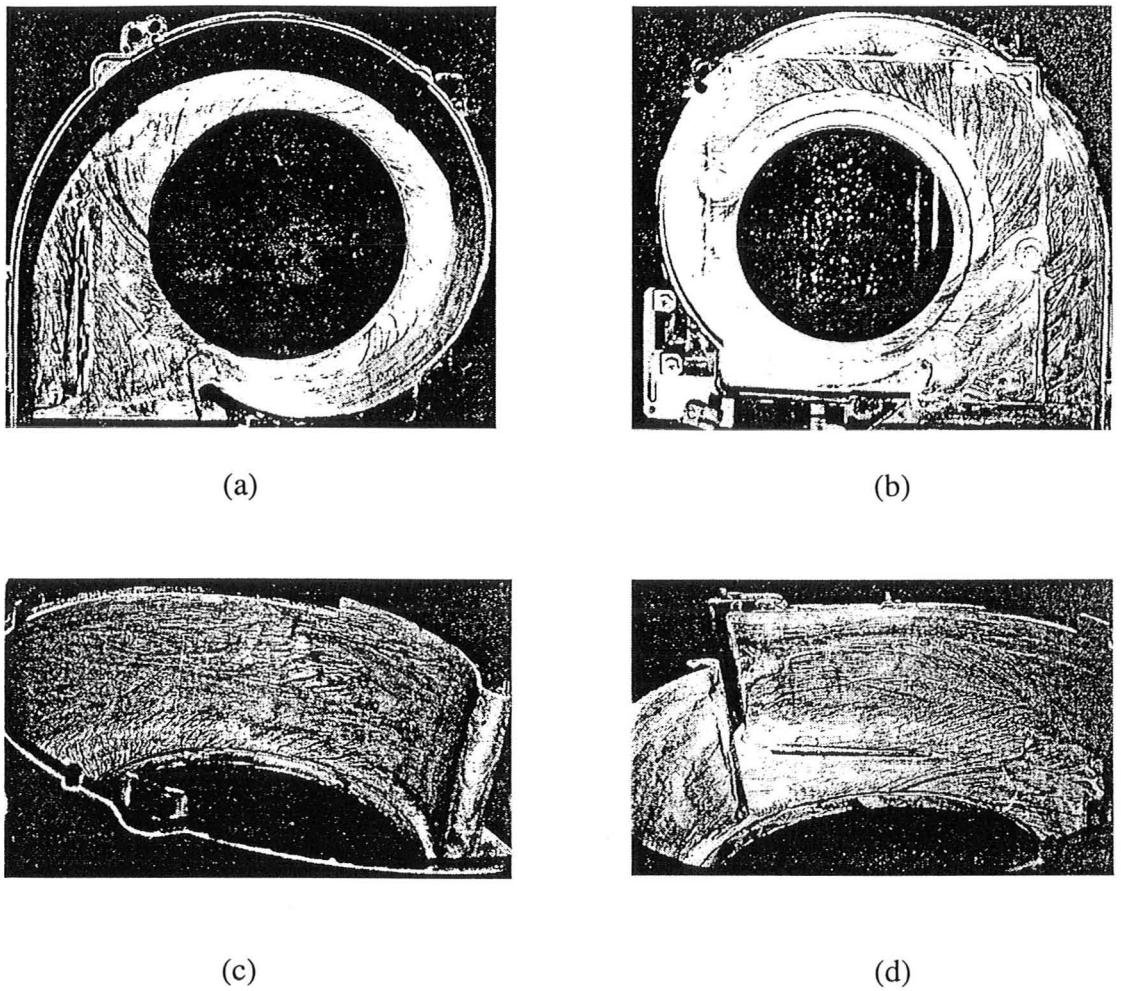

(a) (b)

(c) (d)

Figure 2.7: (a&b). Flow at inlet and opposite sides of the scroll;
(c). flow from scroll midway to the beginning of cutoff; (d). outlet flow,
Ishihara and George (1994)

clearly seen. Figure 2.7c does not show the flow streamlines around the cutoff, where there is a thick dark line, because the flow is strongly turbulent. However, the re-circulation can still be observed near the lower corner. Figure 2.7d depicts the flow pattern at the fan outlet. The flows of the upper and lower parts of the scroll go up and

down; respectively, with moderate slopes. This phenomenon results in a separation line which is also affected by the weak separation in the corner of the scroll. In general, these pictures indicate that the strong broadband noise sources would be expected from the flow separation on the blades and from the high level of turbulence in the re-circulating flow at the blower inlet.

2.4 Automotive HVAC Systems

Noise investigation of automotive air conditioning system is one of the most difficult research areas due to the highly complicated and turbulent flow field in the fan and the evaporator core and the associated complex air ducts. There are just a few published papers on automotive HVAC noise in which anechoic or reverberation room

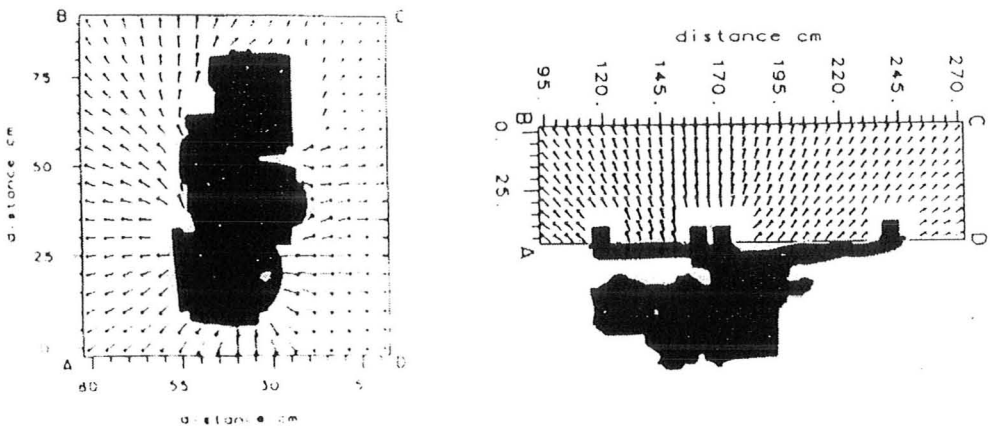

Figure 2.8: Intensity vectors, (a) HVAC system without ducts at 1000 Hz, (b) the complete HVAC system at 500 Hz, Brungart *et al.* (1992)

has been used as the measuring facilities. Brungart *et al.* (1992) used flow visualization that was carried out underwater on an optically clear HVAC system, identical to a real one, in a clear plexiglass tank. In order to determine the role of the fan noise in the whole system, an acoustically isolated fan was used instead of the real fan. Figure 2.8 shows two samples of their results. All of their figures were in the form of intensity vectors around the complete system, with and without the ducts. Based on the magnitudes of these vectors in just two frequencies of 500 and 1000 Hz, they concluded that the fan is the dominant source of noise. However, their vector demonstration for the whole system such as those shown in Figure 2.8 can not be considered as an accurate analysis because it does not give any detailed information related to the sound levels emanating from the outlets of the ducts that driver and passengers hear inside the automobile. However, this work is valuable because it reveals some important flow-noise coupling behaviors around a typical automotive HVAC system.

Humbad and Thawani (1994) studied the source identification and resolution of excessive air-rush noise in a climate control system. They made a series of bench tests in an anechoic room to evaluate the effects of modifying the inlet duct, recirculation ducts and blower cutoff. According to the measured sound pressure levels, they concluded that air rush noise performance can be improved by modification of the cutoff design. However, modification of the inlet and recirculation ducts showed just marginal effects on noise reduction. It should be remembered that the final judgment of an automotive HVAC acoustics is somewhat subjective and is dependent on the passengers. In order to improve the sound quality of an automotive HVAC system, they used an anechoic

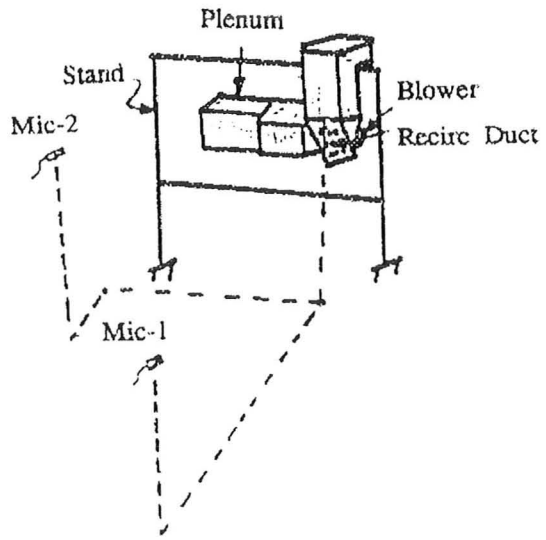

Figure 2.9: Test setup, Humbad and Thawani (1994)

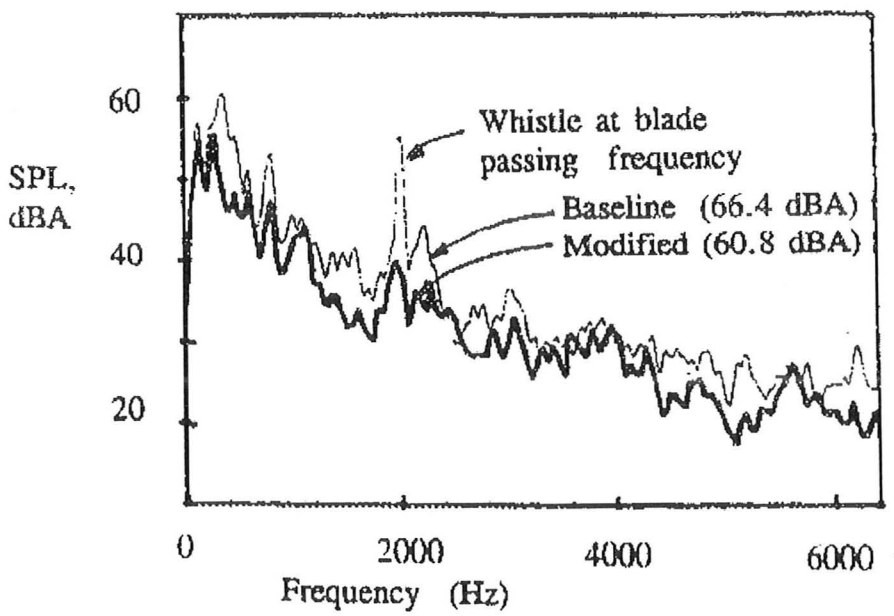

Figure 2.10: Sound pressure level spectrum, blower at high speed, Humbad and Thawani (1994)

room along with a far and a near field microphones. Figure 2.9 shows their setup. A series of bench tests were performed to estimate the effects of modifying the inlet duct, blower inlet and outlet. Figure 2.10 shows typical results for the baseline and modified fans operating under maximum airflow conditions. It should be noted that the vertical axis of this graph is A-weighted sound pressure level and that is the reason the maximum level is about 65 dB which has a typical amount of 80 dB in most of conventional automotive HVAC systems. Again, this figure presents the noise propagating from the complete system and does not provide any information on perceived noise at the outlet of the system ducts.

2.5 Computational Methods

Today, computational fluid dynamics (CFD) is a powerful method to investigate and analyze the noise sources through determination of physical properties and streamlines within the flow field. However, it is still a new branch in flow-noise coupling applications. There are a number of commercial softwares which are able to predict the acoustic properties, yet it is not so accurate and reliable. That is why this area is currently one of the hot spot in aeroacoustics. It should be mentioned that CFD is a tool to calculate the pressure, velocity, density and temperature distributions. These data help to understand where the flow-induced noise sources are. Shen *et al.* (1995) studied airflow in air passages of a plenum to calculate pressure drop between a windshield base and a blower inlet. Toksoy (1995) applied a computational process to a blower design considering flow, noise, and structural integrity. Gronier and Gilotte (1996) simulated

flow fields including individual blade geometry. Their results seemed to be accurate. Werner and Frik (1995) made some modifications on air distribution within the HVAC ducts. Lin *et al.* (1994) investigated the accuracy of a numerical method for prediction of velocity and pressure distribution in an air conditioning duct and compared with experiment. Kondo and Aoki (1985) solved 2- and 3-dimensional flows in a simplified HVAC system with an inlet and outlet ducts, including the evaporator. This work included the effect of non-uniform flow distribution in the front of the evaporator. Ikuta *et al.* (1989) simulated fluid and heat flow in a simplified heater unit and showed a good comparison with flow visualization results. Cho and Kim (1997) analyzed and modified the fluid flow in an HVAC system and compared with empirical results. Fischer (1995) used CFD approach to optimize the shape of the blades and scroll of a centrifugal blower. Since, the description of the procedure is outside the scope of the present study, only some of their results are shown. Figure 2.11 demonstrates the distributions of pressure

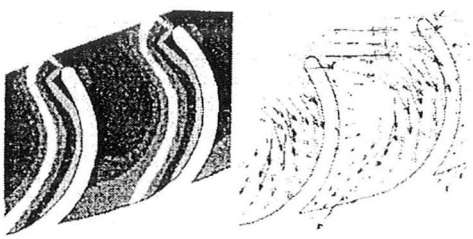

Figure 2.11: Pressure and velocity distributions around the blades, Fischer (1995)

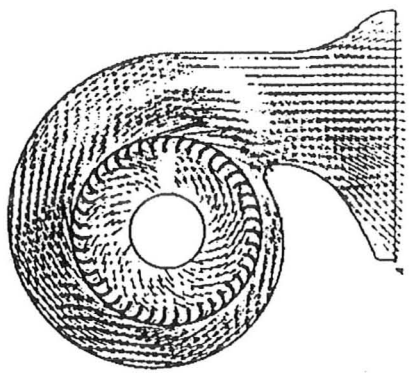

Figure 2.12: Velocity distribution in the blower scroll, Fischer (1995)

and velocity vectors in and around the impeller blades. The cyclic behavior of the impeller was simulated quite well. Figure 2.12 shows the velocity distribution inside the scroll. The flow field showed very good agreement with experiment, especially at the cutoff area. Another exciting CFD research on centrifugal fans was carried out by Humbad *et al.* (1996), shown in Figure 2.13. These pictures demonstrate the velocity vectors in the whole scroll and near cutoff for both baseline and modified designs. The baseline design obviously exhibits a recirculation and highly turbulent area past the cutoff at the evaporator core. The extended cutoff helps to eliminate this recirculation, which is obviously a noise source. Besides, the velocity distribution in the blade and cutoff areas shows a reentry of air into the impeller, while in the new design, it is eliminated. These results are consistent with flow visualization. Thompson *et al.* (1992) solved the acoustic wave equation using a finite element method and compared the results with experimental observations. Figure 2.14 shows the source distribution around the cutoff region. The vorticity shed from the blade tip is due to a dipole source distribution, as described before. However, this source distribution has a dipole nature if the vorticity field experiences rapid changes as the blade passes the cutoff area.

As expressed earlier, CFD modeling is a new method of study of aeroacoustic characteristics of flow fields. It is still required to be compared with experimental data; however, in the future, it will be a useful method to reduce the number of modification tests.

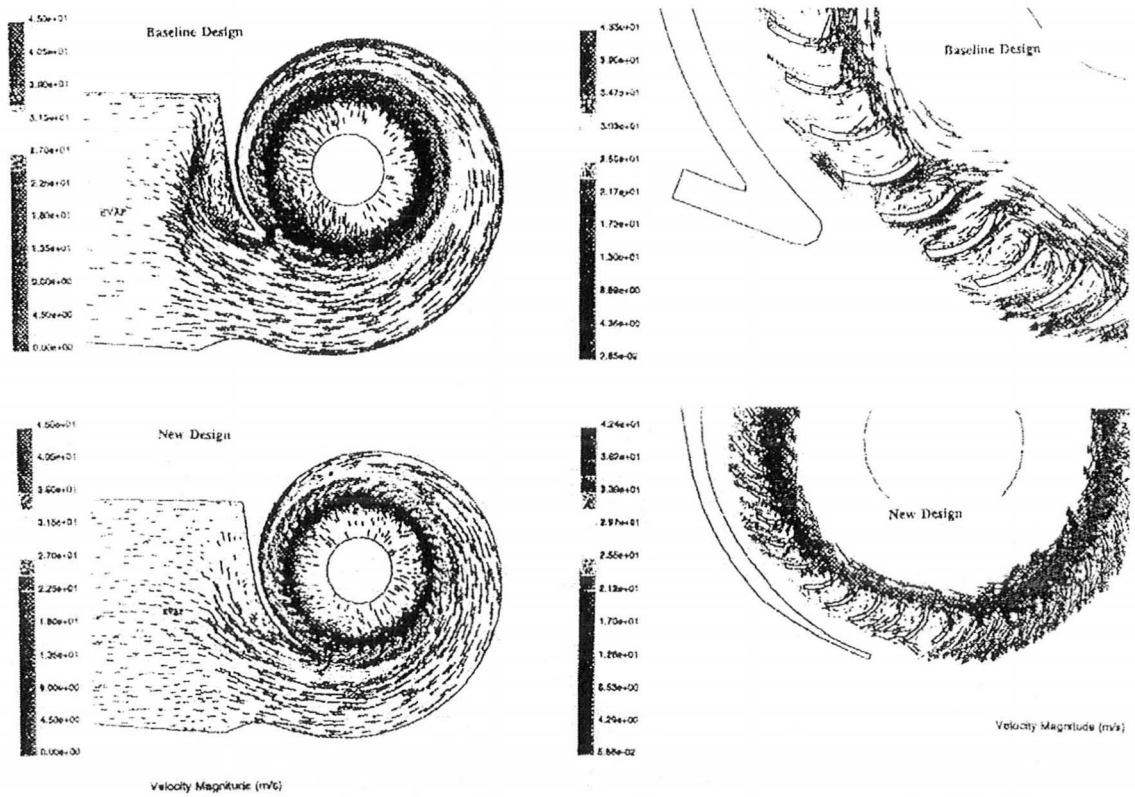

Figure 2.13: Velocity vectors in fan scroll (left) and cutoff (right), Humbad *et al.* (1996)

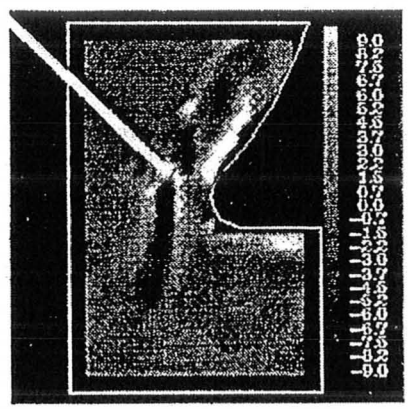

Figure 2.14: Acoustic source distribution in the vicinity of the cutoff, Thompson *et al.* (1992)

2.6 Research Objectives

The above review of literature on automotive HVAC systems and fans can be summarized as follows:

1. Previous studies were mostly focused on fan noise characterization. This trend has been resulted in highly efficient and relatively quiet fans which are currently used in the automotive industry. However, there has been no investigation to clarify the duct flow noise and its comparison with the fan noise.
2. Previous studies on automotive HVAC systems were concentrated on measurement of total noise level of the whole system in an acoustic room. Hence, these studies have not dealt with source identification of various components of the system.
3. No research in the open literature has been found related to the effect of the noise radiated from the fan inlet when HVAC system is working on the recirculation mode.

Considering the above items, it is required to initiate a systematic experimental procedure to characterize and identify the noise sources of automotive HVAC systems in order to understand which elements in the system should be modified. Therefore, the main objective of the present study is to develop an experimental approach which allows the characterization and identification of noise sources in complex automotive HVAC systems.

Chapter 3

Experimental Apparatus and Measuring Technique

3.1 Introduction

The purpose of this study was to identify the noise characteristics and sources in both front and rear climate control systems of a van automobile, shown in Figure 3.1 and 3.2, respectively. Each of the systems has the complete components of an actual HAVC system that is used in the automobile, including blower or fan, evaporator core, plenum, air distributive ducts and louvers. Both systems run by a 12-volt DC motor. The front system is mounted under the vehicle dash panel, in a specific place in the engine compartments. The location of the rear system is above the left rear wheel (driver side), inside the cabin.

There are three recognized methods to measure the noise, each requiring different measurement facilities; i.e., using an anechoic room, a reverberation room, and in-duct sound level measurement. All of these approaches are appropriate and reliable if they are applied properly. Since, at the time of this study, there was no access to any acoustic

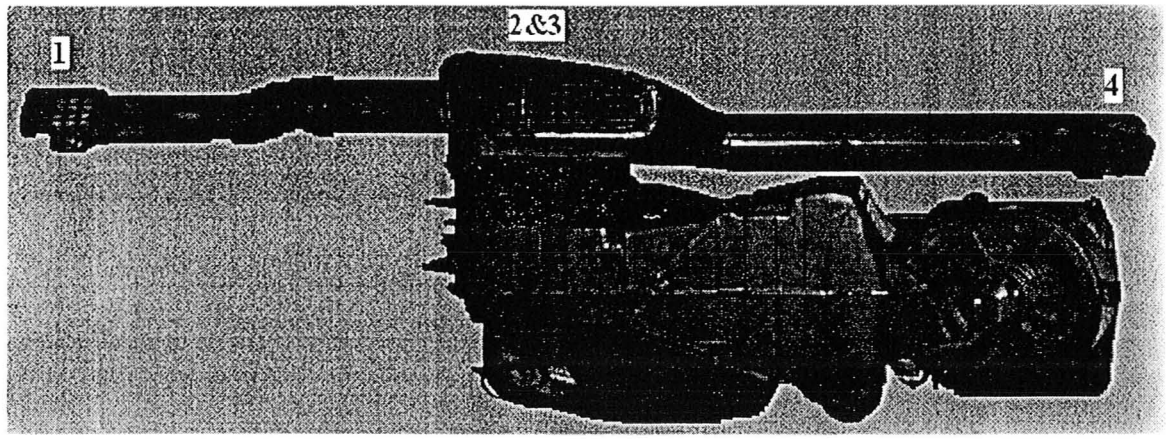

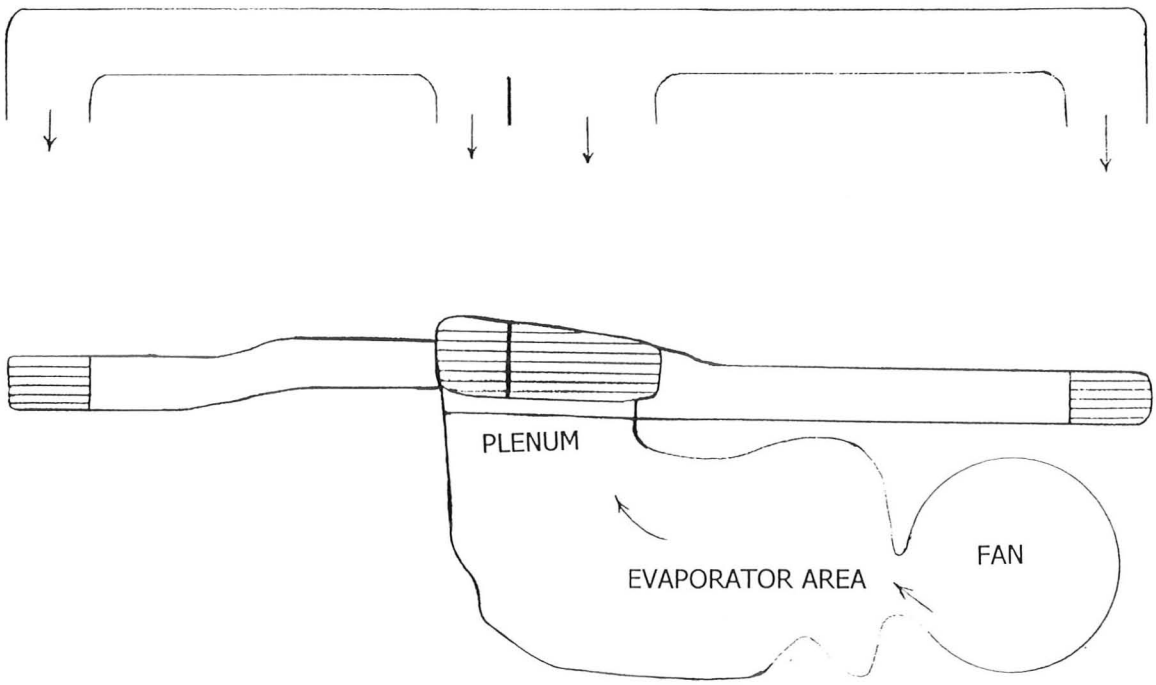

Figure 3.1: Front HVAC system

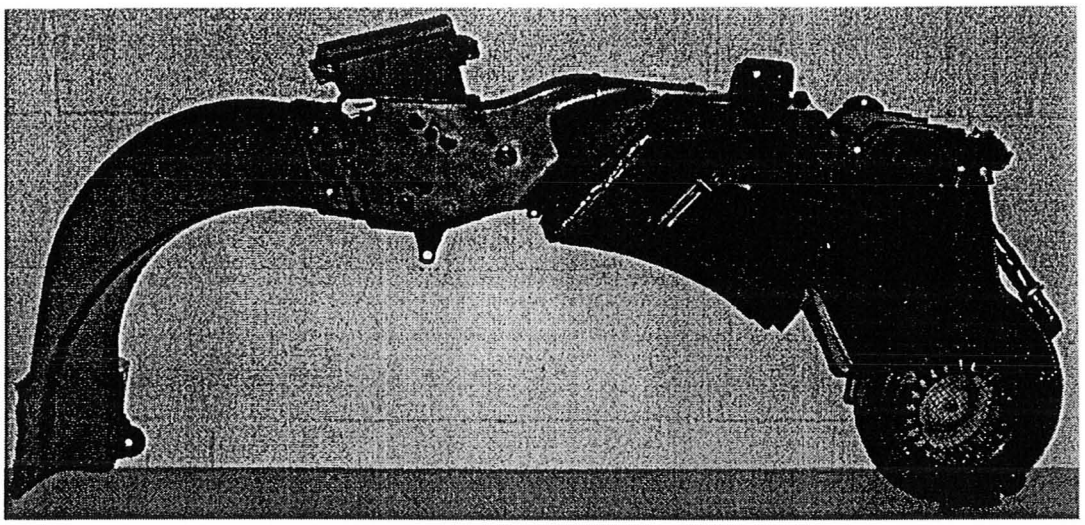

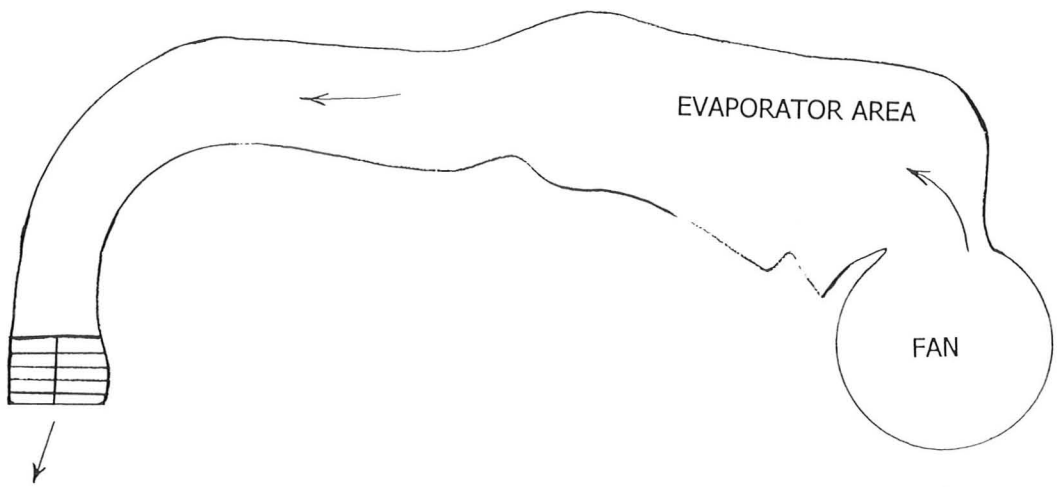

Figure 3.2: Rear HVAC system

room, the third method, which is in-duct noise level measurement, was chosen.

3.2 Apparatus

In-duct sound level measurement is a popular method for certain categories of applications. The test setup consists of a pipe with the noise source located at one of the two ends, and one or more microphones are used to measure of the noise level inside the duct. The procedure seems simple and straightforward; however, there are two important points that should be considered:

1. For any open end pipe or duct, the inside propagating acoustic waves keep the plane wave characteristics up to a certain frequency which is called *cut-off frequency*. For the range of frequencies above the cut-off, the sound pressure distribution at any cross section in the pipe is no longer constant and sound propagation cannot be treated as plane waves.
2. Since the measuring pipe has a finite length, the sound wave propagating from the source down the pipe or duct is reflected at the duct end. This phenomenon results in axial standing waves. In this case, the sound pressure is dependent on the axial location.

Cut-off frequency is a function of pipe diameter and cross-sectional shape, assuming the sound speed is constant. Based on the maximum interested frequency, the diameter of pipe can simply be chosen. For a circular cross sectional duct, cut-off frequency is calculated by the following formula, Blevins (1995):

$$f_{cut-off} = \frac{0.586c}{d} \tag{3.1}$$

where c is the speed of sound and d is the duct diameter. If one would like to get a cut-off frequency 10 kHz, the diameter should be about 2 cm, and if the source has larger dimensions, a transition duct is required to change the size of the cross section. In this case, all the fluid mechanics and flow-acoustic coupling aspects should be taken into account, such as boundary layer separation, turbulent flow and reflected sound effects. In case of presence of temperature gradient, these effects will be intensified. Cummings (1977) solved the wave equation for this special case and showed a very good agreement with experimental results. In the present study, the diameter of the fans and vents outlet are large; hence, in order to go to higher frequency, a transition duct with 7 deg included angle has been used. Transitional pipes or ducts in which the total angle is less than 10 deg are categorized as narrow diffusers or nozzles, as expressed by Lier *et al.* (1999). Roozen *et al.* (1998) also found in this case, area change of the duct has no influence on the flow-acoustic properties and flow separation, even in a pulsating flow. The diameter of the measuring duct is equal to 10 cm resulting in a cut-off frequency about 2020 Hz that is very close to the blade passing frequency of the HAVC fans when operated at maximum load. The experimental set-up is demonstrated in Figure 3.3.

In order to overcome the second problem, an anechoic termination is attached to the end of the test duct to reduce the effect of the standing waves. A three-microphone method is used to decompose the incident and reflected waves. The procedure will be explained in details in section 3.3. The anechoic termination, which has been made in

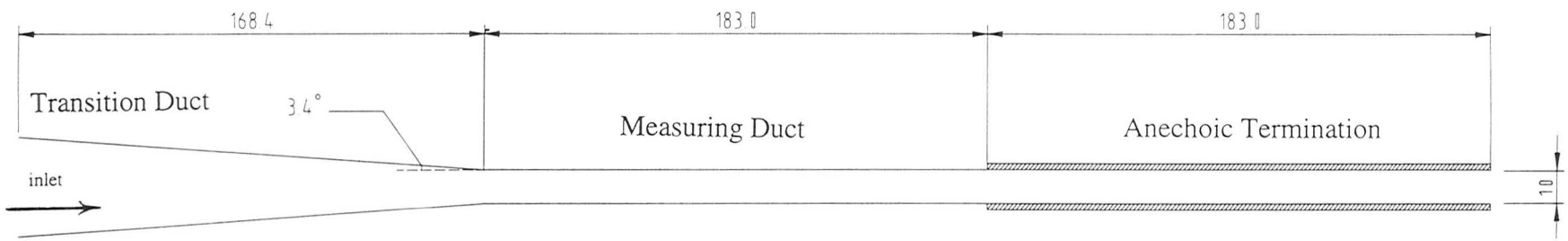

Figure 3.3: Test setup (dimensions are in cm)

the machine shop of the department, is a two-sided slit duct in which the total angle is about 2 deg. This provides a gradual and appropriate sound absorption inside the duct. A highly absorbent type of glass fiber with a total thickness of about 5 cm was wrapped around the duct. The reflection coefficient of this duct will be shown and discussed in section 3.6.

3.3 Three-Microphone Method

The theory of the three-microphone method involves the decomposition of a random signal generated by an acoustic source into its incident and reflected components using transfer function relations between the acoustic pressure at three locations on the wall duct as shown in Figure 3.4. Edge and Johnston (1990) presented one of the most effective procedures of three-microphone method that is used in the current study. The standing wave can be described by general equation, Davis (1988):

$$\boldsymbol{p}(x) = \boldsymbol{p}^{+} e^{-jkx} + \boldsymbol{p}^{-} e^{jkx} \tag{3.2}$$

The bold letters denote complex variables. Assuming:

$$\begin{aligned} \boldsymbol{p}^{+} &= c_1 + jc_2 \\ \boldsymbol{p}^{-} &= c_3 + jc_4 \end{aligned} \tag{3.3}$$

Sunbstituting into 3.2:

$$\boldsymbol{p}(x) = c_1 e^{-jkx} + jc_2 e^{-jkx} + c_3 e^{jkx} + jc_4 e^{jkx} \tag{3.4}$$

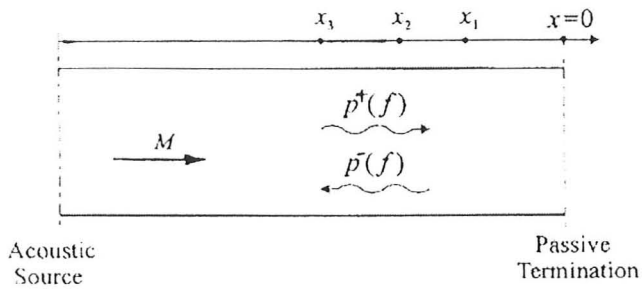

Figure 3.4: Sound field in an acoustic duct

The sum of the squares of the absolute errors between theoretical, $p(x_n)$, and experimental, $p_{exp}(x_n)$, acoustic pressure for all of the three points should be minimum, then:

$$\begin{aligned} E &= \sum_{n=1}^{3} \left| p(x_n) - p_{exp}(x_n) \right|^2 \\ &= \sum_{n=1}^{3} [p(x_n) - p_{exp}(x_n)][\overline{p}(x_n) - \overline{p}_{exp}(x_n)] \end{aligned} \tag{3.5}$$

The bar signs indicate complex conjugates. Since the minimum value of E is desirable, its derivatives with respect to the real and imaginary parts of p^+ and p^- should be zero:

$$\frac{\partial E}{\partial c_i} = 0 \qquad ; \text{for } i = 1 \text{ to } 4 \tag{3.6}$$

After algebraic manipulation and simplification:

$$\sum_{n=1}^{3} \mathbf{Re}\left[p(x_n) \frac{\partial \overline{p}(x_n)}{\partial c_i} \right] = \sum_{n=1}^{3} \mathbf{Re}\left[p_{exp}(x_n) \frac{\partial \overline{p}(x_n)}{\partial c_i} \right] \tag{3.7}$$

where,

$$\frac{\partial \boldsymbol{p}(x)}{\partial c_1} = e^{-jkx} \tag{3.8}$$

$$\frac{\partial \boldsymbol{p}(x)}{\partial c_2} = je^{-jkx} \tag{3.9}$$

$$\frac{\partial \boldsymbol{p}(x)}{\partial c_3} = e^{jkx} \tag{3.10}$$

$$\frac{\partial \boldsymbol{p}(x)}{\partial c_4} = je^{jkx} \tag{3.11}$$

Hence:

$$\sum_{n=1}^{3} \boldsymbol{Re}\left[\frac{\partial \overline{\boldsymbol{p}}(x_n)}{\partial c_i} \sum_{m=1}^{4} \{c_m \frac{\partial \boldsymbol{p}(x_n)}{\partial c_m}\}\right] = \sum_{n=1}^{3} \boldsymbol{Re}\left[\boldsymbol{p_{exp}}(x_n)\frac{\partial \overline{\boldsymbol{p}}(x_n)}{\partial c_i}\right] \tag{3.12}$$

In matrix form, this equation has the following form:

$$\begin{bmatrix} S_{11} & S_{12} & S_{13} & S_{14} \\ S_{21} & S_{22} & S_{23} & S_{24} \\ S_{31} & S_{32} & S_{33} & S_{34} \\ S_{41} & S_{42} & S_{43} & S_{44} \end{bmatrix} \begin{bmatrix} c_1 \\ c_2 \\ c_3 \\ c_4 \end{bmatrix} = \begin{bmatrix} t_1 \\ t_2 \\ t_3 \\ t_4 \end{bmatrix} \tag{3.13}$$

The left-hand coefficients are as follows:

$S_{11} = 1$

$S_{12} = j$

$S_{13} = \cos 2kx + j\sin 2kx$

$S_{14} = -\sin 2kx + j\cos 2kx$

$S_{21} = -j$

$S_{22} = 1$

$S_{23} = \sin 2kx - j\cos 2kx$

$$S_{24} = \cos 2kx$$

$$S_{31} = \cos 2kx - j\sin 2kx$$

$$S_{32} = \sin 2kx - j\cos 2kx$$

$$S_{33} = 1$$

$$S_{34} = j$$

$$S_{41} = -\sin 2kx - j\cos 2kx$$

$$S_{42} = \cos 2kx + j\sin 2kx$$

$$S_{43} = -j$$

$$S_{44} = 1$$

The right-hand coefficients can be calculated as:

$$t_1 = \boldsymbol{p}_{exp}(x)(\cos kx + j\sin kx)$$

$$t_2 = \boldsymbol{p}_{exp}(x)(-j\cos kx + \sin kx)$$

$$t_3 = \boldsymbol{p}_{exp}(x)(\cos kx - j\sin kx)$$

$$t_4 = \boldsymbol{p}_{exp}(x)(-j\cos kx - \sin kx)$$

Note that in equation 3.13, the real parts of the above coefficients are used. These coefficients are calculated in a loop for the desired range of frequency and in each of the three locations of microphones. After all of these steps, the matrix can be solved to determine the coefficients of c_i. Now, everything is ready to find the values of $\boldsymbol{p}^+$ and $\boldsymbol{p}^-$ using equation 3.3; therefore, the reflection coefficient is given by:

$$R = \frac{p^-}{p^+} e^{2jkx} \tag{3.14}$$

Based on this procedure, a computer program was produced in Matlab. The input file of this program is the output file of the Labview program described in section 3.5. Using the acoustic pressures at the three measuring points and their phase angles saved in the Labview output file, the Matlab program decomposes the incident and reflected waves; i.e., p^+ and p^-, respectively.

Since the result of any kind of microphone method is dependent on the locations of the microphones, it is important to know where the best places are. Unfortunately, when the numbers of the microphones are more than two, there is no general or specific rule to find a good axial location for microphones. According to the author's experience during the course of this study, the critical case is when all of the three microphones are located in the nodes. This condition makes the transfer functions undefined and the results will include excessive errors. To avoid this, the results should always be checked with the theory. If the error percentage is unacceptable, the microphones should be relocated but one in a time, then check with theory. Normally, after a couple of time, the appropriate locations can be found.

3.4 Microphones

Three 1/4" pressure microphones were used flush-mounted on the duct wall to measure the sound levels. According to the calibration data and chart provided by G.R.A.S. Sound & Vibration, their sensitivities are in the range of 1.5 to 4 mV/Pa, and

their frequency responses are flat up to 10 kHz. They are calibrated by a pistonphone type 4220 for each test.

3.5 Data Acquisition

The microphones were connected to an amplifier, and the output signals were fed into a National Indtruments PCI-4452 four-channel sixteen-bit sampling input board. A four-channel LabVIEW program was used to collect the data. For all of the measurements, a Hanning window was used for spectral smoothing, 120 ensembles were used in spectral averaging. To get a large bandwidth of frequency, the chosen sampling rate was equal to 32,768 with a resolution of 1 Hz.

3.6 Verification of the Measuring Technique

The result obtained by the procedure explained in section 3.3 is dependent on many factors, including the locations of the microphones, accuracy of measurement, data acquisition technique and the structure of the written program to decompose the incident and reflected waves. Thus, the experimental setup, data acquisition and analysis technique needed to be verified. A good way to verify the method of two- or multi-microphone is to compare its results with the theoretical predictions available for an unflanged open end pipe, Davis (1980). For this purpose, before doing any test on HVAC systems using the test setup shown in Figure 3.3, a speaker was attached to the open end of transition duct and the anechoic termination was replaced with an unflanged pipe.

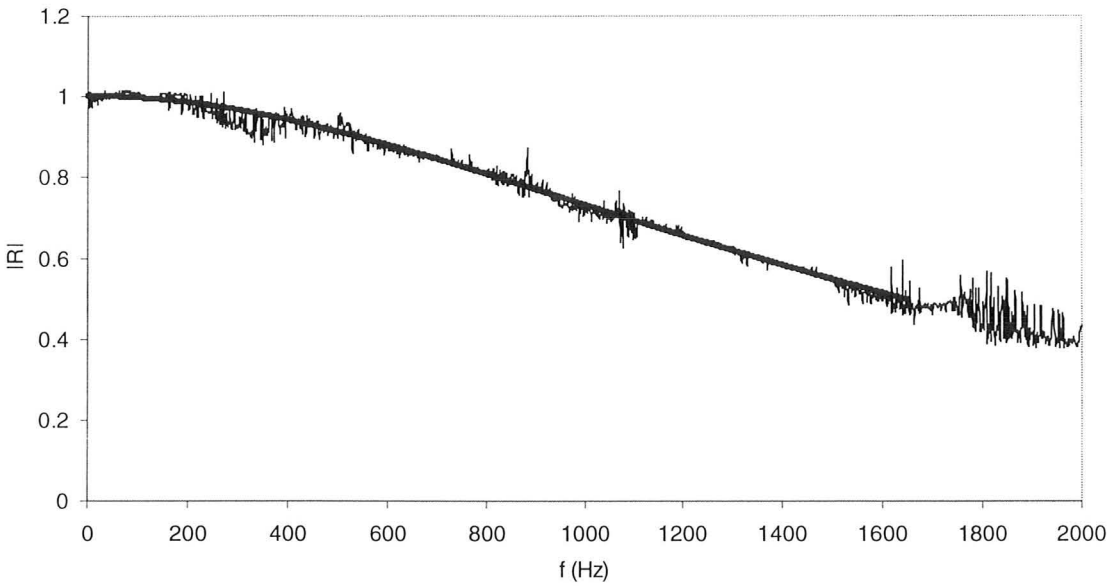

Figure 3.5: Comparison of calculated and theoretical reflection coefficients for the setup with unflanged pipe

Then, a measurement was done for a random noise generated by an HP analyzer and noise generator. The results of this measurement and theoretical prediction are depicted in Figure 3.5. As it is observed, this procedure could model the duct acoustic field. It should be noted that the theoretical approximation is good only for the wave numbers up to $1.5/a$, where a is duct radius. For the present case, this is equal to the frequency of 1650 Hz. It is clear that as the frequency becomes closer to cut-off, the error increases which is due to the change of characteristics of the internal duct waves. The average error is less than 1.7%, which is pretty close to the result of Peters (1993), 1.6%, which has been obtained over a very short range of frequency using the two-microphone method. Therefore, the setup of the microphones, data acquisition and analysis technique have

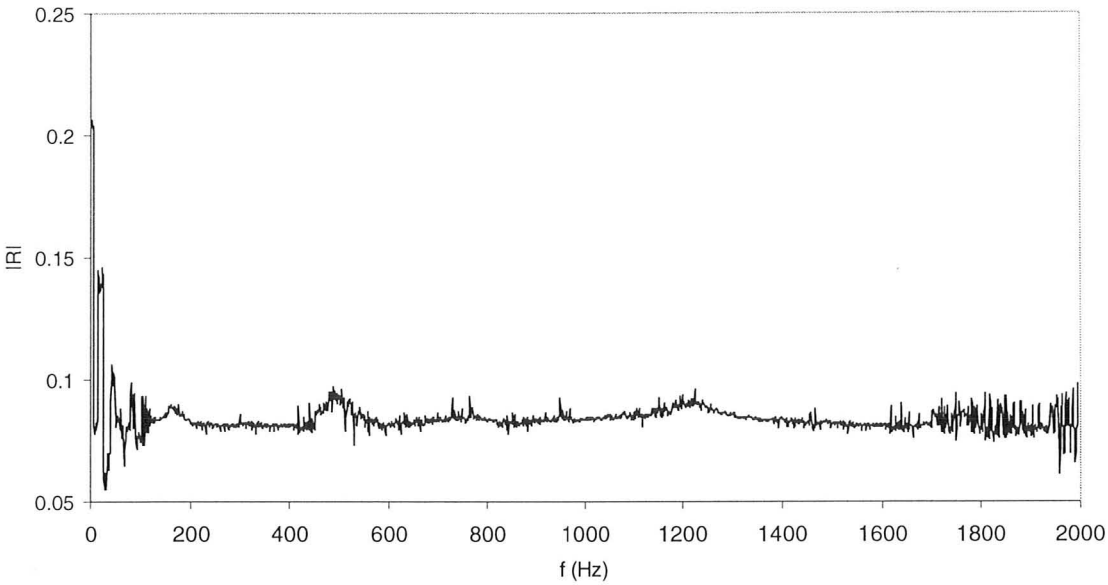

Figure 3.6: Reflection coefficient of the test setup wih anechoic termination

been verified. Next step is to find the value of the refection coefficient of the complete test setup; i.e., including the anechoic termination. To do this, the anechoic termination was used and the tests were repeated. Figure 3.6 shows the result for this case. At low frequencies, some instability is observed, but it diminishes above f = 100 Hz. Again, large errors occur for frequencies close to cut-off. This figure shows that the average pressure reflection coefficient for the present test setup is between 0.08 and 0.09, which is very close to the result of Neise (1975) for a test setup containing an anechoic termination. The only remained concern is while the interested range of frequency is usually up to 10 kHz, how this setup can be useful as its cut-off frequency is about 2 kHz. First of all, it should be mentioned that for the small forward-curved blowers and

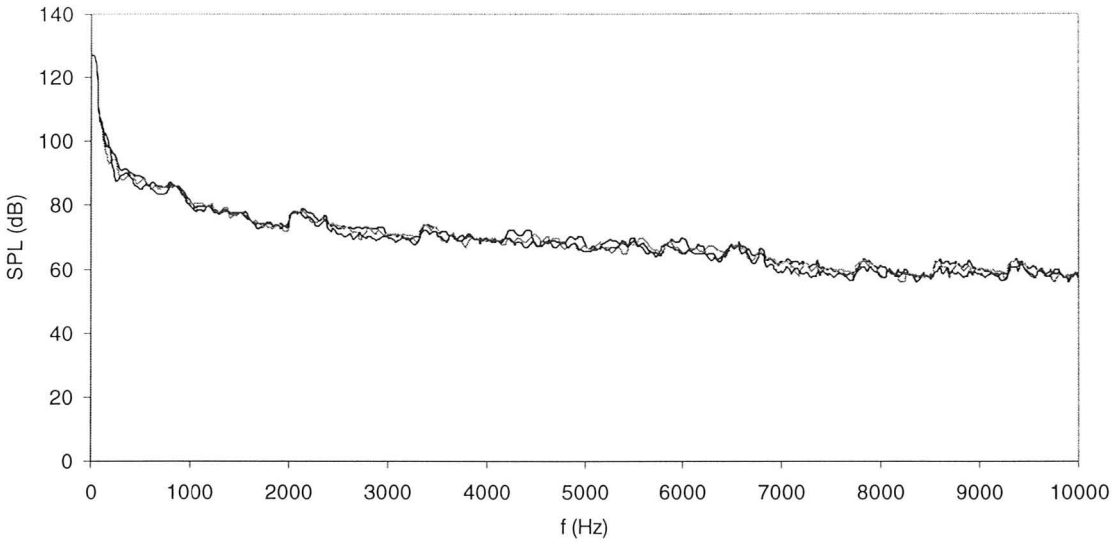

Figure 3.7: Measured sound pressure levels of microphone 1, 2 and 3

automotive air conditioning systems, the most critical frequency range is approximately from zero to 2000 Hz, which is covered by the present setup. However, in order to observe what happens after 2000 Hz, the data measured from each microphone are shown in Figure 3.7 for the range of zero to 10 kHz. It is clear that all of the three curves are pretty much close to each other, which is due to the effect of the anechoic termination. Therefore, all of the graphs that will be demonstrated in the next chapter, for range of frequency between zero and 2 kHz, three-microphone method has been employed, and for 2 kHz to 10 kHz, the average of the data measured by the three microphones has been used.

Chapter 4

Results and Discussion

4.1 Introduction

This chapter deals with the results of all the measurements for front and rear air conditioning systems and their fan sections alone. The spectra of the sound levels of each duct, in the standard and re-circulation modes will be shown and discussed. Then, with cancellation of the effect of flow-noise, an effort is made to pinpoint the relative importance of noise sources; i.e., fan noise and flow noise. In order to complete the discussion, noise tests inside the car are then compared with the laboratory data.

4.2 Front HVAC System

To determine the sound levels of the front air conditioning system, each of its three main ducts was separately connected to the inlet of the test apparatus. The tests were done at maximum working load; i.e., 12 DC volts. Figures 4.1-4.3 show the results.

Each curve is given by a four-character abbreviation. The first and last characters are related to the ducts number 1 and 4 (left and right vents in Figure 3.1), respectively. The two middle characters are assigned for the middle ducts, i.e. ducts number 2&3. Numbers indicate which duct is attached for measurement and the letters "C" and "O" stand for two possible cases of either closed or open for each duct outlet, respectively. For example, "1OOC" means duct number 1 was attached to the test apparatus and being tested, duct number 4 was closed and ducts number 2&3 were open during this measurement. These figures show that the maximum sound level for each duct is produced when all the outlets of the other ducts are closed, and vise versa. One can figure out that this is due to the sound reflection from the closed vents. In fact, in both cases of open and closed vents, there are some reflected waves. These graphs indicate that the reflected waves generated at the passive termination of the open ducts are weaker than the waves bouncing back off the closed end ducts.

In each graph, there are two peaks at low frequencies. Comparing Figures 4.1 to 4.3 with Figure 4.4 clarifies that the first one is affected by the background noise that has a broad peak around f = 63 Hz. It is thought that the second peak demonstrates the air rush noise that high turbulent and separated flows cause in the scroll and at the blower discharge area. This will be explained in the section 4.4. Narrow band sound level spectra are shown in Figure 4.5.

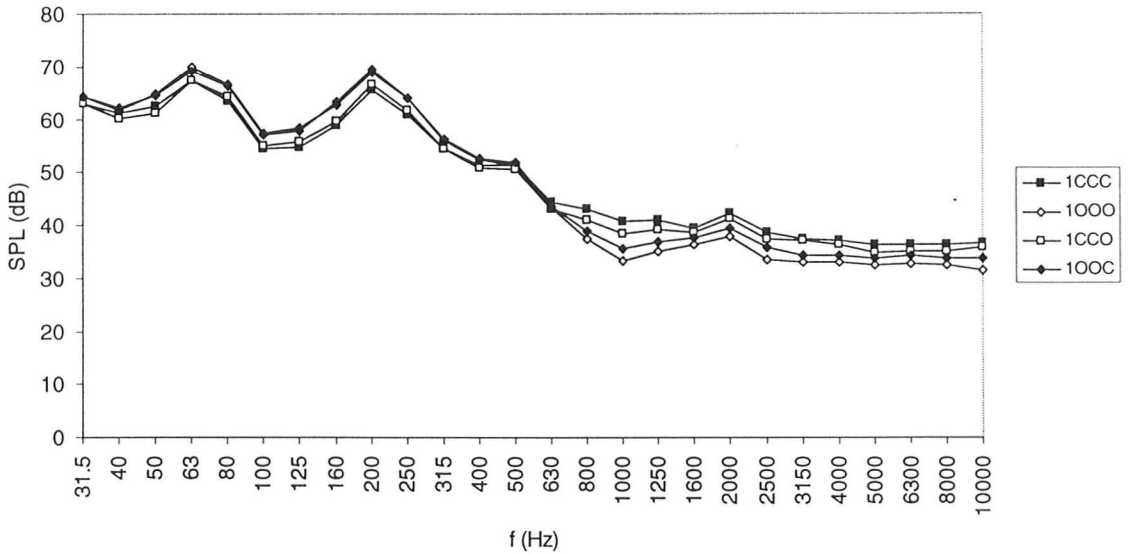

Figure 4.1: Sound levels of duct no.1

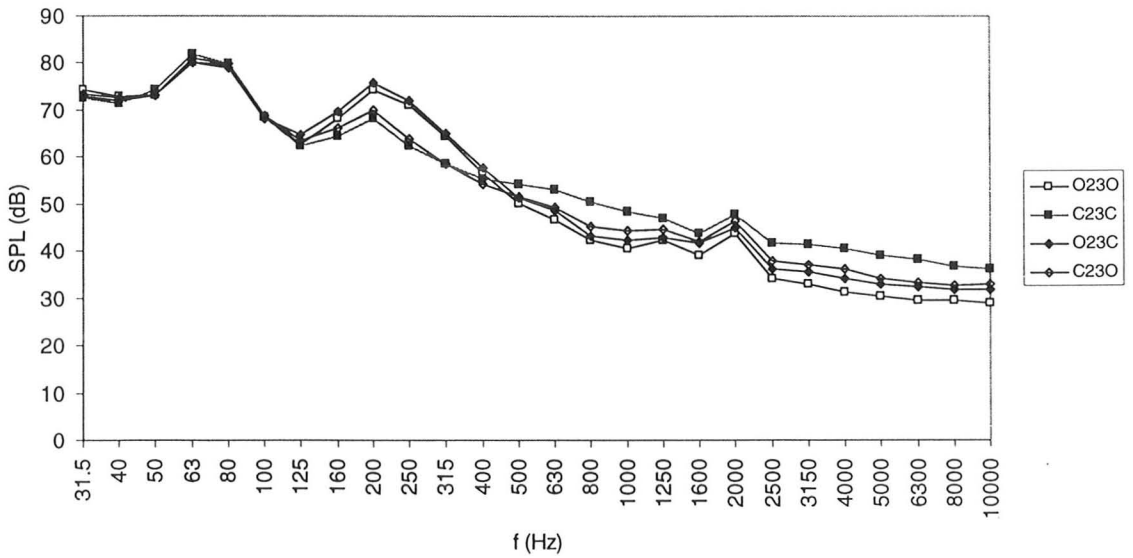

Figure 4.2: Sound levels of ducts no.2&3

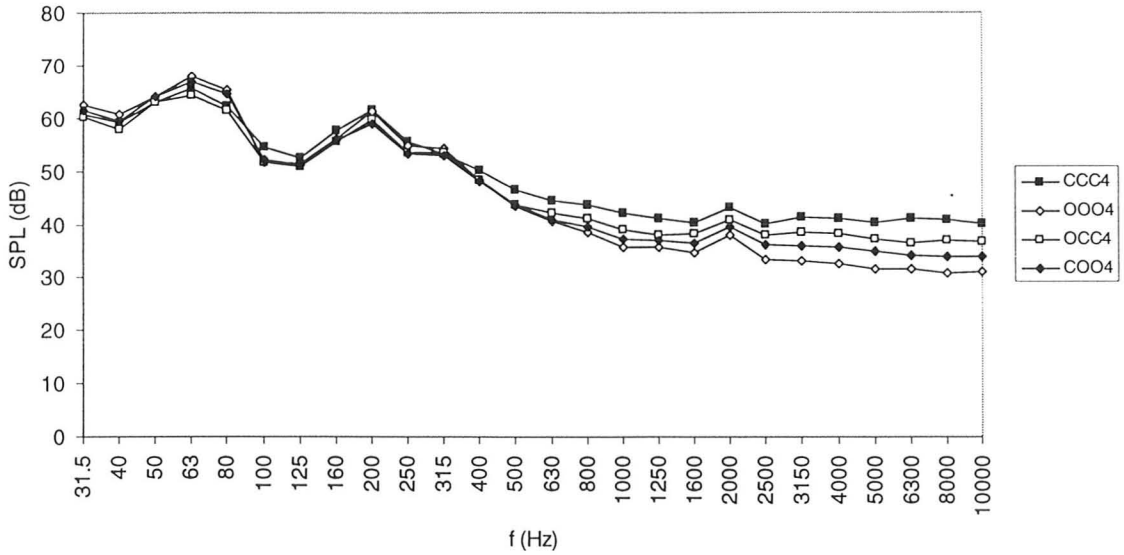

Figure 4.3: Sound levels of duct no.4

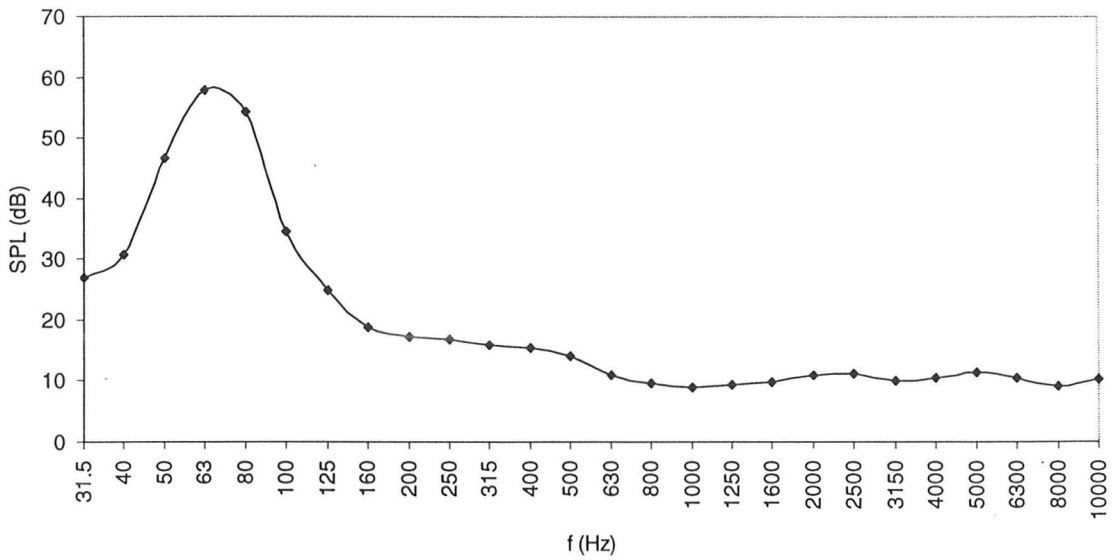

Figure 4.4: Background noise level

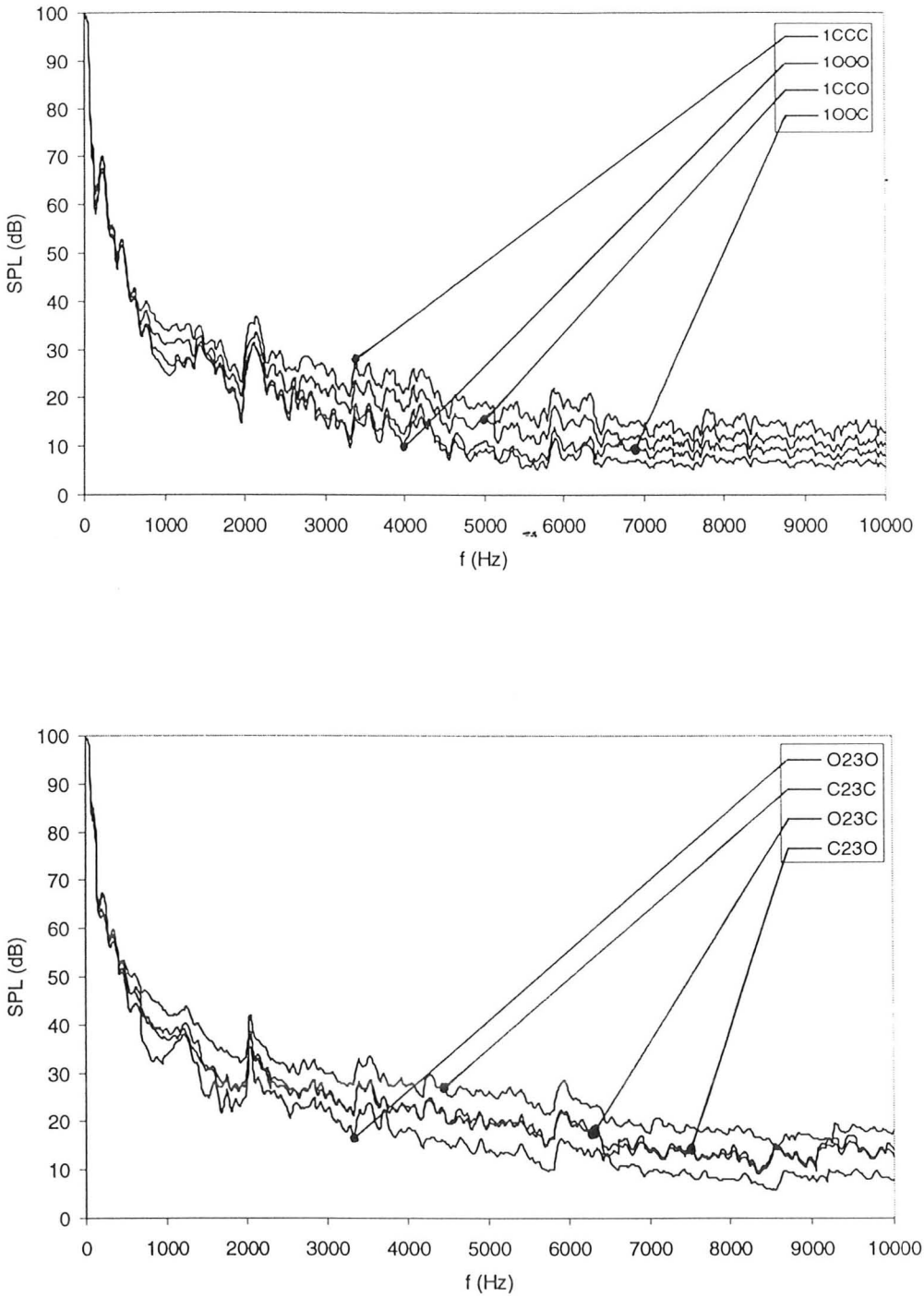

Figure 4.5: Narrow-band sound level spectra for duct number 1, 2&3 and 4

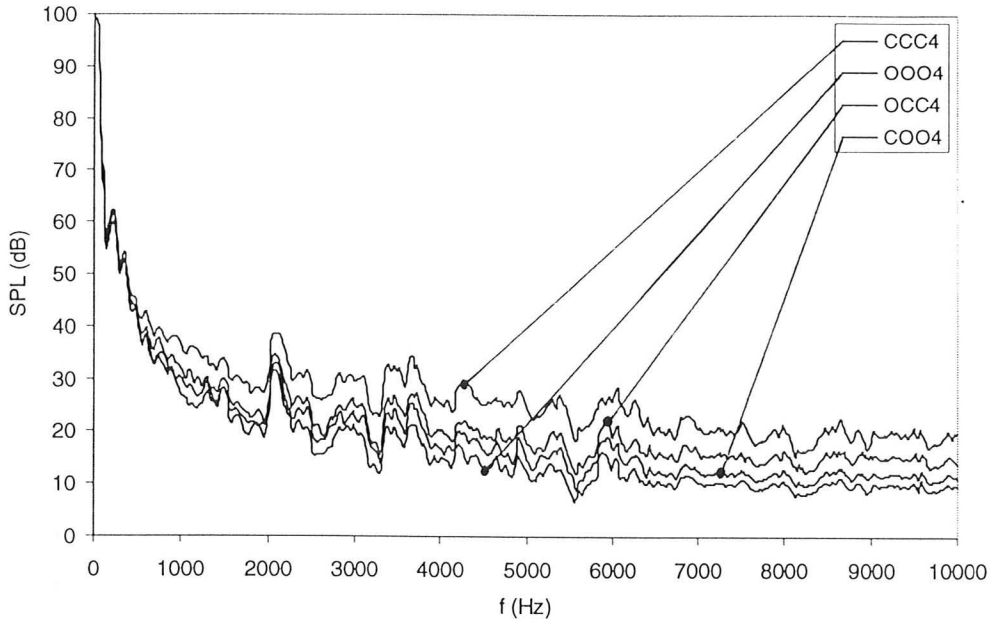

Figure 4.5(Cont'd.): Narrow-band sound level spectra for duct number 1, 2&3 and 4

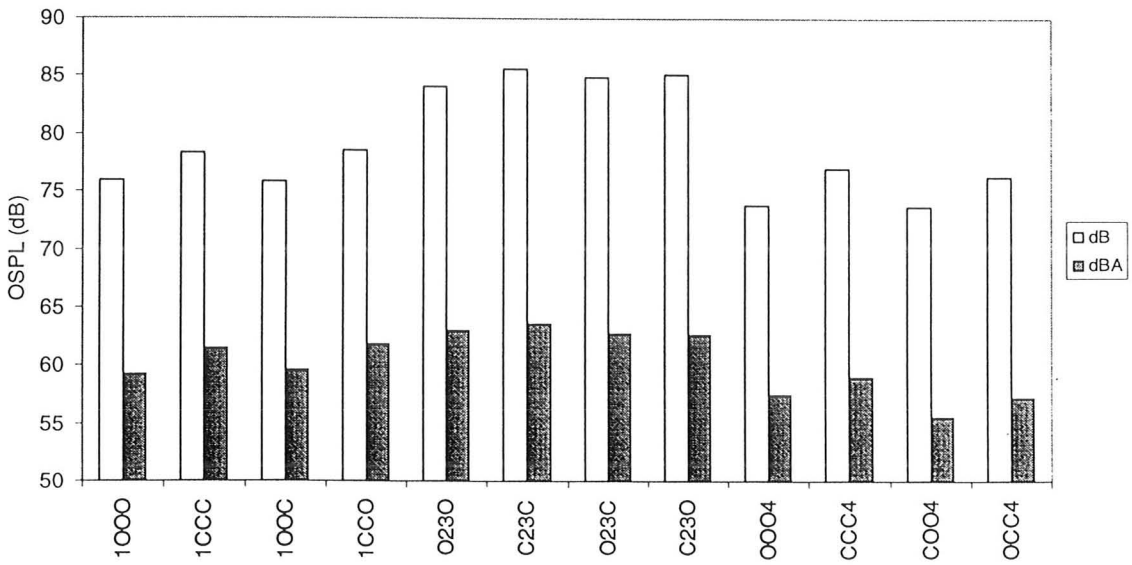

Figure 4.6: Overall sound levels of ducts in different cases

Here, the peaks at the blade pass frequency (BPF) around f = 2000 Hz are observed better than in the one-third octave band spectra. For the frequencies beyond BPF, no important peak or sudden change is seen in the spectra. Since the ducts 2&3 deliver the greatest amount of air from the system, it seems that the noise radiated by each duct is related to the velocity of the airflow passing through. This point is confirmed by the result of the overall sound level shown in Figure 4.6. This figure reflects the fact that ducts number 1 and 4 produces almost same total noise levels and the maximum level belongs to the case that all vents are closed.

In order to investigate the effect of the louvers on the noise levels, all of the above experiments were repeated without any louvers. Louvers that are extensively used in automotive air conditioning systems can be describe as a cascade of small narrow thin plates. Passengers can simply change the angle of attack of the louvers by hand; however, all of the plates of a louver operate at a common angle of attack in every situation. Steady and unsteady inflows passing over these small plates result in different noise generation mechanisms. The following parameters have essential roles to determine the possible mechanism:

1. The nature of the flow; attached or separated, and laminar or turbulent (angle of attack can change the character)
2. The size and geometry of the two ends of the plates
3. Plates spacing

In low speed and incompressible flows, the quadrupole radiation due to turbulence in the wake, boundary layer or even inlet flow is negligible, as discussed by Howe (1978) and

Blake (1986). However, Willmarth (1975) showed that interaction of turbulence with each of the two ends on the plates creates dipole radiation as a result of scattering of the non-acoustic wave number components of turbulent pressure fluctuations. Generally, most of the noise is produced where the flow leaves the plate and has a tonal nature due to the instability in the periodic wake vorticity. This has been explained theoretically by Howe (1976, 1999 and 2000). This is usually important when the wavelength of the turbulent eddies is larger than the plate thickness at the trailing edge. Since the violence of the unsteady motion at the trailing edge is alleviated by vortex shedding into the wake, particularly at high frequencies, as shown by Beranek (1992), the mechanism of noise generation is weaker at leading edge. In present study, results are based on zero angle of attack; hence, there is no locally separated flow on the plates. It is expected that at non-

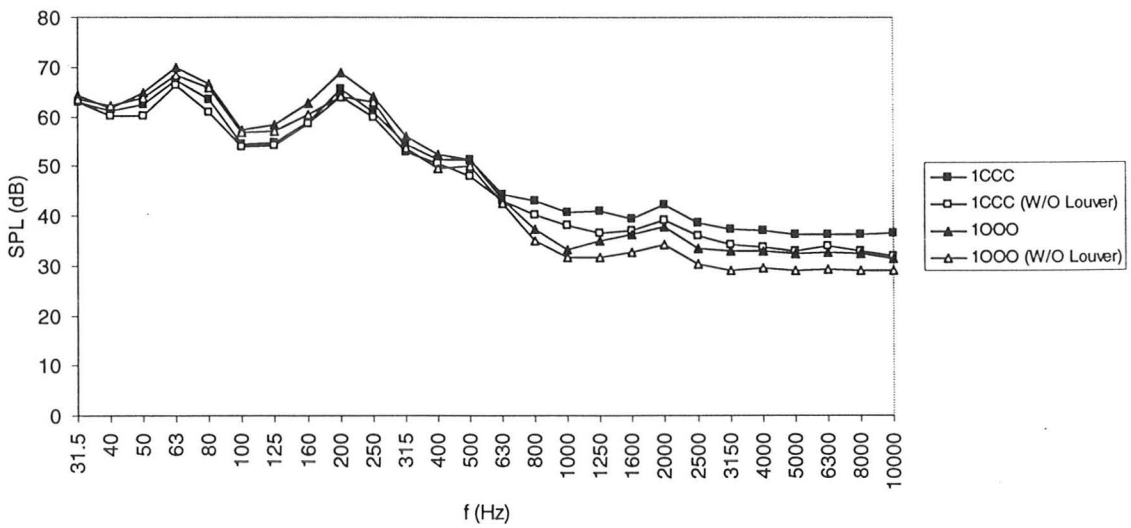

Figure 4.7: Sound level of duct no. 1 – with & without louver

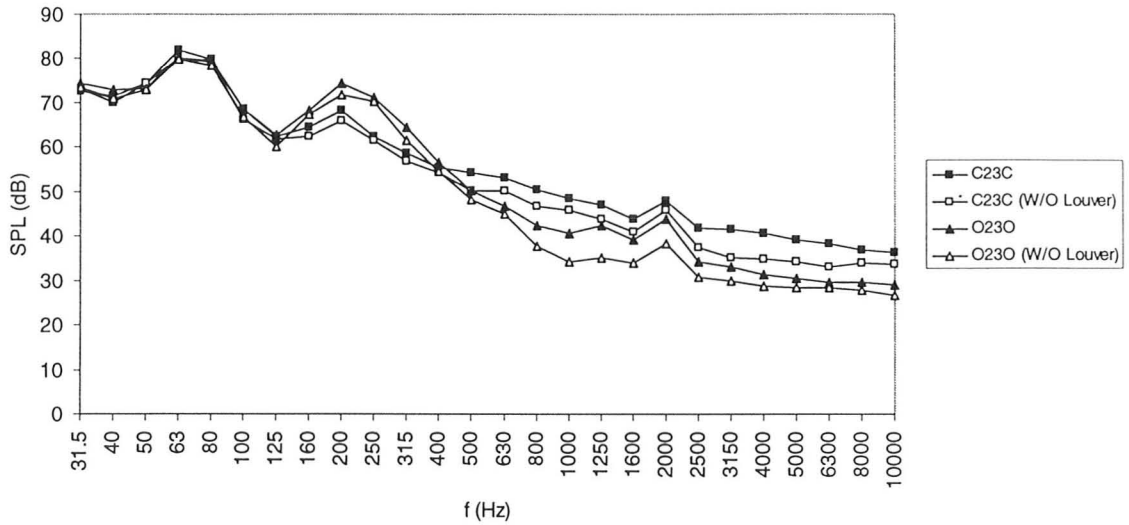

Figure 4.8: Sound level of ducts no. 2&3 – with & without louver

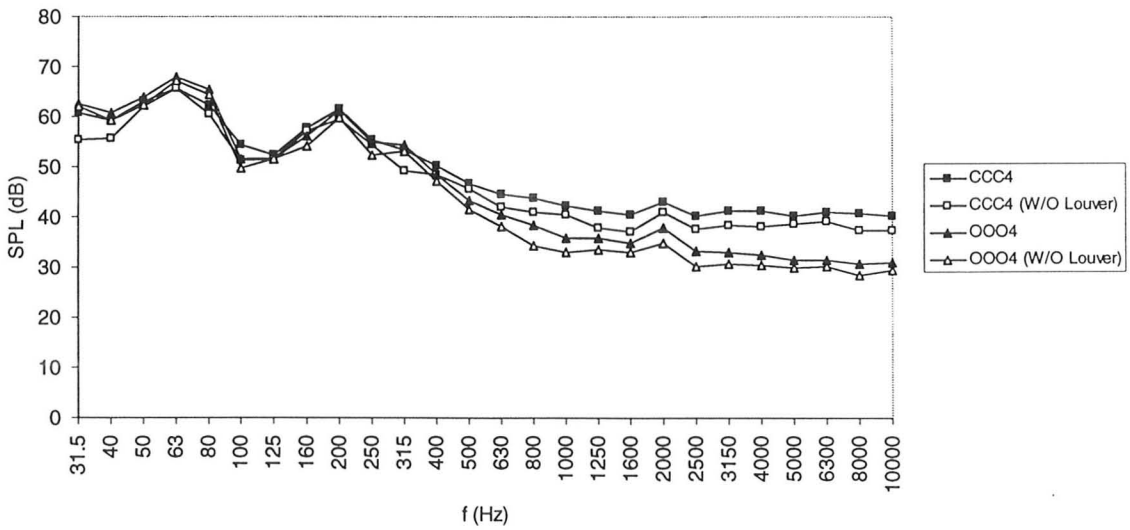

Figure 4.9: Sound level of duct no. 4 – with & without louver

zero angles of attack, noise level shows a broadband character. Figures 4.7-4.9 demonstrate and compare the sound levels of each duct for both cases with and without the louvers. When the louvers were removed, the noise levels decreased. This can be clearly observed in Figure 4.10, which shows overall sound levels for different cases. Another interesting feature about these figures is the crossing of the curves corresponding to the closed and open cases at a frequency near 500 Hz which corresponds to a Strouhal number about 0.1, calculated based on plates thickness. Physical description of this phenomenon is not straightforward, as it is related to the interaction of acoustic waves and non-acoustic pressure fluctuation waves. However, it is thought that for the range of frequency above Strouhal number 0.1, since the other vents are closed, there is more flow rate; hence, the effect of the noise generated by shedding vortices becomes more strong. In addition, the difference between the reflection coefficients in the case of open and closed vents can be another reason for this phenomenon. In the case that the vents are closed, almost 100 percent of the waves are bounced back towards the open vent. When the vents are open, since the reflection coefficient of each of open vent decreases with frequency, the total reflected waves will be less than the closed end case. This seems reasonable because in Figures 4.7-4.9 the difference between open and closed cases increases with frequency which is in good agreement with the trend of decreasing the reflection coefficient with frequency for open end ducts. Therefore, in the case of closed ends, combination of both flow-noise and reflected sound should be considered.

The last important point about front air conditioning system is the case of recirculation mode. In this case, the noise issued from the inlet side of the front fan

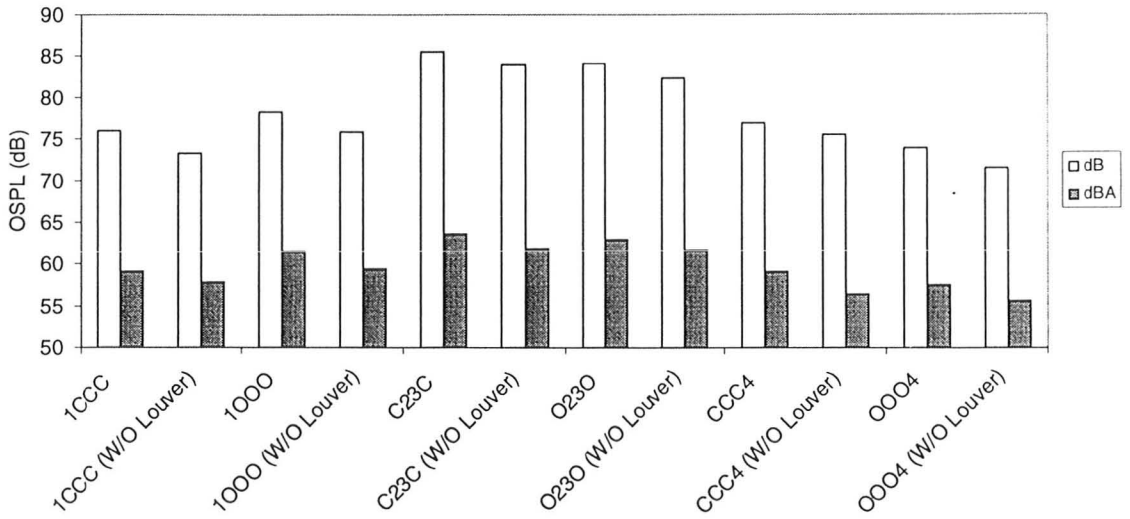

Figure 4.10: Overall sound levels of ducts in different cases – with and without louver

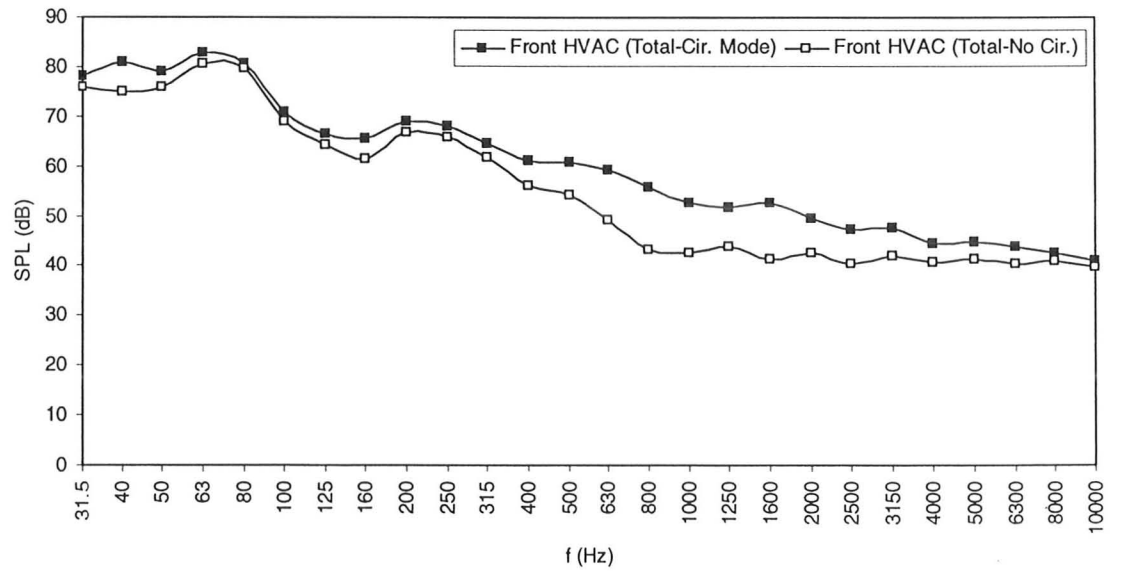

Figure 4.11: Total sound level of front HVAC system

should be taken into account to determine the total noise that can be heard inside the automobile. The measurement of inlet side noise of the front fan will be explained in section 4.4. Therefore, if one adds all the noise levels radiated from ducts number 1, 2&3, 4 and inlet side of the front fan, it will result in the total sound pressure level, shown in Figure 4.11 for the case of recirculation mode. It explicitly shows how much the noise level inside the automobile is affected by the fan inlet side, especially at high frequencies. There will be a comparison between the total noise of the front and rear air conditioning systems in the next section.

4.3 Rear HVAC System

The sound level of the rear air conditioning system was examined in a similar way to the front system, and at the same condition of the motor speed. Figures 4.12 and 4.13 show the results for both cases; i.e., with and without the louver. In both graphs, BPF peaks are clearly observed at f = 2200 Hz. These peaks probably include the cross modes. The trends of the graphs are comparable with the front system. The rear system louver generates more noise, especially above f = 500 Hz. It is really impossible to put the rear louver system into any recognized category of the known louvers. In fact, it should not be called louver, but a curved perforated plate including ten large holes, as shown in Figure 4.14. Hence, its function is similar to a hand guard and it does not provide any directional control of the exit airflow. The blocking areas of this louver can be considered as bluff bodies. Terao and Shoda (1975) studied the sound generated by simple bluff bodies using

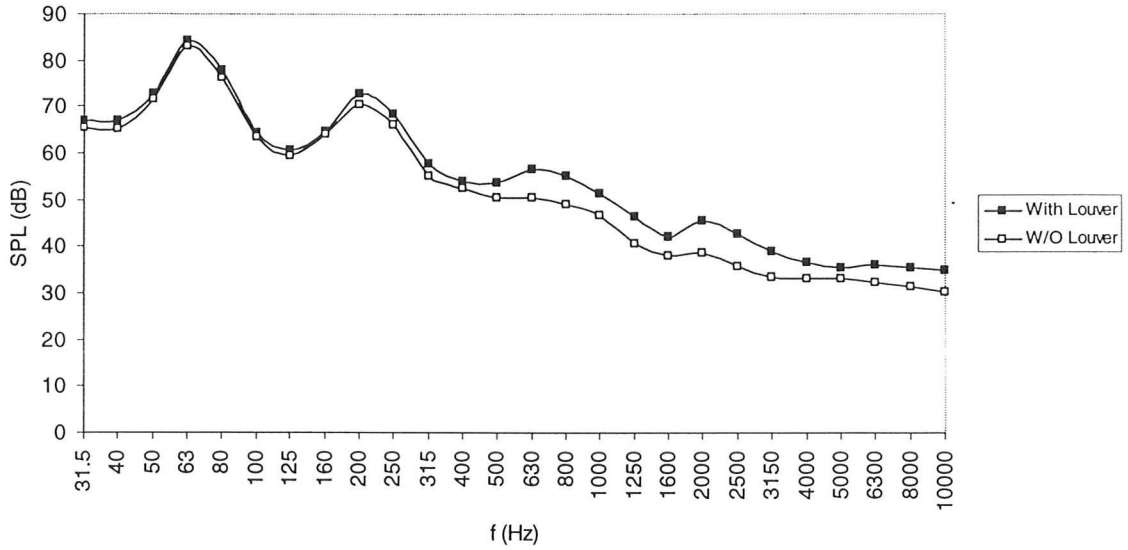

Figure 4.12: Sound level of the rear HVAC duct – with & without louver

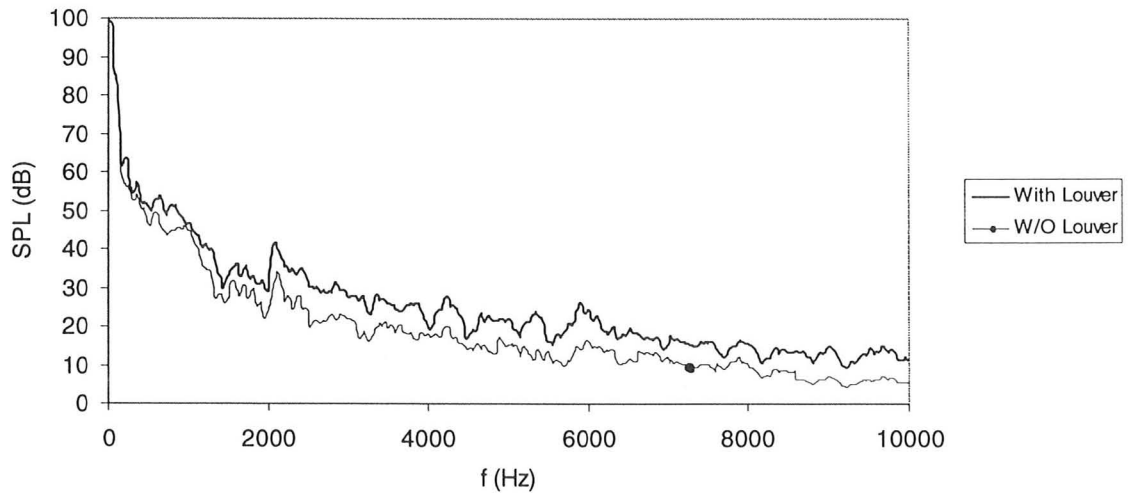

Figure 4.13: Sound level spectra for rear HVAC duct – with & without louver

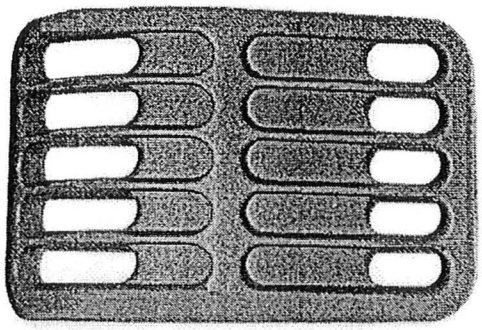

Figure 4.14: Louver of the rear HVAC system

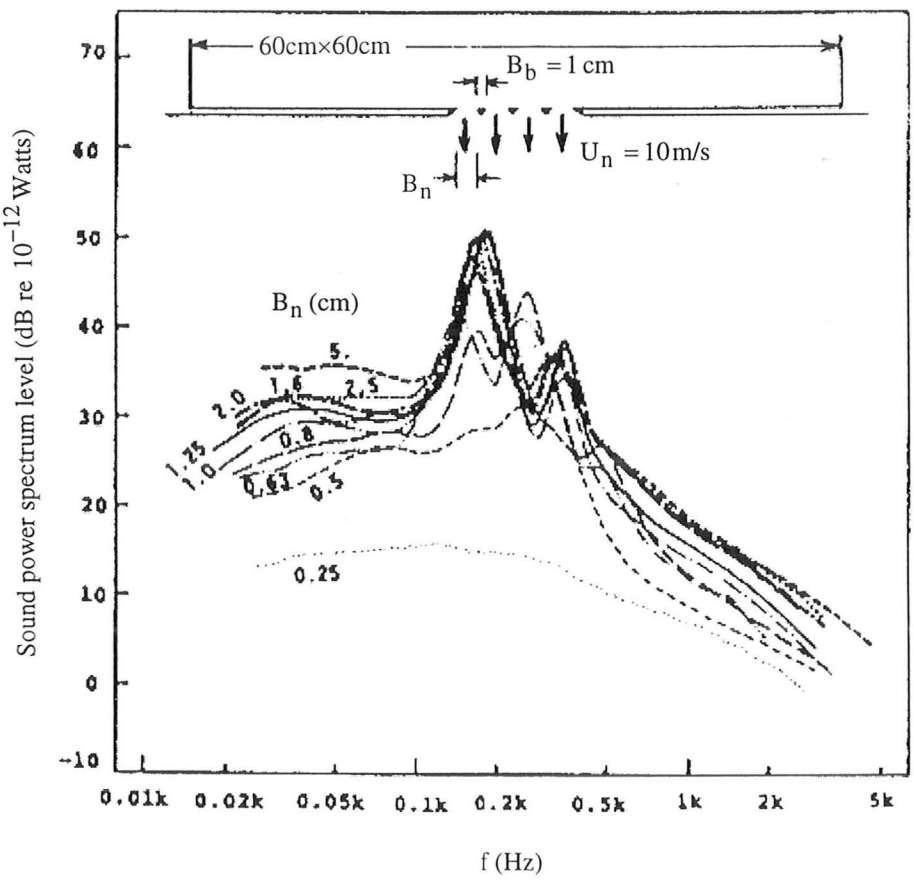

Figure 4.15: Bluff body spectra, Terao and Shoda (1975)

a reverberation room. The configuration of their tested bluff bodies was like a perforated flat plate. The dimensions of the holes and bluff bodies were adjustable. For the case of one hole, their results showed that wider hole produces more noise but at lower frequency. Figure 4.15 is one of their results that is very helpful for the present study. B_n and B_b are the width of the holes and the bluff bodies, respectively. For $B_n \geq 0.5B_b$ a discrete tone is produced associated with a higher harmonic tone. In the range $B_n < 0.5B_b$, the discrete tone disappears and instead a wide spread sound is generated that results in lower noise level. They suggested that the exponent of velocity dependence for each system of bluff bodies is constant over all values of Strouhal numbers and is equal to 5.0. The results of this systematic study can be used to optimize the size of the holes for the louver used in the present rear HVAC system.

It should be mentioned that both inlet and outlet sections of the rear air conditioning system are inside the cabin of the automobile; i.e., the inlet flow is not fresh air. Therefore, to understand how much noise the rear system produces, the effect of inlet side of the rear fan should be considered. The results of the rear fan inlet side is described in section 4.4. Figure 4.16 shows the total noise level of the rear air conditioning system at full speed of the rear fan. As it is obviously seen, inlet side has a significant effect on the total sound level of the rear system.

Now it is appropriate to compare the noise levels of the front and rear air conditioning systems. Figures 4.17 shows the total levels of both systems. In most of the frequency range, the rear system shows more generated noise level. Within the air rush

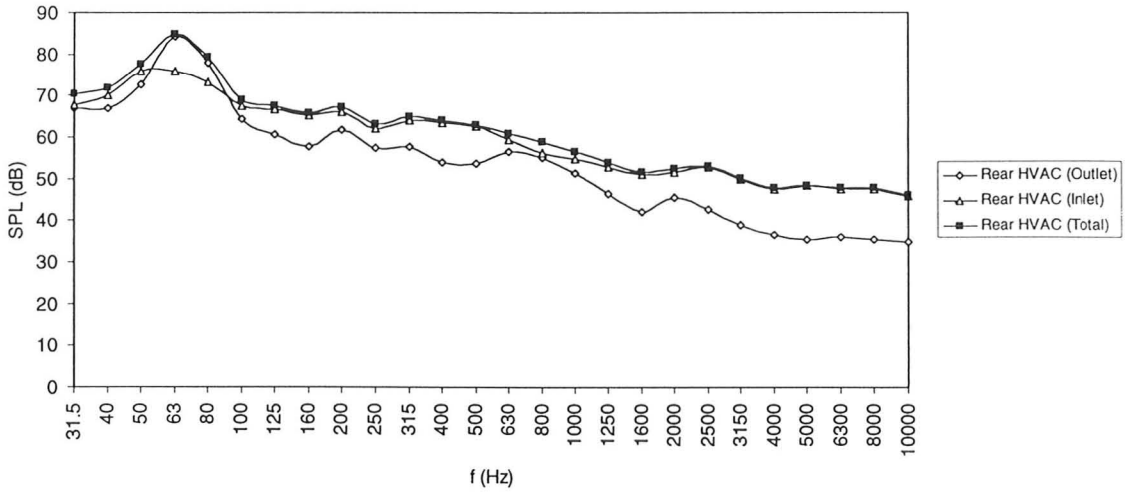

Figure 4.16: Sound levels of the rear HVAC system (Inlet, Outlet and Total)

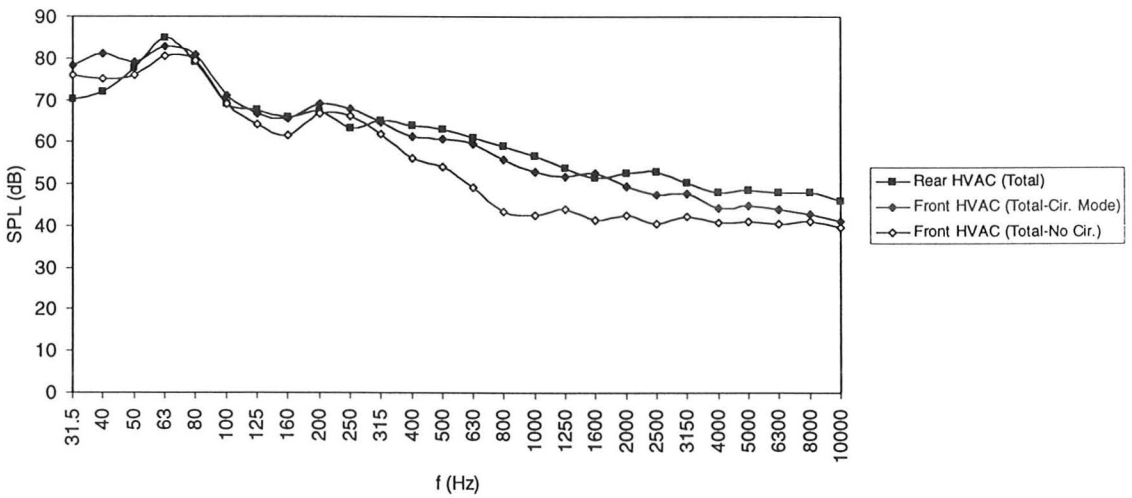

Figure 4.17: Comparison between front and rear HAVC systems noise spectra

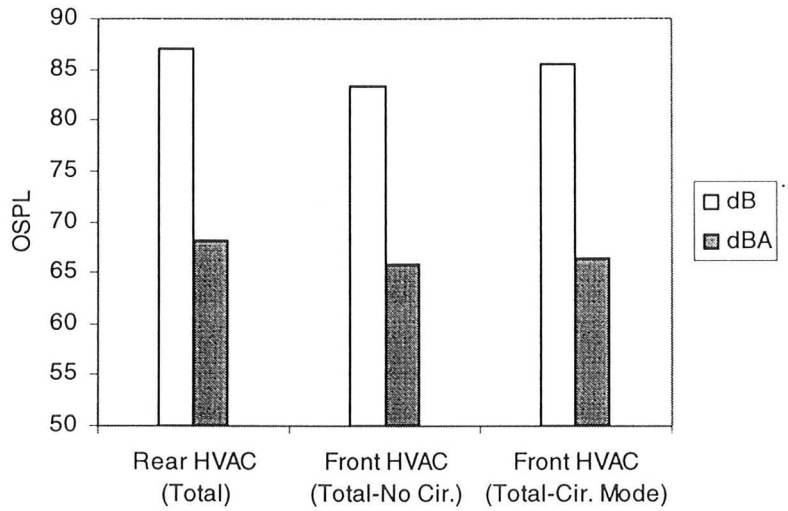

Figure 4.18: Comparison between the overall sound levels of the front and rear HAVC systems

noise frequency range; i.e., f = 150-350 Hz, they have almost same peak value, and thereafter, the rear system produces higher noise level over the rest of the frequency range. Figure 4.18 displays the overall sound level for both systems. It confirms previous conclusions about the rear system.

4.4 Front HVAC System Fan

Front air conditioning system fan, which will be referred to hereafter as the front fan, was attached to the test setup to find detailed data about its noise characteristics. The test was made at different fan speeds. Figures 4.19 and 4.20 show the spectra. The speed RPM = 3000 corresponds to 12 DC volts. Since the impeller has 44 blades, as shown in Figure 4.21, the BPF is 2200 Hz. As the speed decreases from full speed, BPF shifts to

lower frequencies and the sound level decreases. The narrowband spectra clearly show the blade pass frequencies and their corresponding amplitudes. Large fans can generate higher noise levels. Tone production is due to the interaction of the airflow leaving the impeller blade and the scroll, particularly at the cutoff region. In fact, the flow that is coming out of impeller blades is strongly non-uniform and causes severe pressure fluctuations at the cutoff region. This, in turn, generates sound at the blade pass frequency. Increasing the distance between impeller tip and cutoff seems to be a very good method to reduce the noise that will be discussed in the next chapter. Regarding the output sound of the fans, Morfey (1973) says: "*Because centrifugal ventilating fans typically operate at low Mach numbers and with partially stalled flow in the impeller, most of the sound that they generate is at the frequencies where the wavelength is larger than the impeller diameter.*" This is consistent with the present result. Here, the impeller

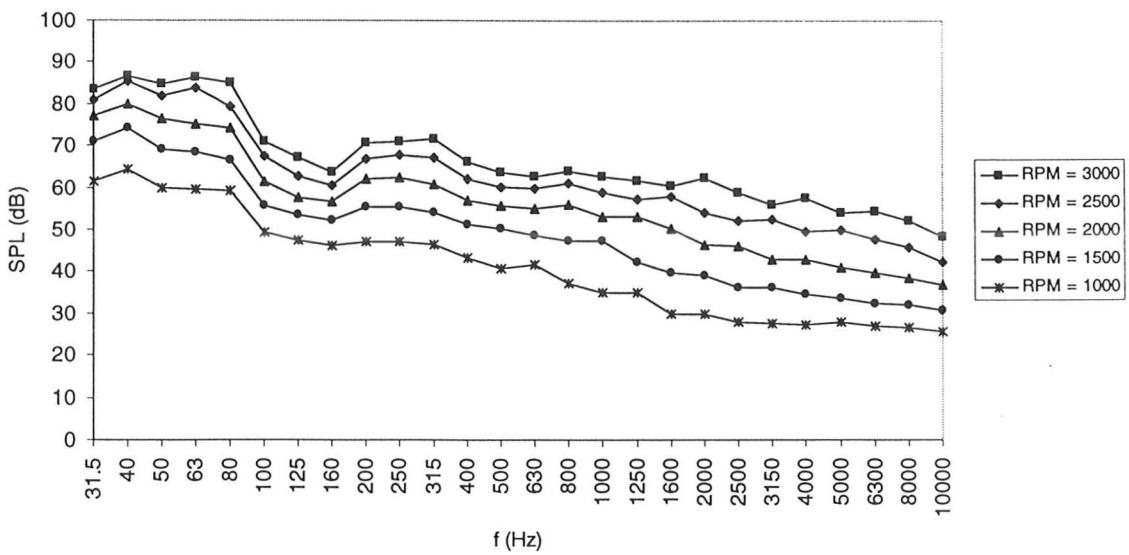

Figure 4.19: One-third octave band spectrum of front fan at different impeller speeds

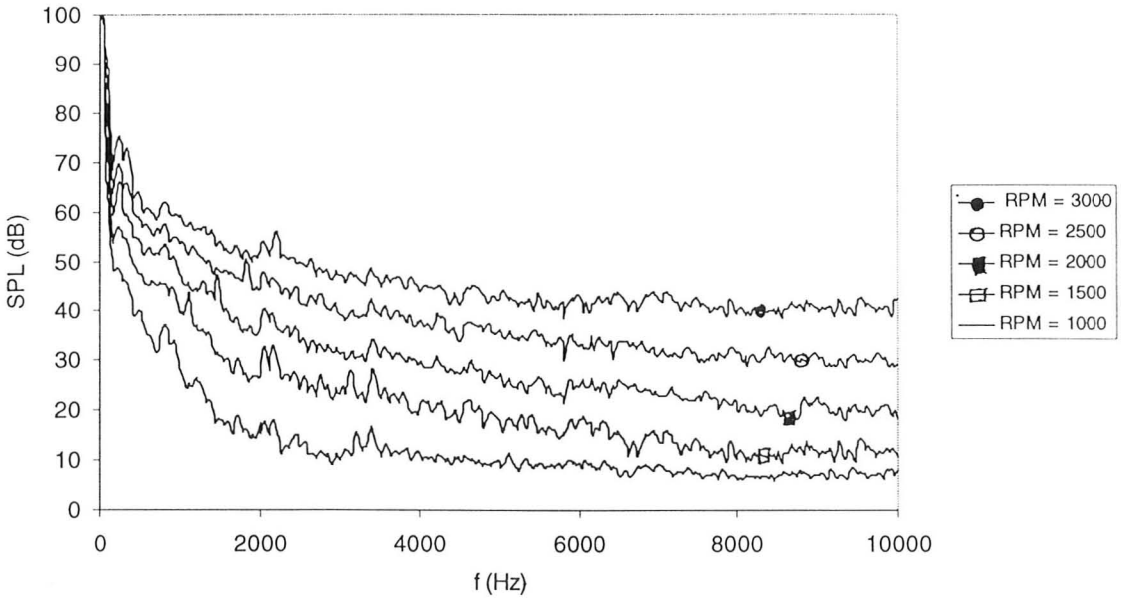

Figure 4.20: Narrowband spectrum of front fan at different impeller speeds

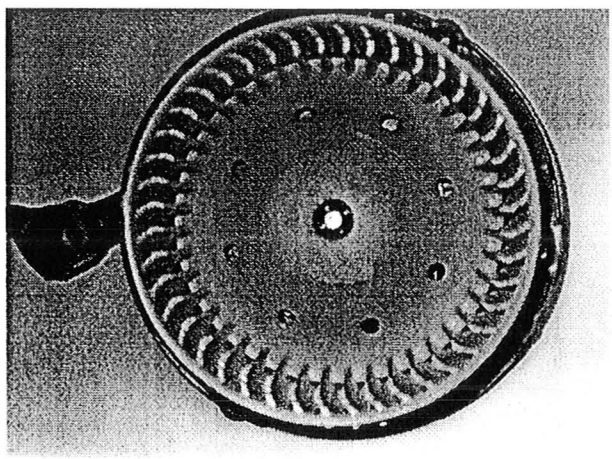

Figure 4.21: Impeller of the fans of the HVAC systems

diameter is 0.15 m, and it is observed that most of important variations, fluctuations and noise production happen below f = 2300 Hz; especially, above f = 4000 Hz, there is no tone or sharp peak and the spectra level becomes nearly constant or decreased. The second peak in Figure 4.19, which usually occurs at the frequency range between 150 Hz to 350 Hz, is related to the air rush noise or rumble noise. Air rush noise is caused by turbulent flow acting on the inside solid surfaces in the space between impeller and scroll, turbulence to turbulence interaction between the flows inside the blades and the circulating flow outside the impeller, and shedding vortices from impeller blades. Besides, the effects of separated flows on the blades and high level of turbulence in the recirculation of the inlet should be added. The first peak that occurs around 50-60 Hz is just due to background noise and some initial frequency instability. The sound level is plotted versus Strouhal number in Figure 4.22, which shows the same spectra but plotted versus the Strouhal number defined by $St.=(f.d/V)(\pi/Z)$ in which Z, V and d are the number of blades, tip impeller velocity and impeller diameter, respectively. In this presentation of Strouhal number, the blade passing frequency should lie at $St.=1$, and the first peak at $St.=2$. This can be seen in the figure. In order to determine the total sound generated by the fan and HVAC systems, it is required to determine the noise level generated by the inlet side of the fan. To do so, the inlet side of the fan section was attached to the setup and the previous measurements were repeated. Figures 4.23 and 4.24 show the results at different speeds of impeller. As it was expected, the trend of the graphs are similar to that of outlet side except that the levels are lower, which means inlet side makes less noise. Figure 4.25 is the total noise produced by front fan at full speed. It

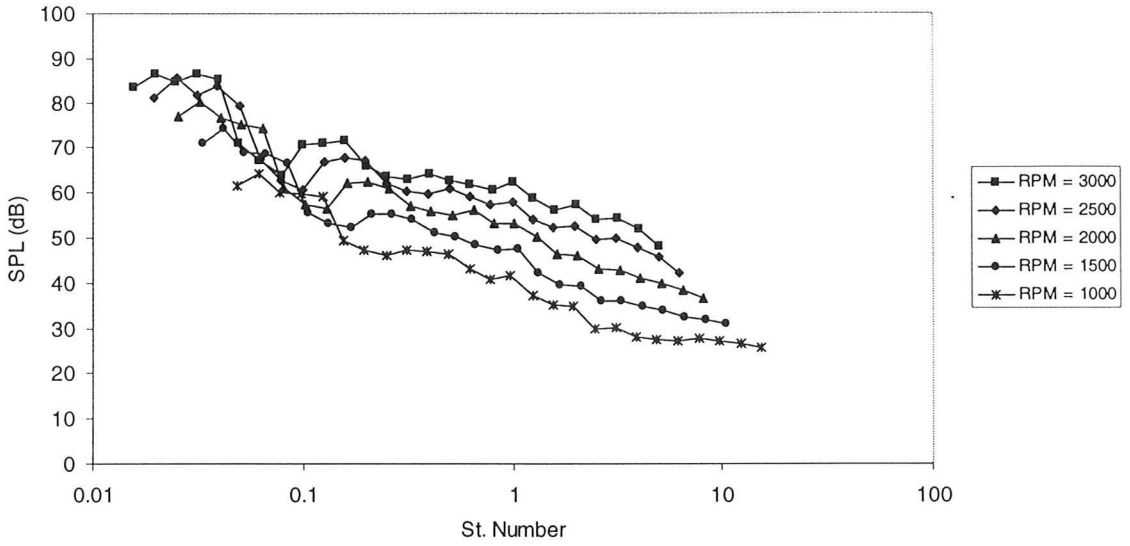

Figure 4.22: Sound pressure spectra of front fan vs. Strouhal number

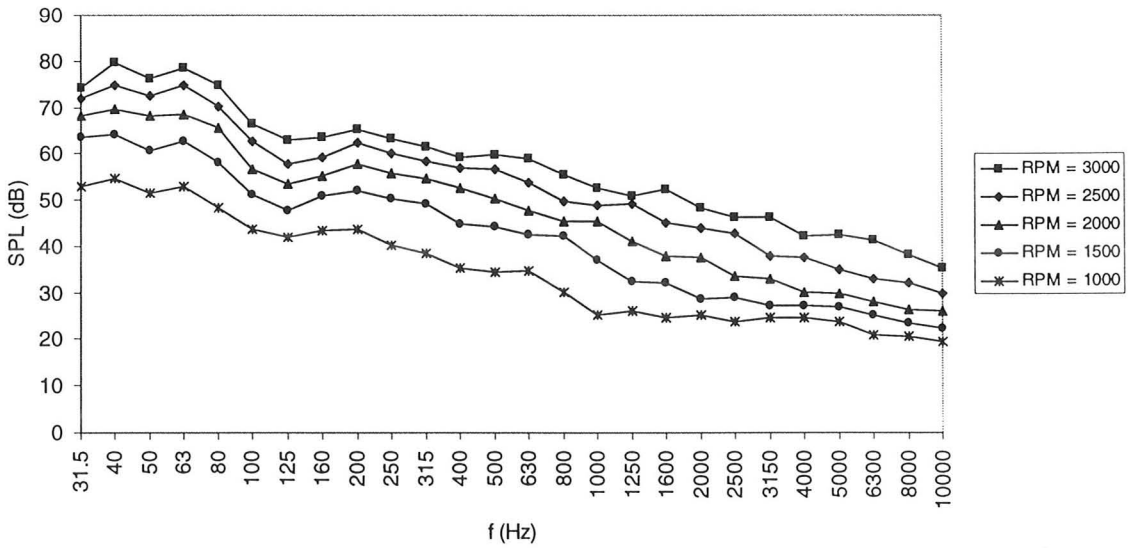

Figure 4.23: One-third octave band spectrum of front fan at different impeller speeds (inlet side)

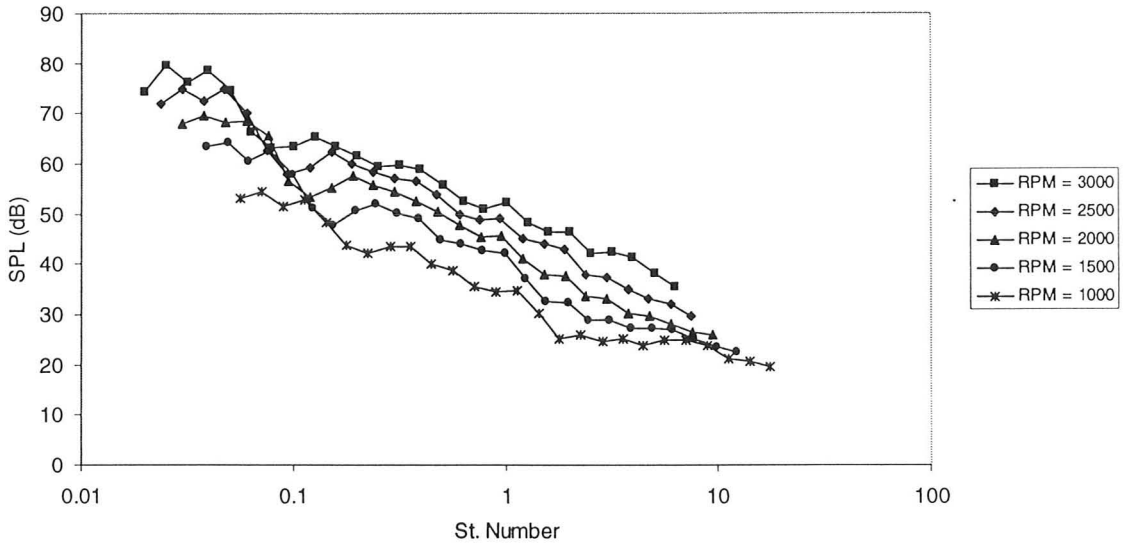

Figure 4.24: Sound pressure spectra of
front fan vs. Strouhal number (inlet side)

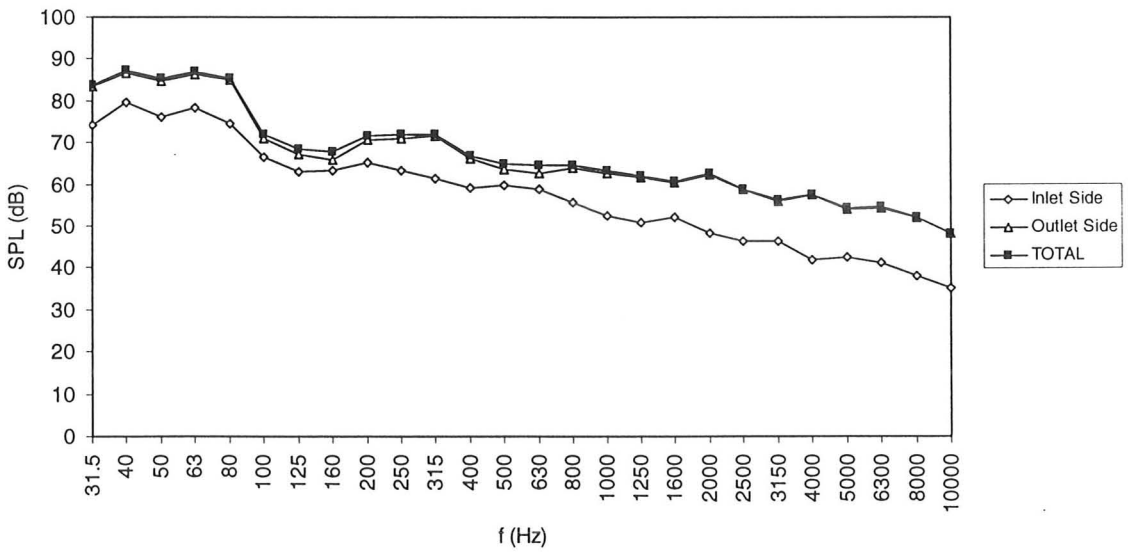

Figure 4.25: Total sound generated by front fan (inlet & outlet sides)

is obvious that the total and outlet noise levels are very close, and one might neglect the effect of inlet side. However, as it was observed, the inlet side has an important effect on total noise level of the whole air conditioning system. Overall sound levels of the inlet and outlet sides of the front fan are given in Table 4.1. Again, the difference between inlet and outlet noise is substantial, as seen in Figure 4.25.

Variation of sound levels in terms of tip speed of fan blades is another important item that most investigators check. According to the fan sound law, which was given by Jorgensen (1961), sound level is proportional to V^5 and is a linear function of $10\log V^5$, in which V is the tip speed of the impeller. However, this proportionality can not be applied for all kind of fans, especially small types, Maling (1963). This has also been suggested by two recent studies on automotive air conditioning system fan, Brungart *et al.* (1992), and Ishihara and George (1994). Although in both publications, the authors mentioned that the sound level of the fan is V^5- dependent, based on the figures shown, this is not accurate. The sound level in those articles are proportional to $V^{4.2}$ and $V^{4.6}$, respectively. This is the reason that Jorgensen (1999) in the new edition of his book indicates that tip speed exponent 5 may vary between 4 and 6; however, the linearity between sound level and log term is always kept. Thus, the sound radiation from

OSPL	dB	dBA
Inlet side	84.45	67.74
Outlet side	92.90	73.80
Total	93.08	74.14

Table 4.1: Overall sound level of the inlet and outlet sides of the front fan

fans is not exactly dependent on V^4, V^6 or V^8, and therefore it can be considered as a combination of monopoles, dipoles and quadrupoles distributions inside the fan. This might be the reason that Neise (1975) says: "*There seems no hope of finding a universal value for the tip speed exponent*".

Here, for the fan under consideration, Figure 4.26 shows the sound level variations with blade tip speed. The overall SPL varies linearly with $10\log V^{4.1}$. This figure also contains the graphs for sound level at different frequencies as a function of fan speed, which is proportional with $V^{5.8}$. These results indicate that the flow field is not governed by dipoles only. This is another evidence that flow-sound coupling inside

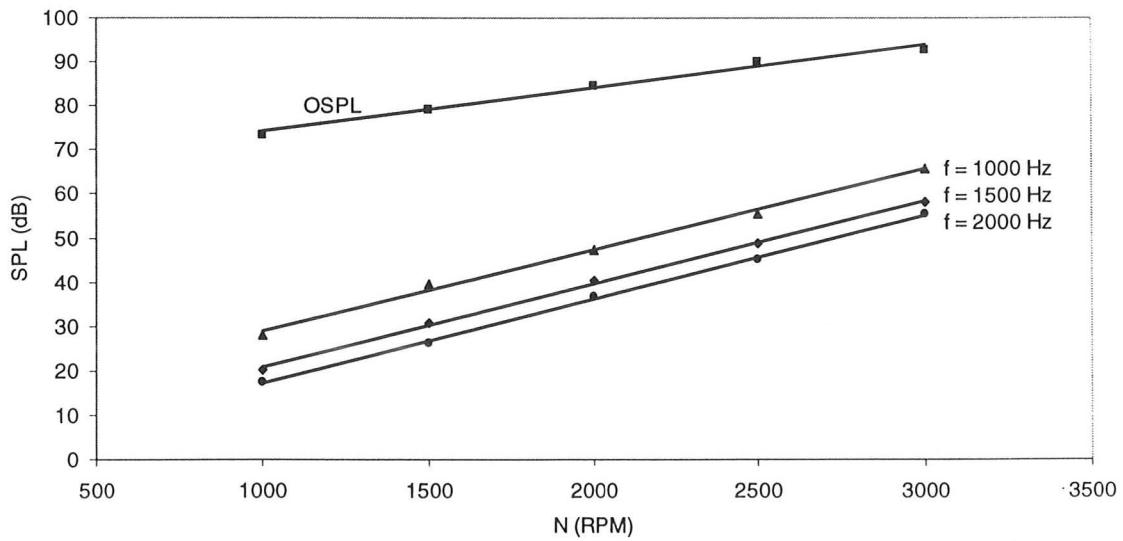

Figure 4.26: Sound level of front fan as a function of impeller tip speed

a centrifugal fan is too complicated to establish a general theory or a comprehensive rule of design and analysis.

4.5 Rear HVAC System Fan

Similar to the front fan, the rear fan was examined to clarify its sound characteristics. Most of the explanations about front fan in the privious section are true for rear fan. Rear air conditioning system fan has the same impeller geometry, but different DC motor, and more importantly, different scroll geometry. At 12 DC volts, the rear fan speed is about 3500 RPM and one would expect more tones. As said before, tones are generated due to the interaction of impeller outflow with the scroll surfaces, especially the cutoff. This mechanism is strongly dependent on the impeller, scroll and cutoff geometries. Since the geometry of the rear air conditioning system and its fan scroll is such that it is mounted on the rear wheel, inside the automobile, its geometry is so compact and is probably not well designed due to space considerations. This is the reason that stronger tones are produced, as shown in Figures 4.27 and 4.28.

The sound spectra versus Strouhal number is demonstrated in Figure 4.29. Again, because of the definition of the Strouhal number used in the previous section, the BPF and tones appears at integer values St.= 1, 2,... at all speeds.

Similar to outlet side, the suction side of the rear fan generates a larger number of tones, but the maximum peak has smaller value, as depicted in Figure 4.30. In the spectrum versus Strouhal number, tons are observed at integer values that are shown in

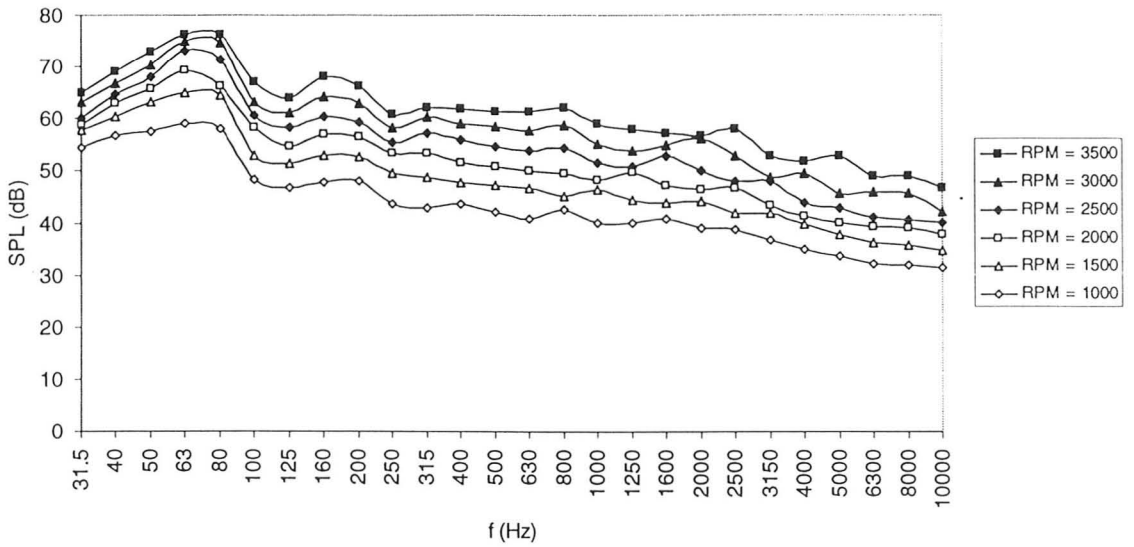

Figure 4.27: One-third octave band spectra of rear fan at different impeller speeds

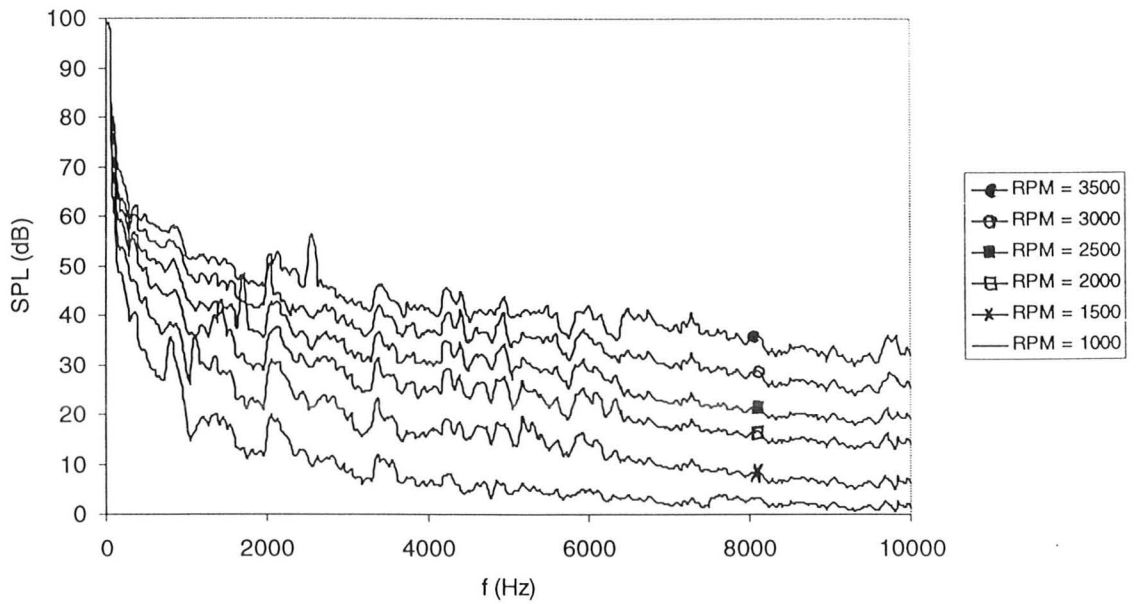

Figure 4.28: Narrowband spectra of rear fan at different impeller speeds

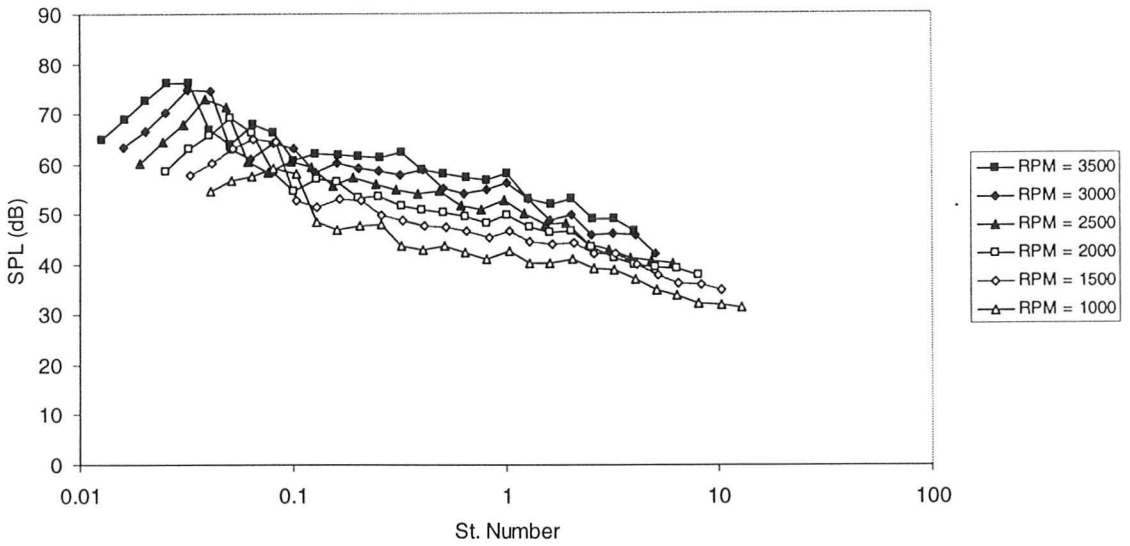

Figure 4.29: Sound pressure spectra of rear fan vs. Strouhal number

Figure 4.31. It should be remembered that the maximum level in these graphs are related to a tip velocity of 3500 RPM, while for front fan was 3000 RPM. That means higher velocity in rear fan does not produce more noise. The only reasonable explanation is the rear fan outflow is less turbulent than the flow leaving the front fan scroll.

The total noise generated by the automotive HVAC system fan can be achieved by adding the inlet and outlet side noise levels which is presented in Figure 4.32. In most of the frequency range, the noise level of outlet side is higher, especially within the frequency of air rush noise, but the difference between inlet and outlet sides for front fan was larger to some extend. Table 4.2 confirms this deduction. The overall sound difference between inflow and outflow is about 1 dB which is not comparable with 8 dB in front fan. The geometry of the casing is definitely the cause of this difference. Besides, in the inlet side of the rear fan there is no duct while an elbow-like box exists in the front

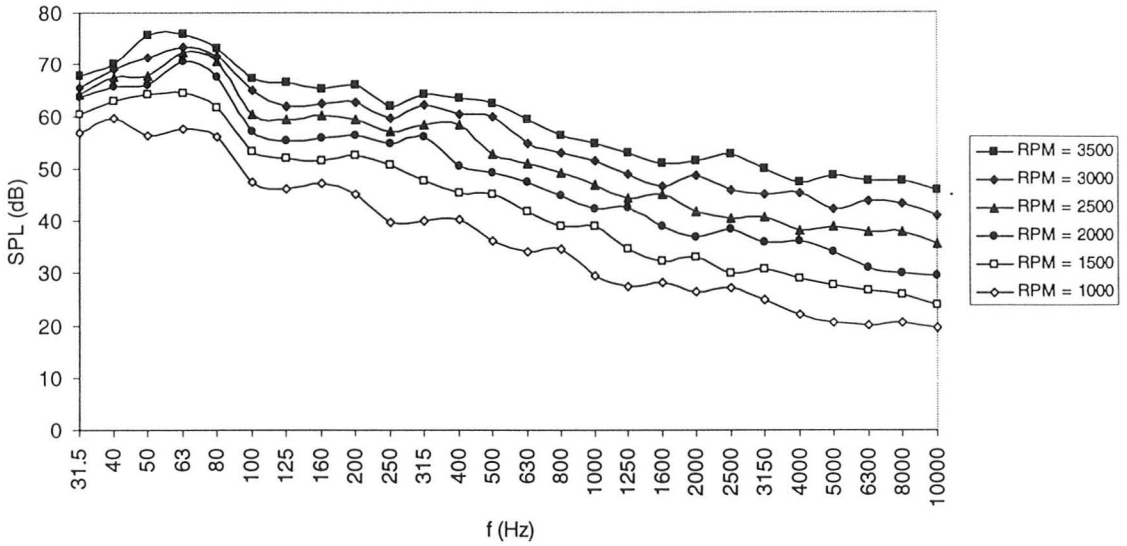

Figure 4.30: One-third octave band spectra of rear fan at different impeller speeds (inlet side)

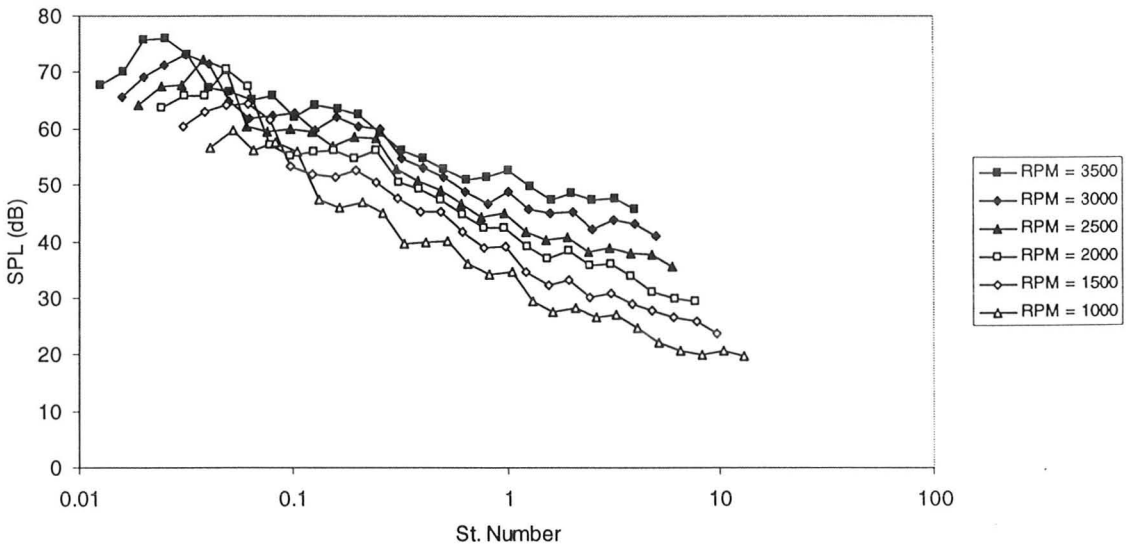

Figure 4.31: Sound pressure spectra of rear fan vs. Strouhal number (inlet side)

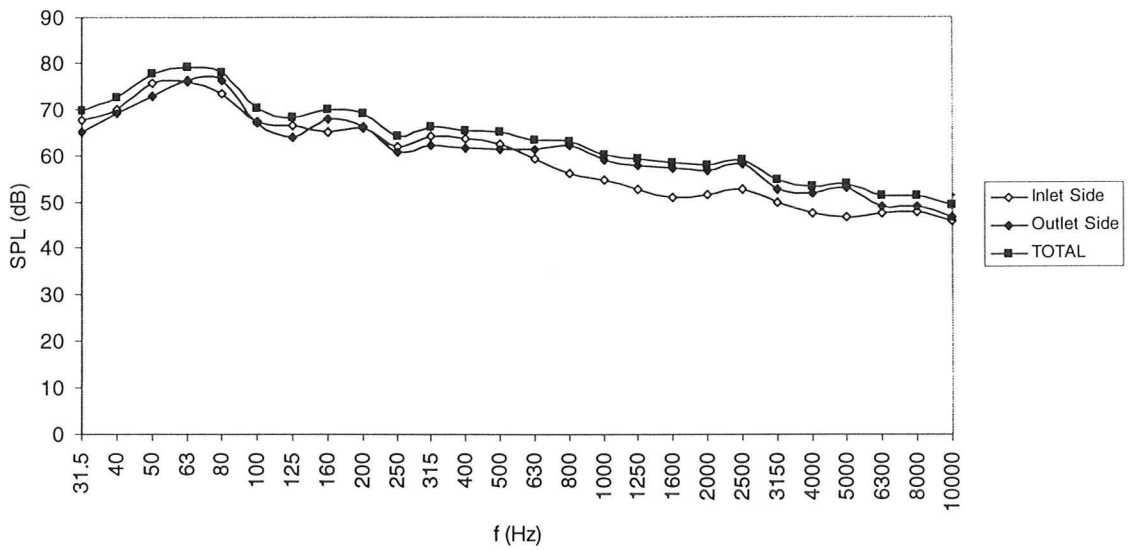

Figure 4.32: Total sound generated by rear fan (inlet & outlet sides)

fan inlet area. The effect of scroll shape and the geometry of outlet duct, that is totally different in the front HVAC system, also contribute to this difference. Therefore, the total noise of rear fan is nearly close to the corresponding values of outlet side noise. However, as it was explained before, the inlet side is a major contributor to the total noise produced by the rear air conditioning system.

OSPL	dB	dBA
Inlet side	81.50	68.46
Outlet side	81.62	70.03
Total	84.57	71.82

Table 4.2: Overall sound level of the inlet and outlet sides of the rear fan

Regarding the variation of sound level of rear fan with respect to impeller blade tip speed, the fan noise was run at different voltages to get different speeds. The relation between voltage and rotational velocity of the fan was determined by an optical and a mechanical tachometer separately, both readings were very close to each other. Thus, it was possible to get the required tip speed by changing the voltage. The results are shown in Figure 4.33 for different three frequencies and overall level. The linearity of the change in sound levels with rotational velocity is clearly observed; similar to the case of the front fan. This subject was discussed in detail for front fan in the previous section. The overall SPL is proportional to logarithm $V^{4.2}$ which is very close to the front fan. Single frequency variations are proportional with $V^{5.9}$. Here, it is impossible to say that all the noise generated in rear fan is just a result of monopole or dipole distributions. The

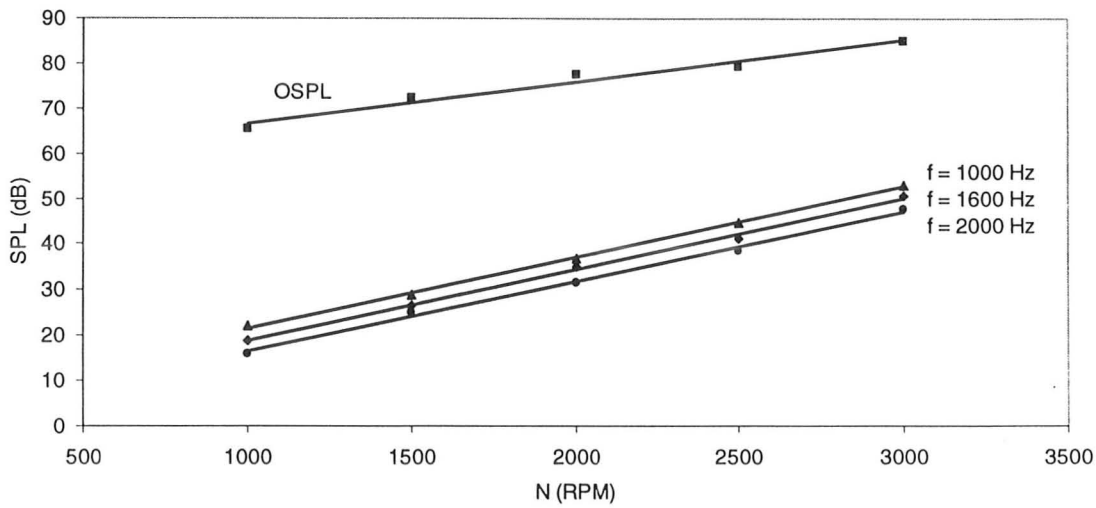

Figure 4.33: Sound level of rear fan as a function of impeller tip speed

fact is there is a complex combination of all simple noise sources in which any kind of direction of alignment, arrangement and strength could be happen. All affords are to reveal the characteristics of these sources in order to make an acoustically effective impeller and scroll for small centrifugal fan.

4.6 Evaluation of the Fan Contribution to HVAC System Noise Generation

In the previous sections, noise sources mechanisms of the air conditioning systems and the related fans were separately investigated. However, it is not clear yet which one is the major noise source. To do this, one can compare the sound level produced by all ducts of the front air conditioning system and the front fan alone. As it is observed in Figure 4.34, the fan alone generates more noise than both possible modes of the front HAVC system. Figure 4.35 demonstrates similar comparison for the rear air conditioning system and the rear fan alone. Overall sound levels in Figure 4.36 summarizes these results. Table 4.3 contains the values of overall sound levels for fans and ducts, with and without the louvers. It is obvious that in all cases, elimination of flow-noise results in lower noise generation. Shortly, this table will be discussed. However, the results described above do not help in pinpointing the primary source of sound generation. In fact, in this form of comparison, neither the effect of the waves reflected from the end of the HVAC ducts nor the role of the acoustic impedance of the evaporator core and plenum regions can be assessed. Hence, Figures 4.34-4.36 do not really give any clear picture about the contribution of the fan in the noise generated by

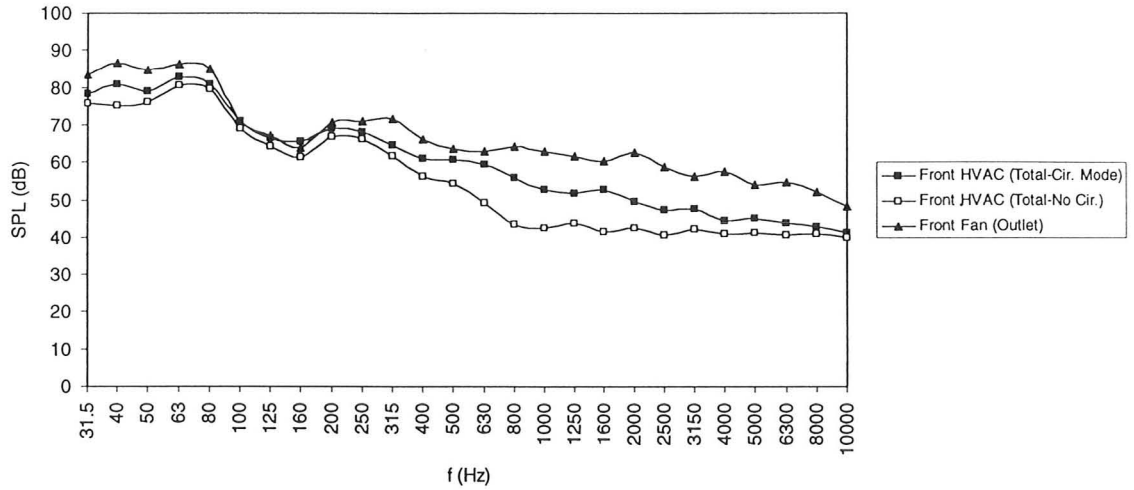

Figure 4.34: Comparison of sound levels produced by front fan and HVAC system

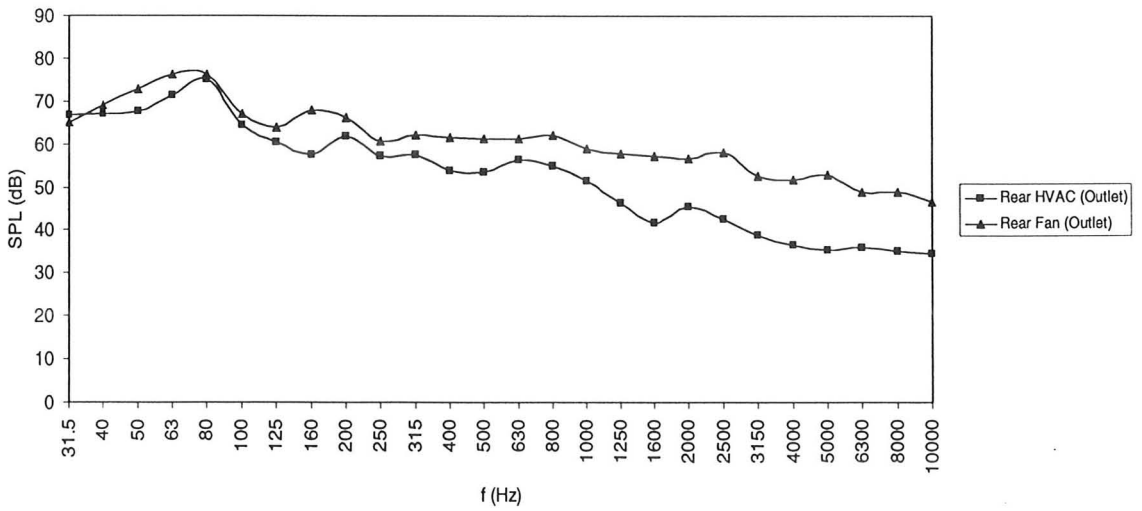

Figure 4.35: Comparison of sound levels produced by rear fan and HVAC system

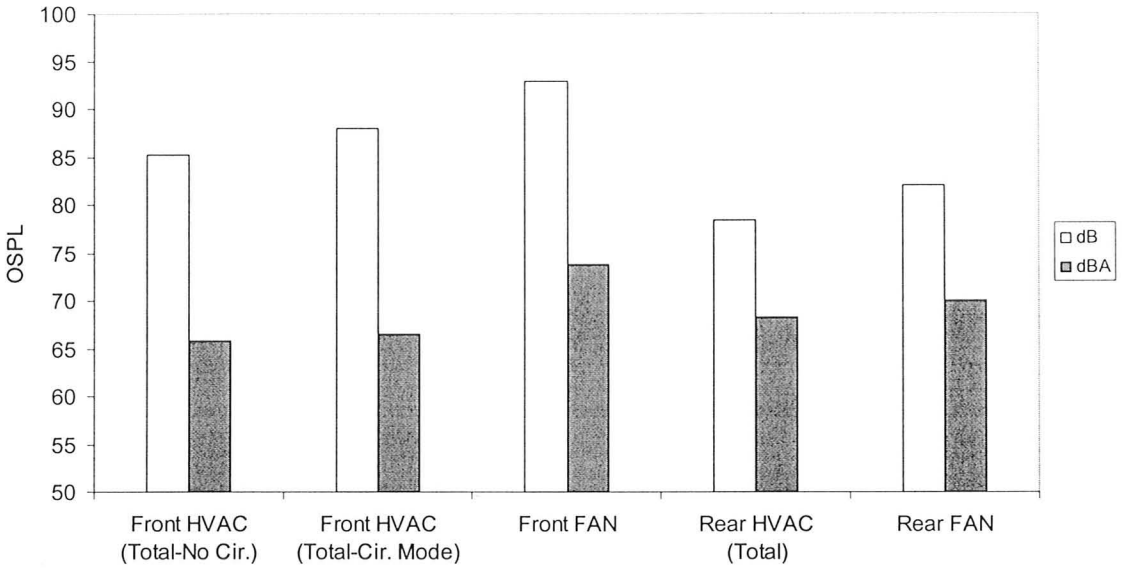

Figure 4.36: Comparison of overall sound levels produced by front and rear fans and HVAC systems

OSPL	With Flow (dB)	No Flow (dB)
Front Fan Scroll	92.90	92.90
Duct No. 1, With louver	78.26	74.40
Duct No. 1, W/O louver	75.83	75.20
Duct No. 2&3, With louver	84.07	81.25
Duct No. 2&3, W/O louver	82.31	81.80
Duct No. 4, With louver	73.86	70.80
Duct No. 4, W/O louver	72.45	71.90
Duct 1+2&3+4, With louver	85.25	82.30
Duct 1+2&3+4, W/O louver	83.50	83.00
Rear Fan Scroll	81.50	81.50
Rear HVAC Duct, With louver	85.84	72.22
Rear HVAC Duct, W/O louver	83.75	76.36

Table 4.3: Comparison of overall sound levels of HVAC ducts and fans, with and without the louvers

the HVAC system. In order to overcome this difficulty, cancellation of the effect of flow-noise inside the HVAC system seems the most effective way. If this could be achieved, it would be possible to understand how much the turbulent flow and the vortex shedding produced in the space between fan and ducts outlet, especially the evaporator region, affect the total noise generated by the system. For this purpose, the impeller was replaced with a speaker in the fan scroll and the tests were repeated for fan alone and complete HVAC system. In each individual case, the speaker was adjusted so that it generates the same total noise level that is produced by the real fans and the systems. Then, all of the previous tests were repeated. Since the sound spectra of the speaker and the fan were different, the only way to get a reasonable conclusion from these tests is to calculate the ratio between output noise levels of the fan and those of ducts, which are given by:

$$\Delta SPL_{(NoFlow)} = SPL_{Speaker} - SPL_{Duct,\ without\ flow} \tag{4.1}$$

$$\Delta SPL_{(WithFlow)} = SPL_{Fan\text{-}alone} - SPL_{Duct,\ with\ flow} \tag{4.2}$$

Figures 4.37-4.39 present the results for the front air conditioning ducts number 1, 2&3 and 4, respectively. The results for the rear system are demonstrated in Figure 4.40. The last two columns show the overall levels. In all the figures, the sound level difference for the case of no-flow is higher than the case with flow up to the frequency 400 or 500 Hz. This means for that range of frequency, the flow-noise is the dominant noise source. Above f = 500 Hz, the trends are reversed and the sound level difference for the case with mean-flow is larger. This indicates that for the higher range of frequency, airflow decreases the fan noise level, but it does not necessarily mean the fan noise is dominant.

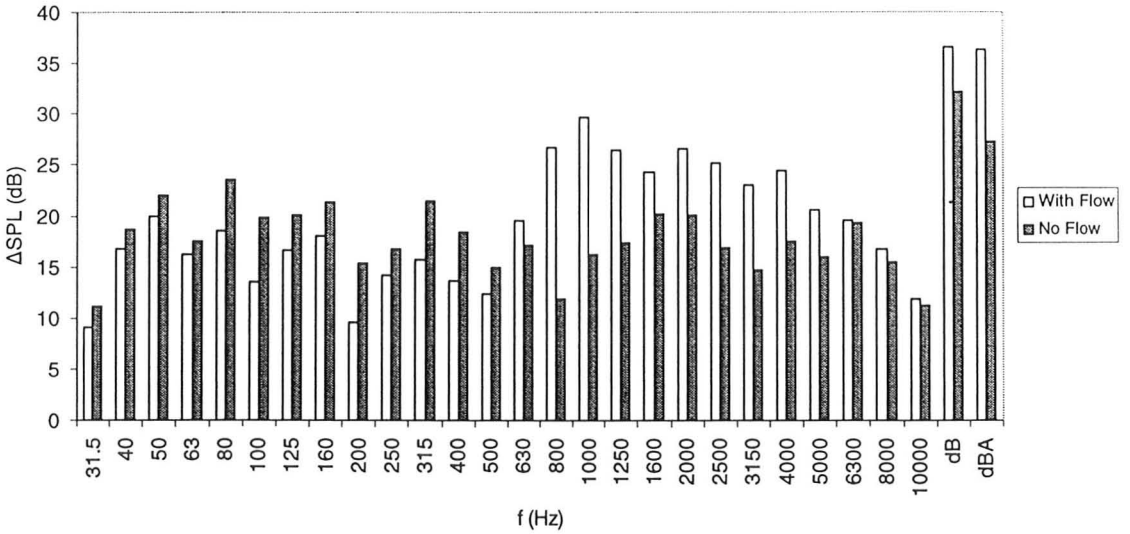

Figure 4.37: ΔSPL for front HVAC system, duct no. 1

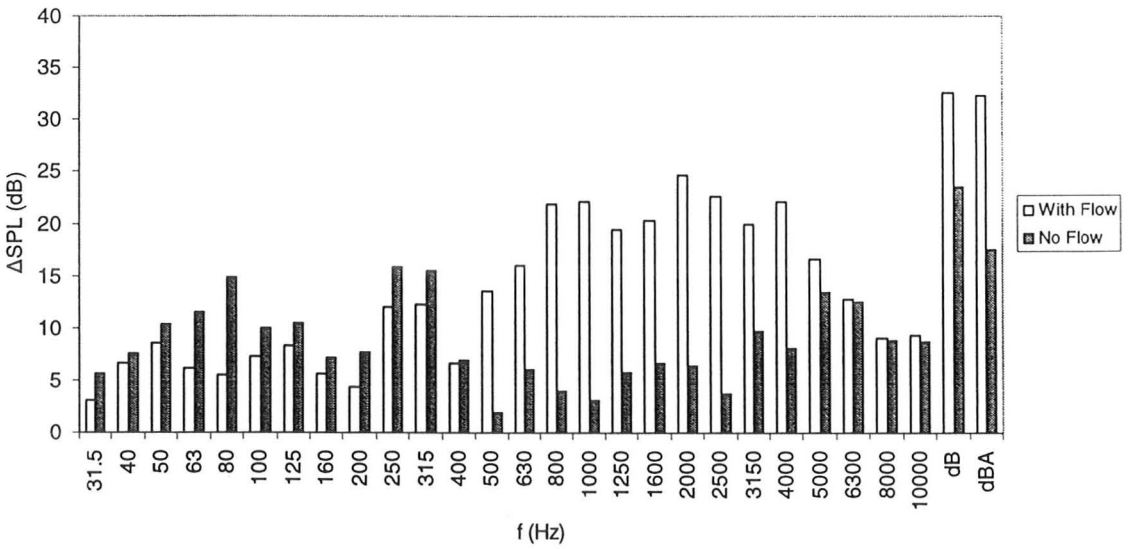

Figure 4.38: ΔSPL for front HVAC system, duct no. 2&3

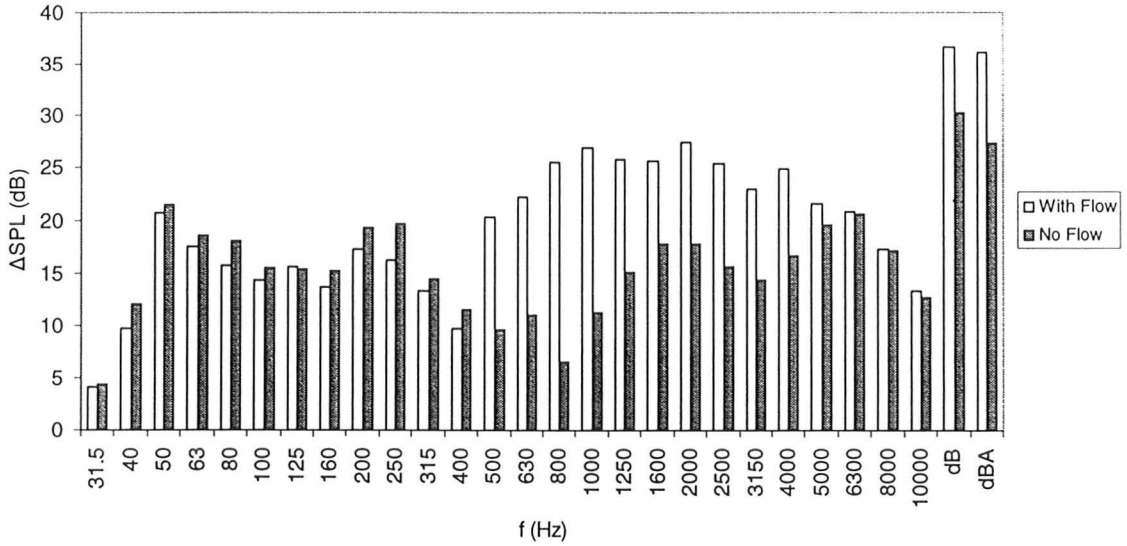

Figure 4.39: ΔSPL for front HVAC system, duct no. 4

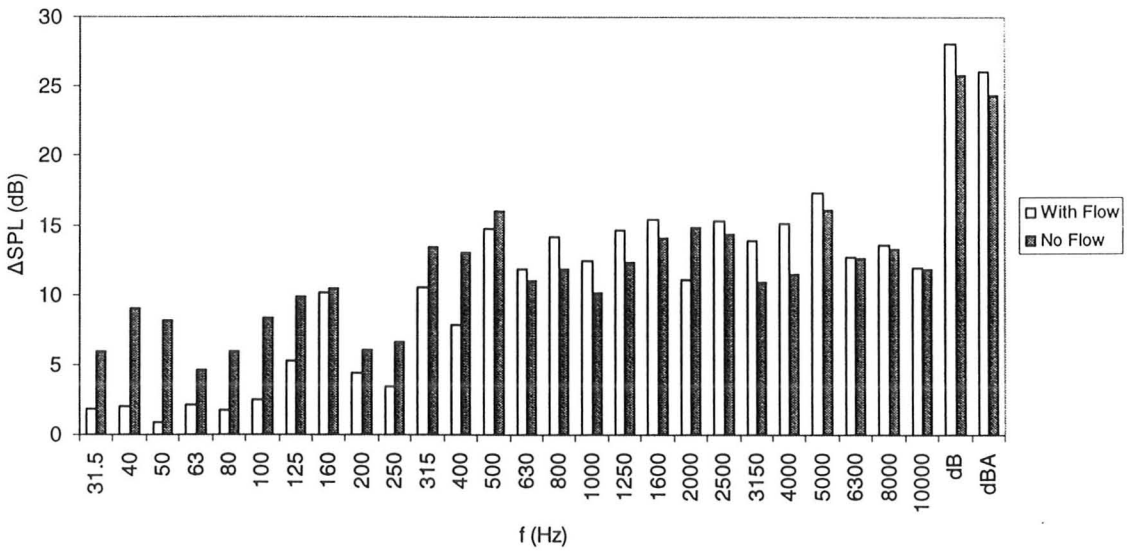

Figure 4.40: ΔSPL for rear HVAC system

It should be noted that the presence of flow not only changes the noise characteristics of the fan section but also generates additional noise resulting from the flow-acoustic coupling phenomenon in the ducting system. Some systematic tests can be developed to find out the accurate flow-noise coupling variations and contribution inside the HVAC ducts in the next step of this project. However, it is obvious that this coupling phenomenon makes it difficult to conclude whether, or not, the fan is the single dominant noise source, although its contribution is undeniable, as seen in Table 4.3. Another reason that makes it impossible to consider the fan as the single dominant source of noise is the levels of the fan noise produced at high frequencies. The spectra in the sections 4.4 and 4.5 show that the centrifugal fans used in these HVAC systems do not really generate a high sound level at high frequencies; especially, the levels at the blade passing frequencies are weak.

It seems that at high frequencies, the difference between no-flow and with mean-flow cases becomes close to each other. This indicates that at this range of frequency, the contributions of flow-noise and fan noise are almost the same in total noise produced. This deduction is in accordance with the results of Brungart *et al.* (1992).

4.7 In-Car Noise Measurement

Some experiments were carried out to measure the noise levels generated by air conditioning systems inside the automobile in order to understand how the outgoing sound waves from the vents combine and interact in the closed space of the car. This could also be considered as a trial to relate the measured data using the present setup in

the laboratory to the test data in the car. For in-car tests, an HP signal analyzer and one of the previously described microphones were utilized to measure the noise levels in a number of points inside the automobile. These locations were: driver, front passenger, left rear passenger (behind the driver), right rear passenger, all for left and right ears. Besides, three arbitrary points between front seats and three other random points between rear seats were selected to measure. The results are shown in Figures 4.41-4.43. These figures are based on the average data between left and right ears and between those three front and rear middle points. The engine of the automobile was not running during the tests. Hence, all these data are just the noise levels of the HVAC systems. Figure 4.41 and 4.42 show the spectra for the front and rear air conditioning systems, respectively. The noise level of the front middle point is higher than the other locations because the microphone was in the jet stream area of the ducts number 2&3. The outlet duct of rear system is located near the car floor and the microphone was not placed in its jet region. That is the reason neither front nor rear middle points show any high noise levels in Figure 4.42. The noise levels increase at high frequencies which is in agreement with the enclosures acoustical characteristics. Comparison between Figures 4.41 and 4.42 reveals that the rear HAVC system produces more noise at nearly all the range of frequency. Figure 4.43 demonstrates the overall sound levels which confirms this observation. Again, the effect of airflow on measurements at the front middle point is clearly seen in the figure. Effect of background noise is obvious at very low frequencies for in-car noise level data. In both Figures 4.42 and 4.43, the measured data using the test setup in the laboratory are compared with the in-car data. The effect of standing waves formed in

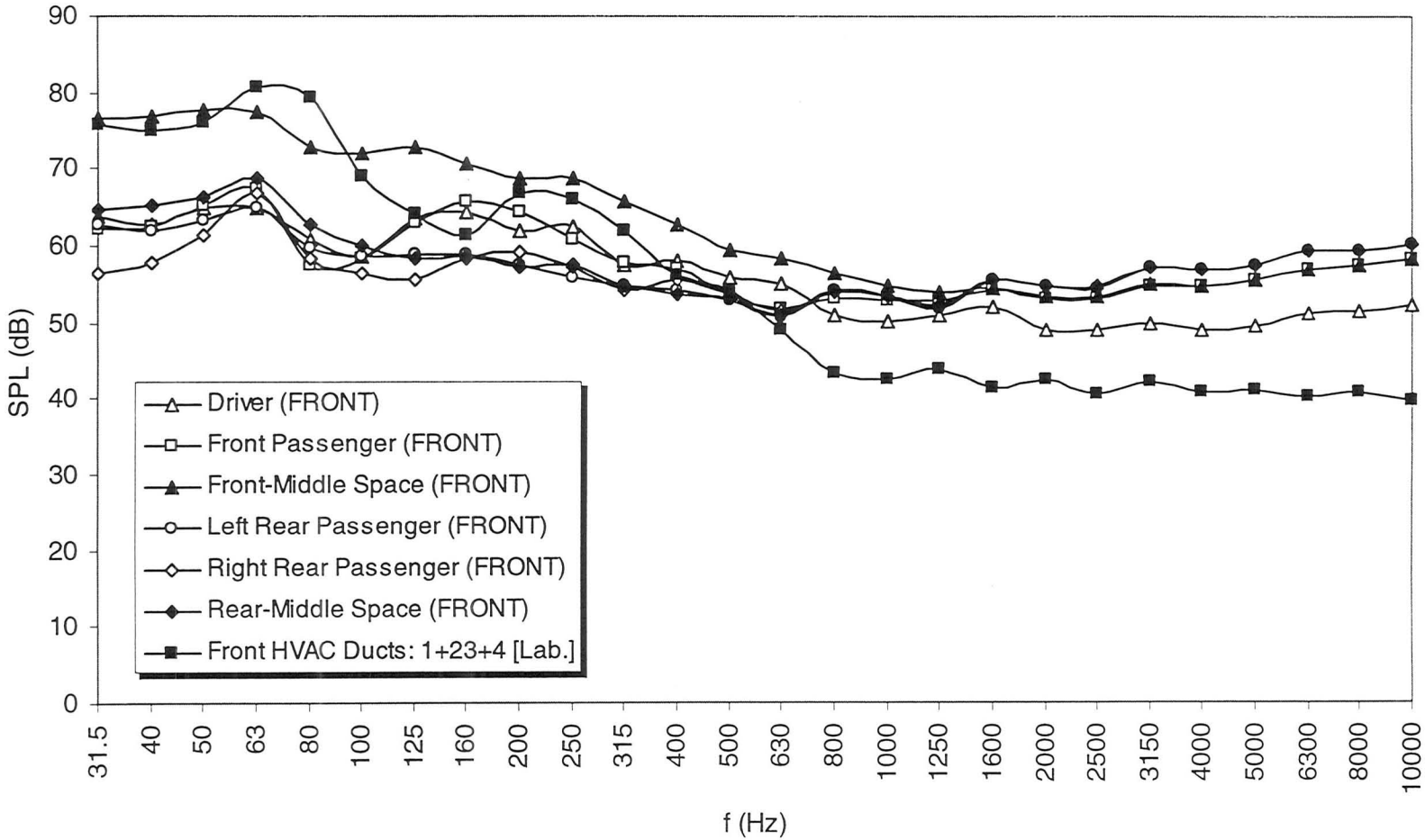

Figure 4.41: In-car SPL spectra for front HVAC system

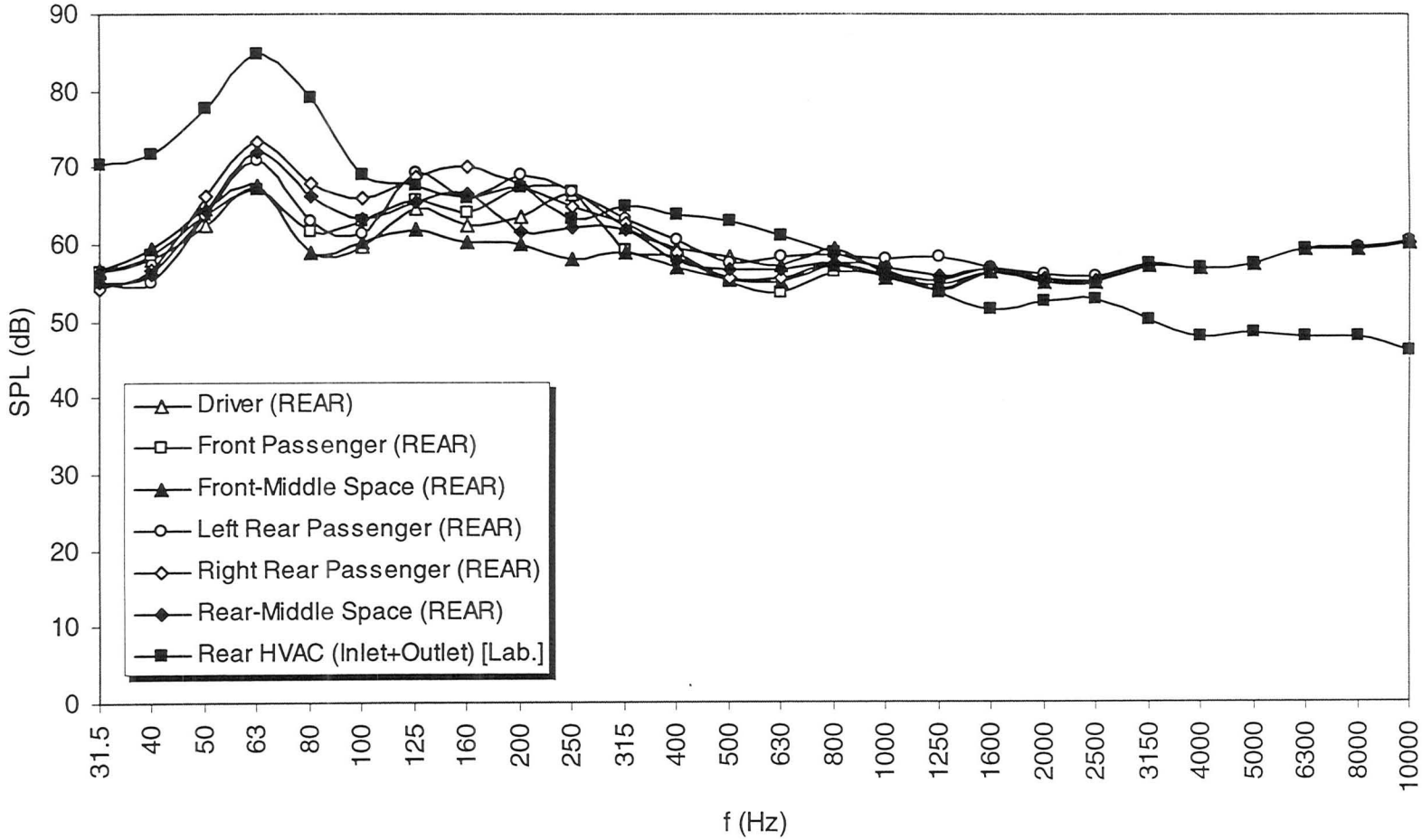

Figure 4.42: In-car SPL spectra for rear HVAC system

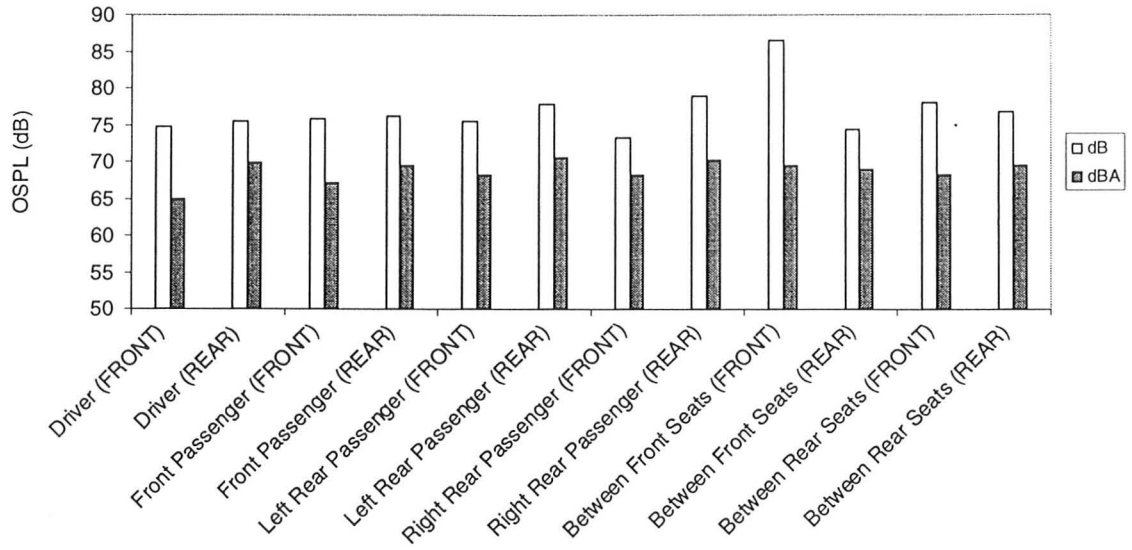

Figure 4.43: Overall sound level for front and rear HVAC systems

the closed area of the car is observed. This is the case that the relation between the sound pressure level and the energy reaching the internal surfaces, including seats and passengers, is no longer the same as for a plane wave. It seems that standing waves affects the sound field in the frequency range over which the wavelength is comparable with the dimensions of the cabin, since at low frequencies that wavelength is 8 to 10 times of the cabin size, they do not contain characteristics of the sound field in an enclosure. In fact, the space of the cabin is similar to a reverberation room, but due to the small volume of the cabin and parallel opposite surfaces, the sound field is not completely diffusive. Besides, all surfaces of reverberation rooms are highly reflective and it is not supposed to be any obstacle inside the room. However, in the cabin of this car, at high frequencies, the sound levels of different locations are very close. This

indicates that the materials which are used inside the cabin of this automobile have good acoustical characteristics so that they provide a nearly diffusive field, especially at high frequencies. In this regard, the shape of the seats should also be considered. Finally, it should be mentioned that a set of possible resonant frequencies always exists for every enclosure.

Chapter 5

Conclusions and Recommendations

The present investigation examined several aspects regarding the noise generated by automotive air conditioning systems and their fan parts alone. The intension of this study was not to find any modification method to reduce the noise levels, but to develop and test a systematic approach which facilitates the characterization of different noise sources and their relative importance. The results obtained using this approach also provide some guidelines for the phase of optimization. After a summary of conclusions of the present study, several methods of modification relevant to automotive HVAC systems will be explained in section 5.2.

5.1 Conclusions

The following items are the most important results of the present study:

1. At low frequencies, up to 500 Hz, the flow-noise produced in the HVAC duct systems is the most important source of noise. This is due to the

combination of both the fan air rush noise and the turbulent and separated flows occurring in the HVAC duct systems.

2. At higher frequencies, above 500 Hz, the produced noise is a combination of both ducts self-generated noise and fan broadband noise. It seems that fan broadband noise has less importance; however, at this level, it is difficult to say which one is dominant over that frequency range. To clarify this, one should determine the acoustic resistance or impedance of the HVAC system ducts. This is not really an easy task and a systematic and sophisticated approach should be initiated.
3. The noise generated by the inlet side of the fans has a small contribution to the total noise produced by the fan section alone. However, when the total HVAC system is considered, the inlet side has a significant influence on the total noise. It also affects considerably the total noise of the front HVAC system when it is working on the recirculation mode. Figure 4.11 shows that it is possible to decrease the noise level by up to 7 dB in the recirculation mode.
4. In the present automotive air conditioning systems, fan is not the *single* dominated noise source, but it has significant contribution at low frequencies in the total noise generated, especially in the recirculation mode.
5. Sound levels propagating from the end of the ducts are higher when all of the other ducts are closed. This is due to the difference between the reflection coefficients for open and closed duct ends.

6. Fan rumble noise was observed at the frequency range from 150 to 350 Hz. Rumble noise is an extremely annoying kind of noise that transfers through the HVAC system ducts and makes the driver and the passengers uncomfortable. Several methods will be explained to reduce this kind of noise in the next section.
7. The outgoing noise levels of the fans and HVAC system ducts are broadband in character. There is no sharp peak in the noise spectra and BPF tones are rather weak. This is in good agreement with the results of Ishihara and George (1994) and Botros *et al.* (1999).
8. Louver is certainly a source of noise. In all cases, removing the louver decreased the noise levels. Front system louvers are like a cascade of small narrow plates. Since the trailing edge of the surfaces has a thickness, shedding vortices occur where the flow leaves the edge. It should also be mentioned that vortex shedding from the present louvers seems to be a random process and has a character of broadband noise. Generally speaking, the frequency of the noise due to the vortex shedding depends on the plate geometry and velocity distribution along the blade surfaces.
9. The above point is more critical for the louver of the rear HVAC system. At low frequencies, where the wavelength is large relative to the dimensions of the louver openings, there would be a great diffraction. The diffracted waves develop as if there is a point source in the opening. Since most of the waves are reflected, a major amount of the sound energy return and do not come out

of the duct and transmit inside the cabin. However, as the frequency increases, more diffracted waves and sound energy are propagated.

10. Fan sound levels vary linearly with $10\log V^n$ in which n is between 4 and 6, depending on the fan type, impeller and scroll geometries.

5.2 Recommendations

In this section, several suggestions are given for future work of the present investigation. As stated before, the present study was focused on the characterization of the noise sources in automotive air conditioning system. The next step would be modification and optimization of the sound quality generated by these systems. Regarding the different sections of the automotive air conditioning system except fan, the following items would be suggested:

1. In order to better understand the role of louvers in noise production, it would be a good idea to mount the louvers one by one at the end of the test setup, and use an acoustically isolated fan to supply the airflow. Under this circumstance, one can study the influence of different parameters on the louvers noise level, such as angle of attack, thickness, geometry and number of the plates and the geometry of the louvers cross section.
2. As mentioned in the previous chapter, the rear HVAC system louver is not a real louver, but a perforated plate acting as a bluff body. Previous test can be applied for this louver to find what the best size and the number of the openings are.

3. It seems that resonator can be employed to reduce the automotive HVAC noise. Recently, Case and Cuddy (2001) studied the effectiveness of a resonator on HVAC duct and showed that it is able to decrease the noise level.
4. In front HVAC system, using absorbent materials at the location of the fan inlet could help to reduce the noise level propagating inside the automobile when it is working on recirculation mode.
5. As a powerful method, flow visualization can be employed to study of the present fans and HVAC systems. Undoubtedly, it will reveal many unknowns about the locations of the turbulent and separated flows which generate higher levels of noise.

Since fan is one of the contributors of air conditioning system noise, several methods for modification of this part is presented:

1. One interesting method to reduce the fan noise level is to control the flow at the blades inlet to postpone the flow separation on the suction side of the blade. This technique was introduced by Saeki *et al.* (1997). Figure 5.1 shows the flow velocity distribution between the blades for a conventional fan. The strong flow separation is seen at the blade inlet. By replacing this blade with a slit blade and decreasing the blade inlet angle of attack, the flow separation will be alleviated at the inflow area. The slit is made near the leading edge of the blade. This also increases the blade pressure gain, but no effect on the total fan efficiency.

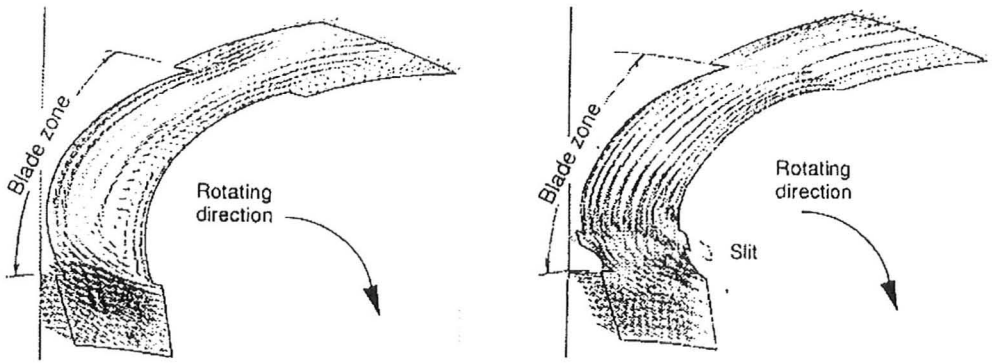

Figure 5.1: Distribution of flow velocity between blades of a conventional fan (left) and a fan with slit blades (right), Saeki *et al.* (1997)

2. Due to the strong pressure fluctuations in the cutoff region, the geometry of the cutoff is an important design factor. Increasing the cutoff radius can result in noise reduction up to 6 dB with same fan efficiency, as shown by Humbad *et al.* (1998). Humbad and Thawani (1994) concluded that semi-inclined cutoff with a 15 mm radius is best from the noise reduction and manufacturing aspects. Inclined cutoff has the ability to reduce the blade passing frequency and overall noise. Increasing the cutoff clearance could be another option to reduce the fan noise without any loss in fan efficiency, as reported by Smith *et al.* (1974).
3. Extension of cutoff is a simple and effective way to decrease the fan noise due to elimination of the recirculated flows. This is demonstrated in Figure 2.10. The extended cutoff stops the reentry of the airflow into the impeller.

4. Another possible method to reduce the fan noise is using transition meshes at blades leading and trailing edges of the impeller, as shown in Figure 5.2. This method was suggested by Khoroshev and Petrov (1971). The inner mesh shifts the blade flow separation downstream. The outer mesh decreases the turbulence level of the blades outflow. However, one should note that the cost of using the transition meshes is a loss in the fan efficiency. For same mass flow rate, the fan with meshes should run at higher speed.

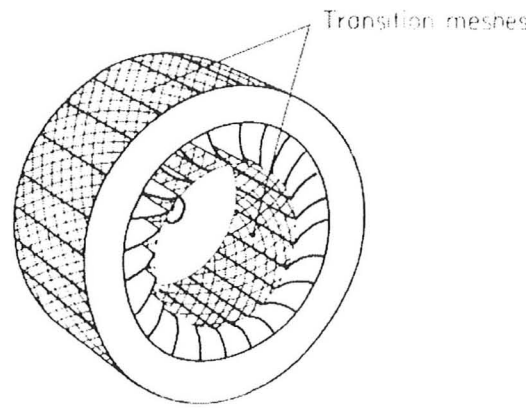

Figure 5.2: An impeller equipped with transition meshes at inner and outer radial sides, Khoroshev and Petrov (1971)

5. The scroll of a small centrifugal fan can be acoustically improved by means of mounting a resonator at the cutoff location, as depicted in Figure 5.3. This method, which is studied by Neise and Koopmann (1980), can be used for fans at different speeds by moving a plug to change the length of the resonator. The resonator length is proportional to the fan speed. Therefore, a

sensor along with a simple electrical controller is required. This method seems highly efficient, especially for reduction of the BPF tone. The fan performance is not influenced by this method.

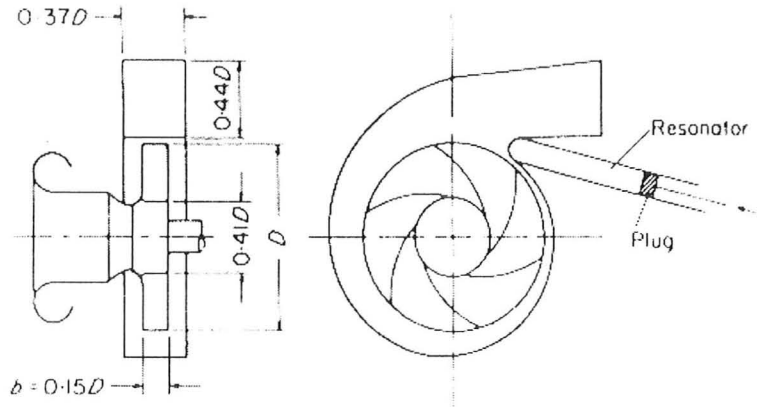

Figure 5.3: A centrifugal fan with a resonator located at the Cutoff, Neise and Koopmann (1980)

6. As it was mentioned earlier, most of the modification methods for scroll are related to the cutoff region. However, as far as the noise generation is concerned, the complete geometry of the scroll is important and should be considered during a design process. As a matter of fact, if one measures the noise of an impeller without the scroll, the spectrum would be flat and uniform, as discussed by Moreland (1974). When it is mounted into the scroll, the overall broadband noise will increase. In addition, scroll geometry has essential effects on the major spectral peaks in fan noise. Width, radius, side geometry and outlet cross section are the most significant parameters in fan scroll design.

7. Acoustical liners attached to the interior scroll of the fan can effectively decrease the outgoing fan noise and the radiated noise from the scroll. This method has been investigated by Bartenwerfer *et al.* (1977). These materials reduce both tonal and broadband noise. There is just a little change in fan performance.

It should be remembered that the effectiveness level of each of the above-mentioned method of noise reduction for the present air conditioning systems or their centrifugal fans is not cleared. They should be tested, especially for the combination of two or more of the above methods.

References

Bartenwerfer, M., Gikadi, T., Neise, W. and Agnon, R., "Noise reduction in centrifugal fans by means of an acoustically lined casing," Noise Control Engineering, Vol. 8, 100-107, 1977.

Beranek, L.L. and Ver, I.L., Noise and Vibration Control Engineering, John Wiley and Sons Inc., 1992.

Blake, W.K., Mechanics of Flow-Induced Sound and Vibration, Academic Press Inc., 1986.

Blevins, R.D., Formulas for Natural Frequency and Mode Shape, Krieger Publishing Co., 1995.

Botros, M.B., Hanna, D.F., Nava and Lai, T.J., M.C., "A new design feature to improve the sound and efficiency of automotive HVAC centrifugal blower systems," Proceedings of the ASME - Noise Control and Acoustics Division, 1999.

Brungart, T.A., Lauchle, G.C. and Tichy, J., "Case History: Acoustic diagnostics of an automotive HVAC system," Noise Control Engineering Journal, Vol. 39, No. 1, 1992, 31-42.

Case, J.J. and Cuddy, W.A., "Application of an acoustical resonator to reduce HVAC blower noise," Proceedings of the Noise and Vibration Conference, Traverse City, Michigan, 2001.

Chanaud, R.C., "Aerodynamic sound from centrifugal-fan rotors," Journal of the Acoustical Society of America, Vol. 37, 1965, 969-974.

Cho, N. and Kim, M., "Numerical investigation of fluid flow in an automotive HVAC module," SAE Paper 971778, 1997.

Cummings, A., "Ducts with axial temperature gradients: an approximate solution for sound transmission and generation," Journal of Sound and Vibration, Vol. 51, No. 1, 1977, 55-67.

Curle, N., "The influence of solid boundaries upon aerodynamic sound," Proceedings of the Royal Society, Series A, Vol. 231, 1955, 505-514.

Davies, P.O.A.L., "Practical flow duct acoustics," Journal of Sound and Vibration, Vol. 124, No. 1, 1988, 91-115.

Davies, P.O.A.L., "Reflection coefficients for an unflanged pipe," Journal of Sound and Vibration, Vol. 72, No. 4, 1980, 543-546.

Doak, P.E., "Acoustic radiation from a turbulent fluid containing foreign bodies," Proceedings of the Royal Society of London, Series A, Vol. 254, 1960, 129-145.

Edge, K.A. and Johnston, D.N., "The secondary source method for the measurement of pump pressure ripple characteristics, Part 1: description of method," Proceedings of the Institution of Mechanical Engineers, Part A, Vol. 204, 1990, 33-40.

Eilemann, A., "Practical noise and vibration optimization of HVAC systems," SAE Paper No. 1999-01-0867, 1999.

Embleton, T.F.W., "Experimental study of noise reduction in centrifugal blowers," Journal of the Acoustical Society of America, Vol. 35, 1963, 700-705.

Ffowcs Williams, J.E. and Hawkins, D.L., "Sound generated by turbulence and surfaces in arbitrary motion," Philosophical Transactions of the Royal Society of London, Series A, Vol. 264, 1969, 321-342.

Fischer, D., "Airflow simulation through automotive blowers using computational fluid dynamics," SAE Paper 950438, 1995.

Goldstein, M., "Unified approach to aerodynamic sound generation in the presence of solid boundaries," Journal of the Acoustical Society of America, Vol. 56, 1974, 497-509.

Goldstein, M., Rosenbaum, B.M., and Albers, L.U., "Sound radiation from a high speed axial- flow due to the inlet turbulence quadrupole interaction," NASA TN D-7667, 1974.

Gronier, P. and Gilotte, P., "Airflow simulation of an automotive blower for a HVAC unit", SAE Paper 960961, 1996.

Howe, M.S., "Contributions to the theory of aerodynamic sound, with application to excess jet noise and the theory of the flute," Journal of Fluid Mechanics, Vol. 71, 1975, 625-673.

Howe, M.S., "A near-wake model for the aerodynamic pressure exerted on singing trailing edges," Journal of the Acoustical Society of America, Vol. 60, 1976.

Howe, M.S., "A review of trailing edge noise," Journal of Sound and Vibration, Vol. 61, No. 4, 1978, 437-465.

Howe, M.S., Acoustics of Fluid-Structure Interaction, Cambridge University Press, Cambridge, UK, 1998.

Howe, M.S., "Trailing edge noise at low Mach numbers, Part 1," Journal of Sound and Vibration, Vol. 225, 1999.

Howe, M.S., "Trailing edge noise at low Mach numbers, Part 2," Journal of Sound and Vibration, Vol. 234, 2000.

Howes, F.S. and Real, R.R., "Noise origin, power and spectra of ducted centrifugal fans," Journal of the Acoustical Society of America, Vol. 30, 1958, 714-720.

Huebner, G.H., "Noise of centrifugal fans and rotating cylinders," ASHRAE Journal, Vol. 5, 1963, 87-94.

Humbad, N.G. and Thawani, P.T., "A systematic case study to improve sound quality of an automotive climate control system," Noise-Con 94, Ft. Lauderdale, Florida, 1994.

Humbad, N.G., Hall, T.J., Terry, J., Hess, G. and Sohaney, R.C., "Case study on reducing automotive blower noise," NCA-Vol. 2, Proceedings of the ASME Noise Control and Acoustics Division, 1996.

Humbad, N., Sohaney, R. and Roan, J., "Centrifugal blower noise and airflow improvements," Noise-Con 98, Ypsilanti, Michigan, 1998.

Ikuta, S., Tanaka, K. and Kato, K., "Numerical simulation of air and heat flow in a heater unit," SAE Paper 890574, 1989.

Ishihara, Y. and George, A.R., "Determination of noise sources in a forward-curved centrifugal blower using flow visualization methods," Noise-Con 94, Florida, USA, 1994.

Jorgensen, R., Fan Engineering, Buffalo Forge Co., Buffalo, N.Y., 1961.

Jorgensen, R., Fan Engineering, Howden Buffalo Inc., Buffalo, N.Y., 1999.

Kind, R.J. and Tobin, M.G., "Flow in a centrifugal fan of the squirrel-cage type," Journal of Turbomachinery – Transactions of ASME, Vol. 112, 1990, 84-90.

Khoroshev, G.A. and Petrov, Y.I, "Some new methods of fan noise reduction," Proceedings of the 7th International Congress on Acoustics, 1971.

Kondo, F. and Aoki, Y., "Prediction method on effect of thermal performance of heat exchanger due to nonuniform air flow distribution," SAE Paper 850041, 1985.

Krishnapa, G., "Some experimental studies on centrifugal blower noise," Noise Control Engineering, Vol. 12, No. 2, 1979, 82-90.

Lier, L., Dequand, S. and Hirschberg, A., "Aeroacoustics of diffusers: an experimental study of typical industrial diffusers at Reynolds numbers of O(10^5)," Journal of the Acoustical Society of America, 1999.

Lighthill, M.J., "On sound generation aerodynamically: I. General theory," Proceedings of the Royal Society, Series A, Vol. 211, 1952, 564-587.

Lin, C.-H., Han, T., and Sumantran, V., "Experimental and computational studies of flow in a simplified HVAC duct", International Journal of Vehicle Design, Vol. 15, 1994, 147-165.

Lyons, L.A. and Platter, S., "Effects of cut-off configuration on pure tones generated by small centrifugal blowers," Journal of the Acoustical Society of America, Vol. 35, 1962, 1455-1456.

Maling G.C., Jr., "Dimensional analysis of blower noise," Journal of the Acoustical Society of America, Vol. 35, 1556-1564, 1963.

Moreland, J.B., "Housing effects on centrifugal blower noise," Journal of Sound and Vibration, Vol. 36, No. 2, 191-205, 1974.

Morfey, C.L., "Tone radiation from an isolated subsonic rotor," Journal of the Acoustical Society of America, Vol. 49, 1971, 1690-1692.

Morfey, C.L., "Rotating blades and aerodynamic sound," Journal of Sound and Vibration, Vol. 23, No. 3, 1973, 587-617.

Mueller, E.A. (Editor), Mechanics of Sound Generation in Flow, Springer-Verlag, Berlin, 1979.

Mugridge, B.D., "Noise characteristics of axial and centrifugal fans as used in industry," The Shock and Vibration Digest, Vol. 7, No. 9, 1975, 93-107.

Neise, W., "Application of similarity laws to the blade passage sound of centrifugal fans," Journal of Sound and Vibration, Vol. 43, No. 1, 1975, 61-75.

Neise, W. and Koopmann, G.H., "Reduction of centrifugal fan noise by use of resonators," Journal of Sound and Vibration, Vol. 73, No. 2, 297-308, 1980.

Neise, W., "Fan noise: generation mechanisms and control methods," Proceedings of the International Conference on Noise Control Engineering, Avignon, France, 1988.

Peters, M.C.A.M., Aeroacoustic Sources in Internal Flows, Ph.D. Dissertation, Eidhoven University of Technology, Netherlands, 1993.

Powell, A., "Aerodynamic noise and the plane boundary," Journal of the Acoustical Society of America, Vol. 32, 1960, 982-990.

Powell, A., "Theory of sound vortex," Journal of the Acoustical Society of America, Vol. 36, 1964, 177-195.

Roozen, N.B., Bockholts, P.E. and Hirschberg, A., "Vortex sound in bass-reflex ports of loudspeakers," Journal of the Acoustical Society of America, Vol. 104, No. 4, 1998, 1914-1919.

Saeki, N., Kamiyama, K., Uomoto, M. and Ishihara, Y., "Development of low noise blower fan," Proceedings of the SAE Vehicle Thermal Management Systems Conference, Indianapolis, Indiana, 1997.

Shen, F.Z., Backer, G.P. and Swanson, D., "HVAC plenum design analysis", SAE Paper 950113, 1995.

Shepherd, I.C. and Lafontaine, R.F., "Measurement of vorticity noise sources in a centrifugal fan," Proceedings of the International INCE Symposium, Senlis, France, 1992.

Smith, W.A., O'Mally, J.K., and Phelps, A.H., "Reducing blade passing noise in centrifugal fans," ASHRAE Transactions, Vol. 80, 1974, 45-52.

Terao, M. and Shoda, T., "On sound generated by bluff bodies in air flow," Inter-Noise75, Japan, 675-678, 1975.

Thompson, M.C. and Hourigan, K. and Stokes, A.N., "Prediction of the noise generation in a centrifugal fan by solution of the acoustic wave equation," International INCE Symposium, Senlis, France, 1992.

Toksoy, C., "Design of an automotive HVAC blower wheel for flow, noise and structure integrity", SAE Paper 950437, 1995.

Werner, F. and Frik, S., "Optimization of an automotive HVAC module by means of computational fluid dynamics", SAE Paper 950439, 1995.

Willmarth, W.W., "Pressure fluctuations beneath turbulent boundary layers," Annual Review of Fluid Mechanics, Vol. 7, 1975.